

FUNCTIONAL ANALYSES OF *ARABIDOPSIS* MAPK GENE FAMILIES

By

SOMRUDEE SRITUBTIM

B.Sc. Khon Kaen University, Thailand, 1994
M.Sc., Simon Fraser University, Canada, 1999

A THESIS SUBMITTED IN PARTIAL FULFILMENT OF
THE REQUIREMENTS FOR THE DEGREE OF
DOCTOR OF PHILOSOPHY

in

THE FACULTY OF GRADUATE STUDIES

(Plant Science)

THE UNIVERSITY OF BRITISH COLUMBIA

October 2005

© Somrudee Sritubtim, 2005

ABSTRACT

In plants, mitogen-activated protein kinase (MAPK) cascades have been implicated in controlling intracellular signaling in developmental processes and in response to many external stimuli, including biotic and abiotic stresses. The hallmark of a MAPK cascade is the participation of three classes of protein kinases (MAPK, MAPKK and MAPKKK) that operate hierarchically to amplify the initial signal. Plant genomes appear to encode an exceptionally rich array of MAPK cascade proteins (at least 20 MAPK and 10 MAPKK homologues have been identified in *Arabidopsis*) but functional analysis of this extensive matrix is just beginning.

To gain insight into the specificity/redundancy of MAPKs and MAPKKs, I have used RT-PCR to examine the expression profiles of each of the identified *MAPKK* and *MAPK* genes in *Arabidopsis*. Gene expression patterns have been examined in various tissues, at several developmental stages and following a series of stress treatments. The findings reveal distinct expression patterns of *AtMKK6*, *AtMPK13* and *AtMPK12* genes.

I have analyzed further the cell and tissue distribution of their expression during development and in response to many external stimuli through use of promoter::*GUS* (β -glucuronidase) reporter plants. On the one hand, my results show that *AtMKK6* and *AtMPK13* promoters are specifically active at the primary root zones where lateral root primordia (LRP) are emerging. Auxin treatment further stimulates the promoter of these genes in emerging LRP, and those promoter activities are suppressed by NPA, an auxin transport inhibitor. The *AtMPK12* promoter, on the other hand, is specifically active in stomatal guard cells and can be induced by high salt and osmotic stress treatments. I have also conducted a phenotypic analysis of *AtMKK6*, *AtMPK13* and *AtMPK12* loss-of-function

mutant plants. Together, these results indicate diverse roles of *MAPKK/MAPK* genes. I show that AtMKK6 and AtMPK13 activities are both associated with the lateral root formation process, while AtMPK12 plays discrete roles during stomatal development.

TABLE OF CONTENTS

ABSTRACT.....	ii
TABLE OF CONTENTS.....	iv
LIST OF TABLES.....	viii
LIST OF FIGURES.....	ix
LIST OF ABBREVIATIONS.....	xi
ACKNOWLEDGEMENTS.....	xiii
 CHAPTER 1: MAPK GENE FAMILY IN PLANTS.....	 1
1.1 INTRODUCTION.....	1
1.2 ROLES OF MAPK PATHWAY COMPONENTS IN PLANTS	3
1.2.1 The role of MAPK pathways in stress signaling in plants.....	4
1.2.1.1 Wounding signaling.....	4
1.2.1.2 Oxidative stress signaling	5
1.2.1.3 Low temperature stress signaling.....	6
1.2.2 The role of MAPK pathways in plant development	7
1.2.2.1 Cell cycle and cytokinesis in plants	7
1.2.2.2 Cell-type specific development:	8
1.2.3 The role of MAPK pathways in plant hormone signaling.....	9
1.2.3.1 Auxin.....	10
1.2.3.2 Abscisic acid	10
1.2.3.3 Ethylene	11
1.3 MAP KINASE PATHWAY COMPONENTS IN <i>ARABIDOPSIS</i>	12
1.4 THESIS OBJECTIVES	16
 CHAPTER 2: MAPKK/MAPK EXPRESSION PROFILING IN ARABIDOPSIS	 18
2.1 INTRODUCTION.....	18
2.2 MATERIALS AND METHODS	21
2.2.1 Plant materials and growth conditions.....	21
2.2.2 Plant treatments.....	23
2.2.3 Total RNA extraction.....	24
2.2.4 RNA sample preparation for RT-PCR.....	24
2.2.5 RT reaction (first-strand cDNA synthesis) prior to PCR.....	25
2.2.6 PCR amplification.....	26
2.3 RESULTS AND DISCUSSION.....	29
2.3.1 Tissue differentiation of the <i>Arabidopsis</i> MAPKK/MAPK gene families: Characteristic profiles in mature and developing organs using RT-PCR data	29
2.3.2 Stress differentiation of the <i>Arabidopsis</i> MAPKK/MAPK gene families.....	37
2.3.3 Three candidate genes with interesting expression pattern for further functional characterization	43
2.3.3.1 The <i>AtMKK6</i> and <i>AtMPK13</i> genes	43
2.3.3.2 The <i>AtMPK12</i> gene.....	43
2.3.4 Perspectives.....	44

2.3.4.1 Expression profiling approach is useful to identify developmentally regulated and stress-responsive genes.	44
2.3.4.2 Spatial and temporal expression can infer gene function in <i>Arabidopsis</i>	46

CHAPTER 3: ARABIDOPSIS MAP KINASE KINASE (ATMKK6) AND MAP KINASE 13 (ATMPK13) ENCODE POSITIVE REGULATORS OF LATERAL ROOT FORMATION 47

3.1 INTRODUCTION.....	47
3.2 MATERIALS AND METHODS	50
3.2.1 Plant materials.....	50
3.2.2 Genomic DNA isolation	50
3.2.3 Molecular cloning of <i>AtMKK6</i> or <i>AtMPK13</i> promoter:: <i>GUS</i> DNA construct and generation of GUS reporter plants	52
3.2.3.1 Cloning of promoters	52
3.2.3.2 Generation of promoter:: <i>GUS</i> fusion DNA constructs.....	53
3.2.3.3 Transformation of <i>Agrobacterium</i>	54
3.2.3.4 <i>In planta</i> transformation of <i>Arabidopsis</i>	56
3.2.3.5 Selection of transformants	57
3.2.4 Histochemical GUS assay.....	58
3.2.5 Resin embedding and cross-sectioning of root tissue.....	59
3.2.6 Hormone treatments.....	60
3.2.7 <i>E. coli</i> (DH5 α) competent cells	61
3.2.8 <i>E. coli</i> transformation.....	61
3.2.9 <i>Agrobacterium</i> competent cells	62
3.2.10 Bacterial growth media	62
3.2.11 <i>Arabidopsis</i> plant growth media	63
3.2.12 Molecular cloning of glucocorticoid-inducible <i>AtMKK6</i> RNAi and <i>AtMPK13</i> RNAi DNA constructs and screening for the mutant plants	63
3.2.13 Phenotypic analyses and plant growth conditions	68
3.2.14 Lateral root analysis.....	69
3.2.15 Total RNA extraction and RT-PCR analysis.....	69
3.3 RESULTS	71
3.3.1 Histochemical localization of GUS activities driven by <i>AtMKK6</i> and <i>AtMPK13</i> promoters during plant growth and development	71
3.3.2 <i>AtMKK6</i> promoter:: <i>GUS</i> activity distribution during plant growth and development.....	72
3.3.3 <i>AtMKK6</i> promoter activity and lateral root formation.....	74
3.3.4 <i>AtMPK13</i> promoter:: <i>GUS</i> activity throughout plant growth and development	76
3.3.5 <i>AtMKK6</i> , auxin and lateral root formation	79
3.3.6 Blocking polar auxin transport with NPA reduces <i>AtMKK6</i> promoter:: <i>GUS</i> activity.....	81
3.3.7 Auxin can reverse the block of <i>AtMKK6</i> promoter:: <i>GUS</i> activity by NPA in both vascular tissue and pericycle cells.	82
3.3.8 <i>AtMPK13</i> and auxin	85
3.3.9 Phenotypic analysis of <i>AtMKK6</i> RNAi transgenic plants	87

3.3.10 Lateral root analysis of <i>AtMPK13</i> RNAi transgenic plants	92
3.4 DISCUSSION	94
3.4.1 <i>AtMKK6</i> is required for lateral root initiation.....	94
3.4.2 Pericycle-specific expression of the <i>AtMKK6</i> promoter is regulated by auxin.	95
3.4.3 <i>AtMKK6</i> and <i>AtMPK13</i> relationship.....	97

CHAPTER 4: *ATMPK12*, AN ARABIDOPSIS MITOGEN-ACTIVATED PROTEIN KINASE IS GUARD CELL-SPECIFIC AND INDUCED BY SALT AND OSMOTIC STRESSES..... 99

4.1 INTRODUCTION.....	99
4.1.1 Stomatal development.....	99
4.1.2 Stomatal function and their regulation through ion channels	106
4.1.3 Involvement of protein phosphorylation in stomatal regulation.....	109
4.1.4 Salt stress signaling.....	110
4.1.5 Ionic stress signaling: the “salt overly sensitive” (SOS) pathway.....	111
4.1.6 Osmotic stress signaling: SOS-independent protein kinases	113
4.2 MATERIALS AND METHODS	116
4.2.1 Plant materials.....	116
4.2.2 Genomic DNA isolation	116
4.2.3 Molecular cloning of <i>AtMPK12</i> promoter:: <i>GUS</i> DNA constructs and generating the <i>GUS</i> reporter plants	116
4.2.3.1 Cloning of the <i>AtMPK12</i> promoter.....	116
4.2.3.2 Generation of promoter:: <i>GUS</i> fusion DNA constructs and transgenic plants	117
4.2.4 Histochemical <i>GUS</i> analysis.....	118
4.2.5 Resin embedding and cross-sectioning of leaf tissue	118
4.2.6 NaCl and mannitol treatments	118
4.2.7 Verification of the <i>AtMPK12</i> SALK transfer-DNA (T-DNA)	119
4.2.7.1 Genomic DNA extraction of the <i>AtMPK12</i> SALK T-DNA	119
4.2.7.2 Identification of a homozygous SALK T-DNA insertional line.....	120
4.2.8 Phenotypic analyses of the homozygous <i>AtMPK12</i> T-DNA insertional mutant (<i>atmpk12</i>) in normal growth conditions.....	122
4.3 RESULTS	123
4.3.1 Histochemical localization of <i>GUS</i> activity driven by <i>AtMPK12</i> promoter during plant development.....	123
4.3.2 <i>AtMPK12</i> promoter activity was enhanced by NaCl and mannitol	132
4.3.2 Characterization of SALK T-DNA insertion lines	136
4.3.3 Phenotypic analysis of the <i>atmpk12</i> plants	137
4.4 DISCUSSION	137
4.4.1 <i>AtMPK12</i> promoter activity pattern is guard cell-specific throughout.....	137
4.4.2 <i>AtMPK12</i> may be required for guard cell development.....	139
4.4.3 Guard cell-specific <i>AtMPK12</i> is involved in osmotic stress response.	140
4.4.5 Concluding remarks	142

CHAPTER 5: OVERALL THESIS DISCUSSION AND FUTURE DIRECTIONS....	143
5.1 TRANSCRIPTIONAL PROFILING APPROACH VERSUS DEVELOPMENTAL SIGNALING.....	143
5.2 CHARACTERIZATION OF DEVELOPMENTALLY REGULATED GENES USING AN INDUCIBLE RNAI APPROACH	144
5.3. FUTURE DIRECTIONS	144
5.3.1 Systematic analysis of the <i>MAPKKK</i> genes.....	145
5.3.2 Use inducible promoters to drive <i>AtMPK12</i> gene constructs in stomata of transgenic plants.....	145
5.3.3 Identification of the MAPK protein network.....	146
5.3.4 Further characterization of the mutant and transgenic plants	146
REFERENCES.....	147

LIST OF TABLES

Table 1.1 List of <i>Arabidopsis</i> MAPK signalling components, adapted from Jonak <i>et al.</i> (2002).....	14
Table 2.1 <i>AtMKK</i> primer sequences for PCR amplification.....	27
Table 2.2 <i>AtMPK</i> primer sequences for PCR amplification.....	28
Table 2.3 The gene expression profiles in all known <i>Arabidopsis</i> MAPK genes.....	30
Table 2.4 The gene expression profiles in all known <i>Arabidopsis</i> MAPKK genes.....	31
Table 2.5 The MPSS data for the <i>AtMPK</i> genes.....	32
Table 2.6 The MPSS data for the <i>AtMKK</i> genes.....	33
Table 2.7 The gene expression profiles in all known <i>Arabidopsis</i> MAPK genes under different stress conditions.....	39
Table 2.8 The gene expression profiles in all known <i>Arabidopsis</i> MAPKK genes under different stress conditions.....	41
Table 3.1 Primer sequences for promoter cloning.....	53
Table 3.2 Primers for the <i>AtMKK6RNAi</i> and <i>AtMPK13RNAi</i> constructs.....	65
Table 3.3 Primers used for checking gene expression of the <i>AtMKK6RNAi</i> (line13).....	70
Table 4.1 Primer sequences for <i>AtMPK12</i> promoter cloning.....	117
Table 4.2 Primers for verification of the <i>AtMPK12</i> T-DNA insertional homozygous line(s) (SALK_074849).....	120

LIST OF FIGURES

Figure 2.1 Grouping of the MAPKK and MAPK proteins.....	20
Figure 2.2 RT-PCR analysis of the expression pattern of the <i>AtMKK6</i> and <i>AtMPK13</i> genes.	34
Figure 2.3 The <i>AtMKK9</i> gene was differentially expressed in organs and during developmental stages.	36
Figure 3.1 Schematic diagrams of pCAMBIA1381Z and pCAMBIA1301 vectors.....	55
Figure 3.2 Schematic diagram describing construction of the <i>AtMKK6RNAi</i> construct	66
Figure 3.3 Glucocorticoid-inducible <i>AtMKK6RNAi</i> interference (<i>AtMKK6RNAi</i>) system .	67
Figure 3.4 Overview of the process for generating <i>AtMKK6RNAi</i> transgenic plants.....	68
Figure 3.5 Promoterless-GUS activity as a negative control for GUS assay.....	71
Figure 3.6 35S promoter-GUS activity as a positive control for GUS assay	72
Figure 3.7 Histochemical localization of GUS activity in <i>AtMKK6</i> promoter:: <i>GUS</i> reporter plants through development from 3 days to 35 days.	73
Figure 3.8 Detailed examination of 10-day old seedlings of <i>AtMKK6</i> promoter:: <i>GUS</i> reporter plants.	75
Figure 3.9 Histochemical localization of GUS activity in <i>AtMPK13</i> promoter:: <i>GUS</i> reporter plants through development from 3 days to 35 days.	77
Figure 3.10 Schematic illustration showing the location of the putative auxin-responsive sequence AuxREPSIAA4 in the <i>AtMKK6</i> promoter region (740 bp).....	78
Figure 3.11 NPA effect on lateral root formation in 17-day-old wild-type <i>Arabidopsis</i> seedlings.....	80
Figure 3.12 NPA (5 μ M) effect on GUS activity in 10-day-old <i>AtMKK6</i> promoter:: <i>GUS</i> reporter seedlings.	81
Figure 3.13 Histochemical localization of GUS activity in lateral root primordia (LRPs) and lateral roots of <i>AtMKK6</i> promoter:: <i>GUS</i> reporter seedlings, upon NPA (5 μ M) treatment and co-treatment of NPA (5 μ M) and IAA (1 μ M).	84
Figure 3.14 Schematic illustration showing the location of two putative auxin-responsive sequences AuxRR-core in the <i>AtMPK13</i> promoter region (1534 bp).....	85
Figure 3.15 Histochemical localization of <i>AtMPK13</i> promoter:: <i>GUS</i> activity in LRPs and lateral roots from 13-day-old reporter seedlings, upon treatment of NPA alone (5 μ M) and co-treatment of NPA (5 μ M) and IAA (1 μ M).	86
Figure 3.16 RT-PCR analysis showing a ~23% reduction in the <i>AtMKK6</i> transcript level in 10-day-old <i>AtMKK6RNAi</i> seedlings (line 13) when the gene silencing was induced by 1 μ M dexamethasone (dex) treatment as compared to that without dex treatment (control).....	88
Figure 3.17 Phenotypic analyses revealed growth defects of <i>AtMKK6RNAi</i> plants.....	90
Figure 3.18 Close-up views of phenotypes from <i>AtMKK6RNAi</i> plants when.....	91
Figure 3.19 <i>AtMKK6RNAi</i> showed ectopic root hairs, when induced by 1 μ M dex	92
Figure 3.20 <i>AtMKK6RNAi</i> and <i>AtMPK13RNAi</i> showed reduction of lateral root number when RNAi silencing was induced by 1 μ M dex.	93
Figure 4.1 Dicot leaf anatomy	100
Figure 4.2 <i>Arabidopsis</i> stomatal development (Nadeau and Sack, 2002b)	101
Figure 4.3 Stomatal clusters in <i>too many mouths</i>	102

Figure 4.4 Developmental basis of stomatal cluster formation in <i>tmm</i> (Nadeau and Sack, 2002b)	103
Figure 4.5 Paired stomata in <i>four lips</i> (Nadeau and Sack, 2002b)	106
Figure 4.6 Guard cell function: stomatal opening and closing	108
Figure 4.7 Salt stress responses in plants and pathways that interconnect them.	111
Figure 4.8 Diagram of the SOS pathway for plant Na ⁺ response, from Zhu, J-K (2000)....	113
Figure 4.9 Salt stress activates several protein kinase pathways, the SOS3-SOS2 kinase pathway, multiple MAPK pathways and other protein kinases e.g. ATHK1, ASK1 and ATGSK1. Modified from (Zhu, 2001a).....	114
Figure 4.10 Diagram of SALK T-DNA verification primer design and PCR product size..	121
Figure 4.11 <i>AtMPK12</i> promoter-GUS activity survey throughout plant development	125
Figure 4.12 Histochemical localization of GUS activity in <i>AtMPK12</i>	130
Figure 4.13 Transverse section of leaf from the <i>AtMPK12</i> promoter:: <i>GUS</i> reporter plant. .	131
Figure 4.14 NaCl causes an increase in GUS activity of the <i>AtMPK12</i> promoter:: <i>GUS</i>	133
Figure 4.15 NaCl causes an increase in GUS activity in leaf guard cells.....	134
Figure 4.16 Mannitol (5%) causes an increase in GUS activity of the <i>AtMPK12</i> promoter:: <i>GUS</i> reporter seedlings.	135
Figure 4.17 PCR screening of <i>AtMPK12</i> T-DNA insertional lines (SALK-074849).....	136
Figure 4.18 Phenotypic analysis of wild-type and <i>atmpk12</i> mutant plants on growth.....	138

LIST OF ABBREVIATIONS

2ip	6-(γ,γ -dimethylallyl-amino) purine
ABA	abscisic acid
AAPK	abscisic acid-activated protein kinase
ACC	aminocyclopropane-1-carboxylic acid
ACS	1-aminocyclopropane-1-carboxylic acid synthase
ANP1/2/3	<i>Arabidopsis</i> NPK1-like protein kinases 1, 2 and 3
At	<i>Arabidopsis thaliana</i>
AtNHX1	<i>Arabidopsis thaliana</i> sodium proton exchanger 1
CTR1	constitutive triple response 1
DEPC	diethyl pyrocarbonate
dex	dexamethasone
EDR1	enhanced disease resistance 1
ERK	extracellular signal-regulated kinase
FLP	four lips
GCR1	G protein-coupled receptor
GPA1	G protein α subunit
GUS	β -glucuronidase
GMC	guard mother cell
IAA	indole-3-acetic acid
LRP	lateral root primordia
M	meristemoid
MAPK (or MPK)	mitogen-activated protein kinase
MAPKK (or MKK or MEK)	mitogen-activated protein kinase kinase
MAPKKK (or MKKK or MEKK)	mitogen-activated protein kinase kinase kinase
MBP	myelin basic protein
MEK	MAPK/ERK kinase
MIPS	Munich Information Centre for Protein Sequences
MMC	meristemoid mother cell
MMK3	<i>Medicago</i> MAPK 3
MPSS	Massively Parallel Signature Sequencing
MS	Murashige and Skoog
NAA	naphthalene acetic acid
NACK1/2	<i>Nicotiana tabacum</i> protein kinase1 activating kinesin-like proteins 1 and 2
NC	neighbour cell or sister cell
NPA	N-1-naphthylphthalamic acid
NPK1	<i>Nicotina</i> protein kinase 1
Nt	<i>Nicotiana tabacum</i>
NtF6	<i>Nicotina tabacum</i> FUS3-like kinase 6
OMTK	Oxidative stress-activated MAP triple-kinase
Os	<i>Oryza sativa</i>
OST1	open stomata 1
PIN	pin-formed
RNA	ribonucleic acid

RT-PCR	reverse transcriptase-polymerase chain reaction
RNAi	RNA interference
SAMK	stress-activated MAP kinase
SDD1	stomatal density and distribution 1
SIMK	salt-induced MAP kinase
SIMKK	SIMK kinase
SIPK	salicylic acid-induced protein kinase
SM	satellite meristemoid
SOS	salt overly sensitive
TMM	too many mouths
WIPK	wound-induced protein kinase
X-Gluc	5-bromo-4-chloro-3-indolyl- <i>beta</i> -D-glucuronic acid, cyclohexylammonium salt

ACKNOWLEDGEMENTS

It has been a terrific intellectual journey. I have had a great experience during my Ph.D. study at UBC with good support and many good people around me. I would like to thank my supervisor, Dr. Brian Ellis, for his scientific guidance and ongoing support. Brian has been the ideal research supervisor for me. He has provided me with excellent guidance, enough space to work independently and a good scientific environment. It has been a privilege to work with an inspirational scientist like Brian.

I would also like to thank my supervisory committee members Dr. James Kronstad, Dr. George Haughn and Dr. Steven Pelech for their scientific advice, encouragement and feedback, especially at the beginning of my Ph.D. They gave me useful guidance at the critical step of my study on how to choose a good research project. I truly appreciate their advice on my work.

Thank you to the chair of my Ph.D. examining committee, Dr. Roy Turkington, the university examiners, Dr. Carl Douglas and Dr. Geoffrey Wasteneys and the external examiner, Dr. Daphne Goring (Department of Botany, University of Toronto) for their time to review my thesis and provide me with comprehensive feedback.

Thanks to Jochen Brumm, my partner who knows my MAPK project very well by now, for his support, scientific discussion, feedback and encouragement for doing good work.

Thanks to Liew, Cherdasak Liewlaksaneeyanawin, for his assistance with my PhD thesis preparation, scientific discussion and friendship.

Thanks to Minako Kaneda for her expert assistance with the preparation of root sections.

Thanks to Dr. Lacey Samuels for the microscope facility, David Kaplan for the green house facility and Sylvia Leung for chemical ordering.

Thanks to Ellis' lab members, Dr. Godfrey Miles, Dr. Marcus Samuel, Dr. Michiyo Matsuno, Dr. Rishi Gill, Alana Clegg, JinSuk Lee, Hardy Hall, Corinne Cluis, Greg Lampard, Ankit Walia and Alexander Lane for sharing the graduate school experience with me and support me in many ways.

Thanks to the directed study students, Raymond Yu and Janet Chung and also thanks to the volunteering students, Vanessa Chan and Kenny Wong for their assistance on my research project.

Thanks to my UBC friends, postdocs and staff from the Department of Botany, Agricultural Sciences and Michael Smith Laboratories and Thai friends for their support during my Ph.D. time.

Thanks to the Natural Science and Engineering Research Council (NSERC) of Canada and the Institute for the Promotion of Teaching Science and Technology (IPST) of Thailand for generous research and educational funding.

Thanks to everyone in my family, especially my grandparents and my parents who always supported me for doing my Ph.D.

CHAPTER 1

MAPK Gene Family in Plants

1.1 Introduction

MAPK (mitogen-activated protein kinase) signaling modules play a central role in transduction of extracellular stimuli and developmental signals into cellular responses in eukaryotic cells (Widmann *et al.*, 1999; Ligterink and Hirt, 2001; Pearson *et al.*, 2001). The first mammalian MAPK was discovered by its ability to phosphorylate microtubule-associated protein 2 (MAP-2) *in vitro* upon a growth factor insulin treatment, and was named MAP-2 kinase (Ray and Sturgill, 1987). MAP-2 kinase was renamed a “mitogen-activated protein kinase” (Rossomando *et al.*, 1989) when it was found to be tyrosine phosphorylated upon stimulation of cells by a variety of mitogens (Cooper *et al.*, 1982; Rossomando *et al.*, 1989). This mammalian MAPK gene was cloned and found to have high homology to previously identified yeast kinases FUS3 and KSS1 (Courchesne *et al.*, 1989; Boulton *et al.*, 1990; Elion *et al.*, 1990). Since this MAPK was not only activated by mitogens, but also by many other stimuli, it was also designated ERK1, for extracellular signal-regulated kinase 1 (Boulton *et al.*, 1990). One hallmark of the MAPK and FUS3/KSS1 kinases was their ability to phosphorylate myelin basic protein, and hence the term “MBP kinases” is sometimes used to refer to this group of kinases. Soon afterward, two MAPK activators were identified, based on their ability to phosphorylate MBP kinases upon growth factor stimulation of cells (Ahn *et al.*, 1991). The MAPK activators were shown to phosphorylate MAPK, indicating that they were indeed upstream protein kinases (Seger *et al.*, 1992). One MAPK activator was cloned and named MEK1 for MAPK / ERK kinase 1, and it was found to be activated

through phosphorylation. (Crews *et al.*, 1992; Crews and Erikson, 1992). After the identification of MEKs, the MEK activators, Raf-1 and MEKK1 were identified (Kyriakis *et al.*, 1992; Lange-Carter *et al.*, 1993). The first indication of an evolutionarily conserved structure for MAPK cascades came from the finding that mammalian MEKK1 and MEK had high homology to the yeast protein kinases STE11 and STE7, respectively, which function upstream of yeast MAPKs, FUS3 and KSS1 (Lange-Carter *et al.*, 1993).

This module architecture, in which activated MAPKKKs (MEKKs) phosphorylate, and thus activate, target MAPKKs (MEKs), which in turn activate MAPKs, has been described in taxa as diverse as yeasts, worms, flies and mammals (Widmann *et al.*, 1999). Sequencing of these genomes has also revealed that the three classes of MAP kinases (MAPKKKs, MAPKKs and MAPKs) always occur as gene families. Functional analysis, which is most advanced in yeast, has demonstrated that despite their structural conservation over evolutionary time, individual gene family members generally play distinct roles, although some degree of functional redundancy is also observed (Herskowitz, 1995; Gustin *et al.*, 1998a).

In the simplest model, MAPK cascades can be viewed as linear information transmission systems. However, biochemical and genetic evidence suggests a more complex module organization in which kinases at one level within the cascade can be activated by more than one upstream effector and can, in turn, act upon more than one target (Cardinale *et al.*, 2002). When combined with the availability of multiple related kinases at each level, and the interaction with modifying proteins such as scaffolds (Pearson *et al.*, 2001; Nakagami *et al.*, 2004) and protein phosphatases (Gupta *et al.*, 1998; Meskiene *et al.*, 2003), this complexity creates a remarkably versatile matrix of signaling capacities.

1.2 Roles of MAPK pathway components in plants

Our knowledge of signal transduction in plants is less well developed than in other phyla, but there is considerable evidence for broad conservation of signalling architecture between plants and other eukaryotic organisms. Over the past decade, a number of plant-signalling components have been isolated. Homologues of heterotrimeric G proteins, phospholipid modifiers, protein phosphatases, receptor kinases, two-component histidine kinases and various other classes of protein kinases have been identified in plants including members of the MAPKKK, MAPKK and MAPK families (Mizoguchi *et al.*, 1997; Ichimura *et al.*, 1998a). MAPKs are proposed to be one of the convergence points in the stress- or defense-signalling network in plants (Zhang and Klessig, 2001).

The regulation of MAPK pathway components occurs at multiple levels, including transcriptional, post-transcriptional, translational and post-translational levels. Evidence for transcriptional regulation of plant MAPK cascade genes has been provided through observed differences in their expression in different organs, tissue and/or cell-types, as well as expression changes induced by extracellular stimuli (Ligterink and Hirt, 2001; Zhang and Klessig, 2001). An example of post-transcriptional regulation is the report of differential splicing of a single *Arabidopsis* NPK1-related protein kinase 1 (ANP1) gene, which has a high homology to *Nicotiana* protein kinase 1 (NPK1) gene, giving rise to two species of ANP1 transcripts, ANP1L and ANP1S. The activity of ANP1S was greater than that of ANP1L, suggesting that this molecular mechanism might be involved in modulating the activity of this protein kinase (Nishihama *et al.*, 1997). At the translational level, changes of MAPK protein levels in response to pathogenic stimuli have been documented (Zwerger and Hirt, 2001). Post-translational regulation is, of course, central to regulation of MAPK cascades, since each level in the cascade is subjected to phosphorylation by its cognate

activator (Jonak and Hirt, 2002; Teige *et al.*, 2004). In addition, some plant MAPK species have been shown to interact with particular upstream kinases using yeast two-hybrid assays (Ichimura *et al.*, 1998b; Mizoguchi *et al.*, 1998; Kiegerl *et al.*, 2000), while genetic approaches such as transient or stable expression of transgenes have likewise demonstrated functional relationships among specific MAPKKs, MAPKKs and MAPKs. Beyond these better characterized examples, input stimuli of many types have been shown to alter the activation states of plant MAPKs, although the identity of the responsive kinase has not always been established (Morris, 2001; Zwerger and Hirt, 2001).

1.2.1 The role of MAPK pathways in stress signaling in plants

When exposed to an environmental stress, plants respond at many levels in an effort to maximize their chances of survival. MAPK pathways have been implicated in signal transduction in response to a broad variety of such stresses (Ligterink and Hirt, 2001; Tena *et al.*, 2001). In this chapter, the involvement of plant MAPKs in response to wounding, oxidative stress and chilling stress is reviewed.

1.2.1.1 Wounding signaling

Wounding in plants could be the outcome of physical injury, herbivore or pathogen attack. Wounding induces a wide variety of cellular responses, including up-regulation of genes involved in healing and defense and MAPK pathway genes have been implicated in these wound-responses. For example, in tobacco, a protein kinase activity of a 46 kDa protein was detected soon after cutting of the leaves (Usami *et al.*, 1995). This 46 kDa protein was proposed to be a MAPK since (1) it could phosphorylate myelin basic protein (MBP), an artificial substrate of MAPK, (2) the active form of the kinase was phosphorylated on both

serine and/or threonine and tyrosine residue(s), and (3) it was shown to be inactivated through dephosphorylation. Transcripts of a tobacco MAPK, WIPK (wound-induced protein kinase) were shown to rapidly accumulate following wounding, a pattern that was correlated with a rapid increase in its protein activity, indicating that WIPK could be involved in the early stages of the response to the wound-stress (Seo *et al.*, 1995; Seo *et al.*, 1999). Similar to the tobacco WIPK, an alfalfa MAPK, SAMK (stress-activated MAP kinase), showed a rapid increase in its mRNA levels and protein activation following wounding (Bogre *et al.*, 1997). Another tobacco MAPK, SIPK (for salicylic acid-induced protein kinase), can also be activated post-translationally by wounding (Zhang and Klessig, 1998). Unlike WIPK, however, SIPK transcript levels were not significantly changed upon wounding. Interestingly, the expression and activation of WIPK appeared to be regulated by SIPK (Samuel and Ellis, 2002; Liu *et al.*, 2003). In *Arabidopsis*, another MAPK, AtMPK4, was shown to be activated by wounding as well as touch (Ichimura *et al.*, 2000). Besides the MAPKs, the *Arabidopsis* MAPKK, AtMEK1, has been shown to be involved in wound-response (Morris *et al.*, 1997).

1.2.1.2 Oxidative stress signaling

When exposed to oxidative challenge, plants have to cope with increased potential for damage resulting from oxidation of proteins, lipids and nucleic acids (Baier *et al.*, 2005). Oxidative stress in plants can be a result of the oxidative burst, a rapid release of reactive oxygen species (ROS) in plant tissues upon pathogen attack (Mehdy, 1994; Bolwell, 1996). The ROS, rapidly produced in plant cells following the perception of a range of stress signals include superoxide anion (O_2^-), hydrogen peroxide (H_2O_2) and hydroxyl radical (OH^\cdot) (Desikan *et al.*, 1996). Besides pathogen-induced stress, abiotic stresses including ozone

exposure, UV-irradiation, wounding and mechanical stresses can induce a rapid oxidative burst (Green and Fluhr, 1995; Yahraus *et al.*, 1995; Schraudner *et al.*, 1996; Huang *et al.*, 2004; Le Deunff *et al.*, 2004). MAPK pathway genes have been implicated in signaling role(s) in oxidative stress responses. For example, AtMPK3 and AtMPK6 have been shown to be activated by H₂O₂ (Kovtun *et al.*, 2000), as has the alfalfa MAPKKK, OMTK1 (oxidative stress-activated MAP triple-kinase 1) (Nakagami *et al.*, 2004). Ozone-generated ROS can induce SIPK activation in association with lesion formation in tobacco plants, and both gain-of-function and loss-of-function modification of SIPK were shown to render the transgenic tobacco plants increasingly sensitive to ROS stress (Samuel *et al.*, 2000; Samuel and Ellis, 2002).

1.2.1.3 Low temperature stress signaling

MAPK pathway genes have been implicated in signaling in response to low temperature stress. For example, *Arabidopsis* AtMEKK1 and AtMPK3, and alfalfa SAMK, showed increased accumulation of transcripts upon exposure to low temperature (Jonak *et al.*, 1996; Mizoguchi *et al.*, 1996). The *Arabidopsis* MAPKKK, AtMAP3K β 3, also showed transcriptional up-regulation upon cold treatment (Jouannic *et al.*, 1999). In contrast, the maize MAPKK, ZmMEK1, which is expressed in meristematic regions of growing plants, showed a decrease in its transcription level upon cold treatment of roots (Hardin and Wolniak, 1998).

1.2.2 The role of MAPK pathways in plant development

1.2.2.1 Cell cycle and cytokinesis in plants

MAPKs have been shown to be involved in regulation of many cell cycle events in yeasts and animals (Pages *et al.*, 1993; Takenaka *et al.*, 1997; Gustin *et al.*, 1998b; Brunet *et al.*, 1999) and evidence for similar roles in plants is beginning to appear. Plant MAPKs have been implicated in the cell cycle or cell-cycle entry based on expression correlated with specific cell-cycle stages and on gene expression and/or kinase activity in proliferating tissues. For example, transcript levels of SIMKK were low in the G1 phase in alfalfa cell cultures but increased during S and G2 phases. The alfalfa MAPK, MMK3, and its tobacco homologue, NtF6 (for *Nicotina tabacum* FUS3-like kinase 6), have been shown to be activated in a cell cycle-specific manner. These kinases were shown to become active specifically in anaphase and telophase of the cell-cycle (Calderini *et al.*, 1998; Bogre *et al.*, 1999). Importantly, MMK3 and NtF6 were shown to have a role in cytokinesis during mitosis. These kinases were immunolocalized at the phragmoplast in late anaphase, and remained localized to the cell plate during telophase.

Besides MAPKs, MAPKKKs have been shown to be involved in cell division in plants. For example, the tobacco MAPKKK, NPK1 was actively expressed in suspension cultured cells (Banno *et al.*, 1993) and in meristematic and developing tissues (Nakashima *et al.*, 1998). NPK1 transcripts also increased upon induction of cell proliferation (Nakashima *et al.*, 1998). The ANP1, ANP2 and ANP3 were also preferentially expressed in proliferating tissues (Nishihama *et al.*, 1997). In addition, NPK1 protein and mRNA were abundant from S to M phases during the cell cycle (Nishihama and Machida, 2000) and this protein is associated with cell-plate formation during cytokinesis (Nishihama *et al.*, 2001). NPK1 was

also shown to interact with the upstream components NACK1 and 2 (NPK1 activating kinesin-like proteins) in a yeast two-hybrid system (Ishikawa *et al.*, 2002). NPK1 and NACK1 were co-localized at the center of the phragmoplast, as was NtF6, a downstream component of NtMEK1, indicating the involvement of these proteins in a MAPK cascade NACK1-NPK1-NtMEK1-NtF6 associated with cell-plate formation (Zwerger and Hirt, 2001; Takahashi *et al.*, 2004). Takahashi *et al.* (2004) have adopted a different nomenclature for these genes; they use NQR1 for NtMEK1, and NRK1 for NtF6.

1.2.2.2 Cell-type specific development:

MAPKs appear to be involved in regulating the growth and differentiation of various plant organs, including pollen grains, root hairs, embryo, and stomata. Specific examples of these associations are discussed below.

Pollen development:

A few MAPK members have been implicated in pollen development. For example, Ntf4 is involved in the process of pollen germination in tobacco. Ntf4 transcripts were restricted to pollen (Voronin *et al.*, 2001), and were actively synthesized at the late stages of pollen development. NTF4 protein activation occurred after hydration of dry pollen grains, but prior to pollen tube growth (Wilson *et al.*, 1997). SIPK, the tobacco MAPK most closely related to Ntf4, was also expressed in pollen and was activated upon pollen hydration (Voronin *et al.*, 2004). The tobacco MAPKK, NtMEK2, was shown to activate both SIPK (Yang *et al.*, 2001) and NtF4 (Voronin *et al.*, 2004). Tobacco plants expressing a loss-of-function version of NtMEK2 exhibited inhibition of germination in the transformed pollen grains suggesting that NtMEK2 may be required for pollen germination, as would be predicted if NtMEK2 is the

cognate MAPKK for NTF4 and SIPK. In addition, the tobacco MAPKs, Ntf3 and Ntf6, were found to be expressed in pollen (Wilson *et al.*, 1993; Wilson *et al.*, 1997; Prestamo *et al.*, 1999).

Stomatal and early embryo development:

To date, the *MAPKKK* gene, *YODA* (*YDA*) is the only member of the plant MAPK gene family known to have a role in stomatal development. *Arabidopsis yda* mutants form clusters of guard cells in the epidermis of the cotyledons, instead of the usual spatial distribution. Loss-of-function mutations in *YODA* led to formation of excessive numbers of guard cells, while constitutive activation of *YDA* produced plants that completely lacked guard cells (Bergmann *et al.*, 2004). Together these results indicate that *YDA* acts as a cell-fate switch, and has a negative role in stomatal guard cell development in *Arabidopsis*.

In addition to stomatal development, *YDA* was suggested to regulate the first cell-fate decision in embryogenesis (Lukowitz *et al.*, 2004). The loss-of-function *YDA* mutant zygotes were impaired in elongation and the gain-of function *YDA* mutants displayed suppressed embryonic development. However, other components in a *YDA*-containing MAPK cascade remain to be discovered.

1.2.3 The role of MAPK pathways in plant hormone signaling

Plant hormones play important roles in both developmental processes and stress-related responses, and it is therefore not surprising to find evidence for involvement of MAPK pathways in plant hormone signaling. In this section, evidence for MAPK signaling associated with plant hormone regulation is reviewed.

1.2.3.1 Auxin

The plant hormone auxin regulates many growth and development processes including apical dominance, lateral root formation, root hair formation and vascular tissue differentiation (Hobbie and Estelle, 1994; Abel and Theologis, 1996). The initial indications for a role of protein kinases and/or phosphatases in auxin signaling came from experiments in soybean plants and pea epicotyl segments, which demonstrated an effect of auxin on overall protein phosphorylation patterns (Reddy *et al.*, 1987; Poovaiah *et al.*, 1988). Mizoguchi and co-workers (1994) first reported specific involvement of a MAPK in auxin signal transduction. They demonstrated that auxin-starved tobacco BY-2 cells treated with the synthetic auxin, 2,4-dichlorophenoxyacetic acid (2,4-D) displayed rapid and transient activation of 46 kDa protein kinase that was capable of using myelin basic protein (MBP) as a substrate. The tobacco MAPKKK, NPK1, was subsequently reported to be transcriptionally up-regulated following auxin treatment (Nakashima *et al.*, 1998). However, the ectopic expression of tobacco NPK1 in maize protoplasts was able to inhibit auxin-induced gene expression, indicating that this kinase might negatively regulate auxin responses (Kovtun *et al.*, 1998). In *Arabidopsis* protoplasts, constitutively active ANP1, ANP2 and ANP3 were shown to suppress the auxin-responsive promoter, GH3, indicating that ANPs may be a functional orthologue of the tobacco NPK1 (Kovtun *et al.*, 2000).

1.2.3.2 Absciscic acid

Absciscic acid (ABA) plays a role in a wide variety of physiological processes in plants, including seed maturation and germination, stomatal regulation and responses to abiotic stresses including dehydration, high salt, osmotic stress and low temperature (Leung and Giraudat, 1998). Protein kinase signaling appears to be integral to ABA regulatory processes.

Two protein phosphatases belonging to the type 2C (PP2Cs) class (Leung *et al.*, 1997) (ABI1 and ABI2) were shown by mutational analysis to be involved in regulation of germination, stomatal closure and root growth, and both kinase and phosphatase inhibitors were shown to block ABA-mediated expression of a dehydrin gene in pea (Hey *et al.*, 1997). A specific serine/threonine protein kinase, AAPK (for ABA-activated protein kinase) has been found to be involved in Ca^{2+} -independent ABA signaling in guard cells of fava bean (Li and Assmann, 1996).

MAPKs have also been implicated in ABA signaling. In barley aleurone protoplasts, ABA induced a rapid and transient activation of MAPK activity, which was identified by cross-reaction with a phospho-ERK1-specific antibody (Knetsch *et al.*, 1996). A tyrosine phosphatase inhibitor, phenylarsine oxide (PAO), was able to block this MAPK activation, and also blocked ABA-induced gene expression (Knetsch *et al.*, 1996). Besides ABA signaling, MAPKs have been implicated in activating ABA biosynthesis.

1.2.3.3 Ethylene

The gaseous plant hormone, ethylene (C_2H_4), serves as an important regulator of plant physiological processes including fruit ripening, leaf and flower senescence, leaf abscission, and sex determination, as well as defense responses to various stresses and pathogen attack (Johnson and Ecker, 1998).

The first evidence of a role for protein phosphorylation in ethylene signaling came from the work of Raz and Fluhr (1993), who showed that rapid protein phosphorylation was induced upon ethylene treatment of tobacco leaves. The general kinase inhibitor K252a was able to block both this protein's phosphorylation and the ethylene-induced physiological responses.

MAPKs have been specifically implicated in ethylene signal transduction in plants. Mutational analysis showed that CTR1 (constitutive-triple-response1), which encodes a protein with high homology to Raf-like MAPKKK, negatively regulates ethylene responses (Kieber *et al.*, 1993). Ouaked and co-workers (2003) identified four ethylene-activated protein kinases, including one alfalfa MAPKK (SIMKK), two alfalfa MAPKs (SIMK and MMK3), as well as one *Arabidopsis* MAPK (AtMPK6). These protein kinases were proposed to act downstream of CTR1 in a MAPK cascade because transgenic *Arabidopsis* plants ectopically over-expressing SIMKK exhibited constitutive AtMPK6 activation, and also displayed a triple response similar to the *Arabidopsis ctr1* mutant in the absence of aminocyclopropane-1-carboxylic acid (ACC-a precursor of ethylene biosynthesis). In addition, MMK3 and SIMK exhibited rapid activation within five minutes of treatment with ACC. However, Liu and Zhang (2004) recently showed compelling evidence that AtMPK6 was not involved in ethylene signalling, but rather was involved in regulating the ethylene biosynthesis pathway. They reported that AtMPK6 was required for ethylene induction in this transgenic system, and found that selected isoforms of 1-aminocyclopropane-1-carboxylic acid synthase (ACS), the rate-limiting enzyme of ethylene biosynthesis, are substrates of AtMPK6. Furthermore, they reported that phosphorylation of ACS2 and ACS6 by AtMPK6 led to the stabilization and accumulation of ACS protein and, therefore, increased levels of cellular ACS activity and ethylene production.

1.3 MAP kinase pathway components in *Arabidopsis*

Current data collectively implicate MAPK modules as important components of signal transduction in plants, but the full scope and centrality of their participation remains unclear. The sequencing of the *Arabidopsis* genome in 2001 allowed, for the first time, the description

of the full complement of MAPK-encoding genes in a plant (MAPK Group, 2002). In *Arabidopsis*, more than 80 MAPKKK, at least 10 MAPKK and 20 MAPK homologues have been identified (Table 1.1). This analysis revealed that this model plant genome encodes more members of each level of MAPK cascades than any other eukaryotic species examined to date, indicating that higher plants may have evolved to place a greater reliance on this signaling modality than have other kingdoms. However, this is difficult to evaluate, since only fragmentary information is available concerning the functionality of the MAPK components encoded in the *Arabidopsis* genome.

Screens for mutant phenotypes have identified a small number of AtMKKK genes that play important roles in specific physiological responses, including AtCTR1 (Kieber *et al.*, 1993) and AtEDR1 (Frye *et al.*, 2001). Double-mutant combinations have revealed the roles of ANP family of *Arabidopsis* MAPKKKs in cell division and growth (Krysan *et al.*, 2002). Yeast two-hybrid screens and yeast mutant complementation analysis have provided some initial insight into the roles played by the MAPK kinase kinases, AtMEKK1 (Ichimura *et al.*, 1998b), and AtANP1, 2 and 3 (Nishihama *et al.*, 1997). The functions of the great majority of the 80+ AtMAPKKKs, however, remain a mystery. Interestingly, despite the extensive mutant screening carried out in *Arabidopsis* over the last two decades, only one MAPK mutant, *Arabidopsis mpk4* (Petersen *et al.*, 2000) and a small number of MAPKKK mutants such as *edr1* and *ctr1* (Kieber *et al.*, 1993; Frye *et al.*, 2001) have been discovered, based on phenotype. This may mean that most deficiency phenotypes are subtle and/or growth-stage specific, or that sufficient redundancy exists within the MAPK gene families to

Table 1.1 List of *Arabidopsis* MAPK signalling components, adapted from Jonak *et al.* (2002)

Common Name	Number*	Group	Number*	Name members
MAPK	20	A	3	MPK3/6/10
		B	5	MPK4/5/11/12/13
		C	4	MPK1/2/7/14
		D	8	MPK8/9/15/16/17/18/19/20
MAPKK	10	A	3	MKK1/2/6
		B	1	MKK3
		C	2	MKK4/5
		D	4	MKK7/8/9/10
MAPKKK	80	MEKK-like	21	MEKK1, ANP1-3, MAP3K ϵ 1
		ZIK	11	ZIK1
		Raf-like	48	EDR1, CTR1
MAPKKKK	10	Ste20/PAK-like	10	-

* As predicted by analysis of the *Arabidopsis* genome

suppress a deficiency phenotype. Alternatively, homozygous recessive mutants may not be readily recovered due to the severity of the deficiency.

Routing within the *Arabidopsis* MAPK cascades, as in other taxa, appears to be constricted at the MAPKK level, where only ten family members occur, before expanding again to engage twenty downstream MAPKs. This pattern indicates that multiple cascade signal inputs could be converging upon the MAPKKs, which must then integrate and distribute those signals to the appropriate suite of downstream targets, most likely specific MAPKs or subsets of MAPKs. The activities and specificities of MAPKK family members are thus of particular interest.

Among the AtMKKs, stress response functions have been ascribed to AtMKK1 and 2, which can activate AtMPK4 (Huang *et al.*, 2000), and to AtMKK4 and 5, which have been shown to be able to activate AtMPK3 and 6 (Asai *et al.*, 2002). MKK2 (AtMKK2) is

involved in mediating cold and salt stress tolerance in plants (Teige *et al.*, 2004). AtMKK2 has been shown to be activated by cold and salt stress and by the stress-induced MAPK kinase kinase MEKK1, and to directly target MPK4 and MPK6 in yeast two-hybrid, *in vitro*, and *in vivo* protein kinase assays. Accordingly, plants overexpressing MKK2 exhibited constitutive MPK4 and MPK6 activity, constitutively upregulated expression of stress-induced marker genes, and increased freezing and salt tolerance. In contrast, *mkk2* null plants were impaired in MPK4 and MPK6 activation and were hypersensitive to salt and cold stress. AtMKK6 (or ANQ1) appears to be actively involved in regulation of cell plate formation during cell division (Soyano *et al.*, 2003). There is no information available concerning the behavior or function of the remaining five AtMKKs.

At the MAPK level, a large family of kinases is available to transmit signals from the various MAPK modules to appropriate targets within the cell. The twenty AtMAPKs cluster into four discrete structural classes (MAPK Group, 2002), and within a cluster the protein sequences show strong similarity. Nevertheless, even closely related AtMAPKs such as AtMPK3, 4 and 6, appear to play different biological roles. For example, AtMPK4 function has been shown to be essential for proper growth and development (Petersen *et al.*, 2000), while loss-of-function mutants of AtMPK3 or AtMPK6 do not display any obvious morphological phenotype (X. Li, personal communication). *atmpk4* mutants are also affected in regulation of systemic acquired resistance (SAR) during the plant's response to pathogen attack (Petersen *et al.*, 2000), but the biochemical connection between growth regulation and modulation of SAR remains unresolved. AtMPK3 and AtMPK6 also rapidly respond to recognition of an incompatible pathogen (Asai *et al.*, 2002) but the interplay, if any, between these activation events and the negative regulation by AtMPK4 of the subsequent appearance of SAR has not been determined. AtMPK3 and AtMPK6, as well as AtMPK4, are also

rapidly activated by a number of other biotic and abiotic stresses (Mizoguchi *et al.*, 1996; Ichimura *et al.*, 2000; Kovtun *et al.*, 2000; Nuhse *et al.*, 2000; Desikan *et al.*, 2001; Yuasa *et al.*, 2001; Droillard *et al.*, 2002; Zhang *et al.*, 2002), including the downstream signaling induced by binding of the bacterial elicitor, flagellin, to the *Arabidopsis* FLS2 transmembrane receptor (Asai *et al.*, 2002). AtMPK13 (ANR1) appears to be involved cell plate formation during cytokinesis (Soyano *et al.*, 2003) but its targets and specific function are unknown. Little is known about the expression of the remaining seventeen AtMPKs, or about their biological roles. Thus, while mutant screens and similar gene-by-gene approaches have provided some valuable insights, definition of the full potential for signal transduction through MAPK cascades in *Arabidopsis* requires a more systematic analysis.

1.4 Thesis objectives

The general objective of this study was to gain further insight into the biological role of the MAPK gene family in plants, and how these kinases are organized into a signaling network. *Arabidopsis* was used as the biological system because of its rich cell physiology and genetic resources, as well as the full description of its MAPK gene family derived from the genome sequence. These resources make it possible to link genes and their possible biological function(s) based on gene expression patterns and correlations with physiological /developmental events in *Arabidopsis* plants. Manipulations of gene expression can then be used to confirm hypotheses based on those correlation patterns.

Specific objectives:

- I. Systematic expression analyses of the complete array of *AtMPK* and *AtMKK* genes, using reverse transcriptase (RT)-PCR with gene-specific primers. These data were used to select candidate genes with the most interesting expression pattern for further detailed functional characterization (Chapter 2).
- II. Functionally characterization of these candidate genes through two approaches; (1) histochemical localization of gene expression using gene-specific promoter::*GUS* reporter plants and (2) phenotypic analyses of transgenic or mutant plants in which expression of the candidate genes has been modified. The candidate genes chosen from expression profiling (objective 1) were *AtMKK6* and *AtMPK13* (described in Chapter 3) as well as *AtMPK12* (Chapter 4).

CHAPTER 2

MAPKK/MAPK Expression Profiling in *Arabidopsis*

2.1 Introduction

In this chapter, I have systematically explored the expression of the entire identified *Arabidopsis* MAPK gene family members for *AtMKK* and *AtMAPK* genes. There were two aims to this study. First, I wanted to develop an overview of the transcription activity of these thirty genes during growth and development of *Arabidopsis* plants, as well as in response to a limited set of relevant stresses. My second aim was to identify interesting individual candidate genes for further detailed functional characterization. I anticipated that the expression survey might also reveal examples of co-expression patterns of discrete genes in specific organ/tissue types or developmental stages. This could implicate their possible biochemical function in the same cascade.

The *Arabidopsis* MAPK gene family members encoded in the genome have been previously identified and grouped based on their putative amino acid sequences (MAPK Group, 2002). This study also assembled the limited data regarding function for both the *Arabidopsis* genes and their orthologs from other plant species. In addition, another studies assembled the available information on their biochemical properties (phosphorylation and physical interaction) (Ichimura *et al.*, 1998b). Sequence alignment placed the putative AtMKKs into four groups (A-D), and the AtMPKs also into four groups (A-D) (MAPK Group, 2002 and Figure 2.1). The phylogenetic grouping of the putative AtMKKs and AtMPKs, when considered together with the limited functional information, indicates that these groups may represent broad function-related modules (groups). The first such module

consists of group A MAPKKs and group B MAPKs, since some members of both groups appear to have functions associated with cell division. (In this thesis, I have referred to it as the cell-division module, see Figure 2.1). The second module consists of the group B MAPKK, AtMKK3, and group C MAPKs. In yeast two-hybrid assay, AtMKK3 was also shown to physically interact with AtMPK1, which is a member of group C MAPKs (Ichimura *et al.*, 1998b). There is very limited information on the function and gene expression for the gene members in this module. The third putative module consists of group C MAPKKs and group A MAPKs whose function was associated with stress response (referred to here as the stress response module). This proposed module is based on the knowledge that AtMKK4 and AtMKK5, members of group C MAPKKs were shown to activate AtMPK3 and AtMPK6, members of group A MAPKs. The fourth putative module consists of group D MAPKKs and group D MAPKs, whose members' function and gene expression are completely unknown. Overall, most of the *MAPK* gene family members in *Arabidopsis* remain uncharacterized and very little experimental data are available on their gene expression and biological function.

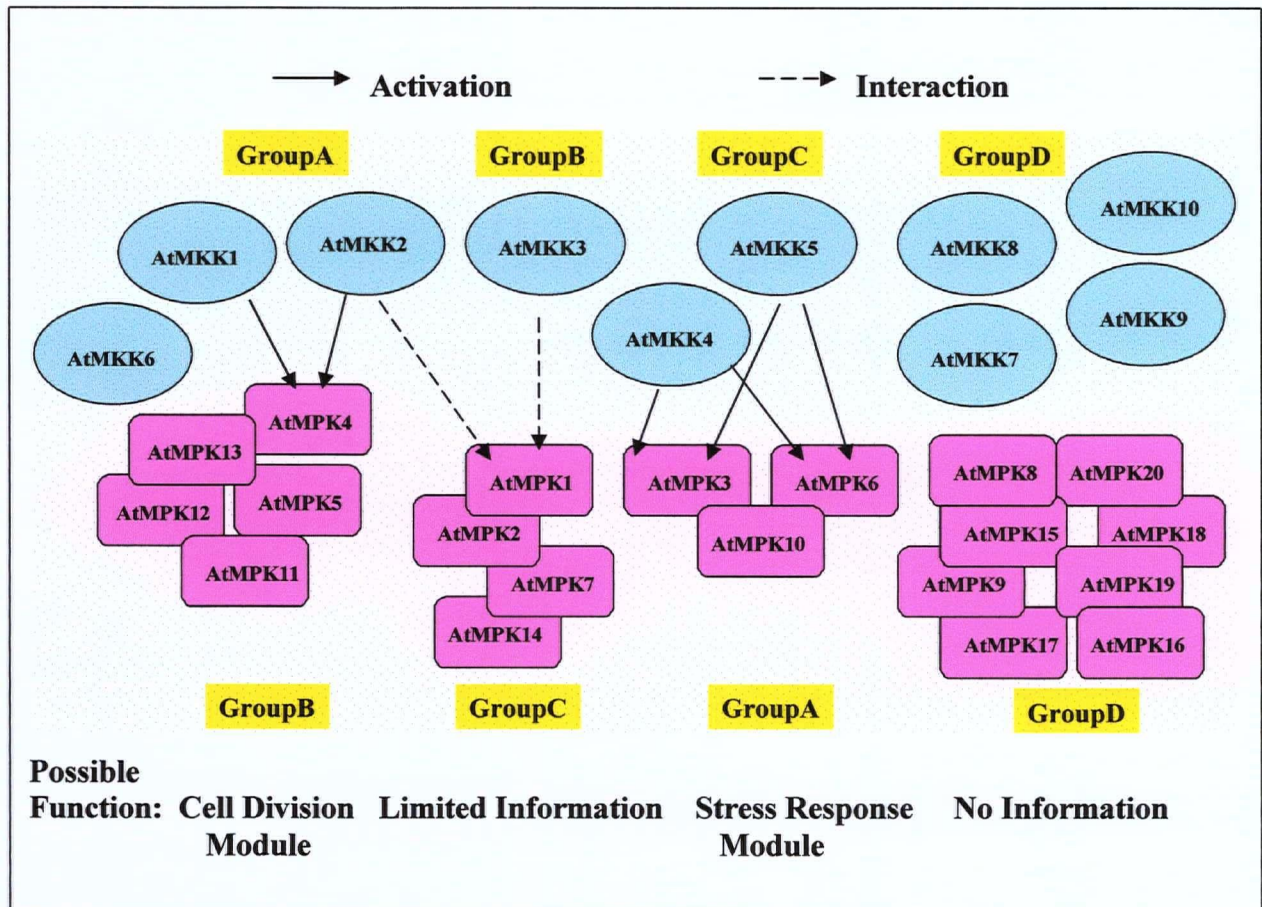


Figure 2.1 Grouping of the MAPKK and MAPK proteins

Phylogenetic grouping based on their putative amino acid sequences. The proposed functional grouping is based on functional and biochemical data for both *Arabidopsis* and orthologues from other species. This figure was adapted from MAPK Group (2002) and (1998b).

2.2 Materials and Methods

2.2.1 Plant materials and growth conditions

Unless indicated otherwise, *Arabidopsis thaliana* (Columbia ecotype, Col-0) was grown in soil at 22-24°C under a 16-hour photoperiod. Two sets of plants were prepared for parallel tissue collection, and were harvested separately for RNA extraction. All the tissue samples were harvested at the indicated time points. Tissues were harvested from 8-10 different plants at 15.00-17.00, pooled, immediately frozen in liquid nitrogen and stored at -80°C until further analysis.

Leaf tissues:

The rosette leaves of 21-day old plants were harvested.

Bolting stem tissues:

The bolting stems of 25-day old plants were harvested.

Flower bud tissues:

The flower buds of 25-day old plants were harvested.

Root tissues:

The *Arabidopsis* plants were grown hydroponically at 25°C under continuous light and the roots of 34-day old plants were harvested. The surface-sterilized seeds were sown on sterile rafts (Sigma M4417) floating on 100 mL of 0.5x MS (Murashige and Skoog) growth medium in Magenta boxes (6-8 seeds per box). The 0.5x MS growth liquid medium contained 0.5x MS salts (Invitrogen), 1x MS vitamins (Sigma M3900), 0.5% sucrose and 0.5 g/L MES. The medium pH was adjusted to 5.8 and autoclaved prior to use.

Callus tissues:

To generate callus, hypocotyls and leaf tissues from 3-week-old aseptically-grown plants were aseptically excised and cultured on callus-induction medium for 34 days. Callus induction medium contained 1x MS salts (4.3 g/L), 200 mg/L glycine, 1x vitamins, 10 μ M naphthalene acetic acid (NAA), 5 μ M 6-(γ,γ -dimethylallyl-amino) purine (2ip), 3% sucrose, 0.3% agar and 0.1% phytagel, pH 5.6. 1x vitamins contained 1 mg/L nicotinic acid, 1 mg/L pyridoxine.HCl, 1 mg/L calcium panthothenate, 1 mg/L thiamin.HCl, 0.01 mg/L biotin and 1 mg/L L-cysteine.HCl.

4-day old and 2-week old seedling tissues:

Surface-sterilized seeds were sown on $\frac{1}{2}$ x MS medium containing $\frac{1}{2}$ x MS salts, 1x MS vitamins (Sigma, Cat No. M3900), 0.5% sucrose and 0.5 g/L MES, 0.8% phytagar, pH 5.8. The seeds were kept at 4°C in petri dishes wrapped with micropore tape and kept in the dark for 2 days and then grown at 25°C under continuous light for either another 4 days or 2 weeks before the seedlings were harvested.

Secondary hypocotyl tissues:

Plants were grown in soil at 22-24°C and covered with plastic and aluminum foil during the first 10 days to induce long hypocotyls. After the plastic and aluminum foil were removed, the plants were grown in soil at 22-24°C under 16-hour photoperiod for 3 months before the secondary hypocotyls were harvested.

Leaf tissues from various developmental stages:

The plants were grown in soil at 22-24°C under 16-hour photoperiod. The rosette leaf tissue was harvested at 1-week, 2-week, 3-week, 4-week and 5-week stages.

2.2.2 Plant treatments

Two sets of plants were prepared for each treatment and each set was harvested separately for RNA extraction. The parallel control plants were grown under the same conditions and were harvested at the same time points, except that the control plants were not treated with ozone, were not wounded and were not shifted to chilling temperature. All rosette leaf samples were harvested from 8-10 individual plants, pooled, immediately frozen in liquid nitrogen and stored at -80°C until further analysis.

Ozone treatments:

The ozone treatments were performed by exposing 26-day-old plants to 300 ± 50 ppb ozone continuously for 8 hours in an ozone fumigation chamber. Ozone was generated with a Delzone ZO-300 ozone generating sterilizer (DEL Industries, San Luis Obispo, CA, USA) and monitored with a Dasibi 1003-AH ozone analyzer (Dasibi Environmental Corp., Glendale, CA, USA).

Wounding treatments:

The 26-day-old plants were cut 10 times with a blade on the left and right sides of each leaf, avoiding the mid vein. The leaf-wounded plants were allowed to stand for 8 hours before the wounded leaves were harvested.

Chilling treatments:

The 26-day-old plants were held at 5°C for 8 hours. The rosette leaves were then harvested.

2.2.3 Total RNA extraction

Total RNA extraction was performed using by TRIzol[®] Reagent according to the manufacturer's instructions. Total RNA was isolated using a modified TRIZOL extraction method. Approximately 1 g plant material was ground in liquid nitrogen using a mortar and pestle, re-suspended in 15 mL TRIZOL reagent (Invitrogen, Carlsbad CA, USA), vortexed and incubated at 65°C for 5 min with regular mixing. Cell debris was pelleted by centrifugation for 30 min at 12,000 g and 4°C and the supernatant was extracted with 3 mL chloroform. After centrifugation for 20 min at 12,000 g, the aqueous phase was recovered and RNA was precipitated at room temperature for 5 min with 0.5 volume 0.8 M sodium citrate and 0.5 volume isopropanol. After centrifugation for 30 min at 12,000 g, the pellet was washed with 70% ethanol and re-centrifuged. The RNA pellet was air dried for 5 min and re-suspended in 200 µl RNase-free water. Following a spectrophotometric determination of RNA concentration, the RNA was precipitated with 2.5 volumes of ethanol and a 1/10 volume of 3 M sodium acetate at -20°C overnight, and subsequently pelleted at 12,000 g for 30 min at 4°C. The precipitate was washed with 70% ethanol, re-centrifuged, air dried and re-suspended in RNase-free water to an approximate concentration of 1 µg RNA/µL. The actual concentration was determined spectrophotometrically.

2.2.4 RNA sample preparation for RT-PCR

The following components were added to an ice-cold, RNase-free, 1.5-mL microcentrifuge tube: 3.6 µg total RNA sample, DNase I reaction buffer (1X final concentration), 4 units DNase I and DEPC-treated water to make a final volume of 40 µL. The reaction mixture was incubated for 15 min at room temperature. To inactivate the DNase I, EDTA solution was

added to a final concentration of 25 mM EDTA and the mixture was heated at 65 °C for 10 min. The resulting RNA sample was free of genomic DNA and was ready to use in the subsequent RT reaction.

2.2.5 RT reaction (first-strand cDNA synthesis) prior to PCR

The following components were added to a nuclease-free microcentrifuge tube: 4 µL (300 ng/µL) random hexaprimers, 3.6 µg DNase I-treated total RNA, 4 µL 10 mM dNTP mix (10 mM each dATP, dGTP, dCTP and dTTP) and sterile, distilled water to make a final volume of 48 µL. The mixture was heated to 65 °C for 5 min and quickly chilled on ice. It was then briefly centrifuged and the following components were added: 16 µL 5X first-strand buffer, 8 µL 0.1 M DTT and 4 µL (40 units/µL) RNaseOUT™ Recombinant Ribonuclease Inhibitor (Gibco BRL). The contents were gently mixed and incubated at 25 °C for 2 min and then 4 µL (200 units/µL) SUPERScript™ II RNase H⁻ Reverse Transcriptase (Gibco BRL) was added and mixed gently. The resulting mixture was incubated at 25 °C for 10 min and then at 42 °C for 50 min. The reaction was stopped by heating the sample at 70 °C for 15 min. To remove RNA complementary to the cDNA, 2 µL (2 units/µL) *E. coli* RNase H was added and incubated at 37 °C for 20 min. The cDNA-containing solution was stored at -20 °C until used for amplification.

2.2.6 PCR amplification

The following components were added to a sterile 1.5-mL microcentrifuge tube to prepare a master mix which contains a final concentration of 1X PCR buffer minus Mg^{++} , 0.25 mM dNTP mixture, 1.5 mM $MgCl_2$, 0.2 μM forward primer, 0.2 μM reverse primer, 0.2 μM Histone H1 forward primer, 0.2 μM Histone H1 reverse primer, 2 units/ 50- μL reaction Platinum[®] Taq DNA polymerase (GIBCO BRL) and sterile distilled water to make up a required volume. The master mix contents were mixed gently, centrifuged briefly and aliquoted to 0.2-mL microcentrifuge tubes. Each cDNA (RT reaction) of the same volume ($\leq 1 \mu L$) was then added to the individual microcentrifuge tube. The tubes were incubated in a Biometra T-gradient thermal cycler at 94 °C for 5 min to denature the cDNA template and activate the enzyme. The PCR amplification was performed 30-36 cycles as follows: denaturing at 94 °C for 1 min, annealing at 57 °C for 1 min, extending at 72 °C for 1 min. The reaction was maintained at 72 °C for 10 min after cycling and then maintained at 4 °C. The amplification products were analyzed by agarose gel electrophoresis (0.8% agarose) and visualized by ethidium bromide staining. Molecular weight DNA standards (1 Kb) were used on the same gel. All primer sequences for amplification of *AtMKK* and *AtMPK* genes are presented in Table 2.1 and Table 2.2, respectively.

Table 2.1 *AtMKK* primer sequences for PCR amplification. Lower case letters represent the restriction enzyme sites.

Gene Name	Gene ID	Restriction Enzyme Site	Sequences (5'-3')	Predicted PCR Product Length (bp)
AtH1	At2g30602	EcoRI	ccggaattccggGGTTAAAGTCAAAGCTTCTTTTAAGA	726
		XhoI	ccgctcgagcggGAGTGAAGAAACCATCACATTATA	
AtMKK1	At4g26070	XhoI	ccgctcgagcggATGAACAGAGGAAGCTTATGCCCTA	1079
		XhoI	ccgctcgagcggCTAGTTAGCAAGTGGGGAATCAAAG	
AtMKK2	At4g29810	XhoI	ccgctcgagcggATGAAGAAAGGTGGATTCAAGCAATAA	1116
		XhoI	ccgctcgagcggATGGTGATATTATGTCTCCCTTGTAAG	
AtMKK3	At5g40440	XhoI	ccgctcgagcggATGGCGGCATTGGAGGAGCTAAAG	1587
		XhoI	ccgctcgagcggCTAATCTAAGTTTGTAATATAAAG	
AtMKK4	At1g51660	EcoRI	ccggaattccggGAAGAACGAATCAATTTAAGCCTG	1521
		EcoRI	ccggaattccggTGGGATACATGCACCATCATAAG	
AtMKK5	At3g21220	XhoI	ccgctcgagcggATGAAACCGATTCAATCTCCTTCTGGA	1134
		XhoI	ccgctcgagcggGGAAAAATGTCAGGAAAACTACG	
AtMKK6	At5g56580	BamHI	cgcggatccgATGGTGAAGATCAAATCGAAGTTG	1095
		XhoI	ccgctcgagcggTTATCTAAGGTAGTTAACAGGTGG	
AtMKK7	At1g18350	BamHI	cgcggatccgATGGCTCTTGTTTCGTAAACGCCGTCA	948
		EcoRI	ccggaattccggCTAAAGACTTTCACGGAGAAAAGG	
AtMKK8	At3g06230	BamHI	cgcggatccgATGGTTATGGTTAGAGATAATCA	906
		EcoRI	ccggaattccggCTATCTCTCGCTTGCTTTCTTGCGTA	
AtMKK9	At1g73500	EcoRI	ccggaattccggATGGCTTTAGTACGTGAACGTCGTCA	957
		EcoRI	ccggaattccggTCAAAGATCTTCCCGGAGAAAAGGATGA	
AtMKK10	At1g32320	BamHI	cgcggatccgATGACACTTGTTAGAGAACGACGTCA	942
		EcoRI	CcggaattccggCTATCTGTTTTTCACAAAAGAATGACG	

Table 2.2 *AtMPK* primer sequences for PCR amplification. Lower case letters represent the restriction enzyme sites.

Gene Name	Gene ID	Restriction Enzyme Site	Sequences (5'-3')	Predicted PCR Product Length (bp)
AtMPK1	At1g10210	EcoRI XhoI	ccggaattccggATGGCGACTTTGGTTGATCCTCCTAA ccgctcgagcggTGTTACAGACACACATCAAGCTTG	1384
AtMPK2	At1g59580	BamHI EcoRI	cgcgatccgcgATGGCGACTCCTGTTGATCCACCTAA ccggaattccggGTACAAACGTTACAGACACTTAAG	1363
AtMPK3	At3g45640	BamHI EcoRI	cgcgatccgcgATGAACACCGGCGGTGGCCAATACA ccggaattccggCTAACCGTATGTTGGATTGAGTGCTA	1137
AtMPK4	At4g01370	BamHI EcoRI	cgcgatccgcgATGTCGGCGGAGAGTTGTTTCGGAAG ccggaattccggAGAGATTTGATAACAAAAGCAGAG	1242
AtMPK5	At4g11330	XhoI XhoI	ccgctcgagcggATGGCGAAGGAAATTGAATCAGCG ccgctcgagcggTTAAATGCTCGGCAGAGGATTGA	1155
AtMPK6	At2g43790	BamHI BamHI	cgcgatccgcgATGGACGGTGGTTCAGGTCAACCG cgcgatccgcgTTGAGACCCATCCCCTTCAACATC	1393
AtMPK7	At2g18170	BamHI EcoRI	cgcgatccgcgATGGCGATGTTAGTTGAGCCACCA ccggaattccggACAAGCCTTAACCTACTTAGTAACA	1392
AtMPK8	At1g18150	XhoI XhoI	ccgctcgagcggATGGGTGGTGGTGGGAATCTCGTCGA ccgctcgagcggCTATTAAATACAACAAATCAAACCCAA	1920
AtMPK9	At3g18040	EcoRI EcoRI	ccggaattccggATGGATCCTCATAAAAAGGTTGCA ccggaattccggTCAAGTGTGGAGAGCCGCGACC	1557
AtMPK10	At3g59790	BamHI EcoRI	cgcgatccgcgATGGAGCCAACTAACGATGCTGAGA ccggaattccggTCAATCATTGCTGGTTTCAGGGTTGA	1206
AtMPK11	At1g01560	BamHI XhoI	cgcgatccgcgATGTCAATAGAGAAACCATTCTTCG ccgctcgagcggTTAAGGGTTAACTTGACTGATTCA	1134
AtMPK12	At2g46070	BamHI EcoRI	cgcgatccgcgATGGATTTAGTGTCTTCAAGAGATA ccggaattccggTCAGTGGTCAGGATTGAATTTGACAGA	1245
AtMPK13	At1g07880	BamHI EcoRI	cgcgatccgcgATGGAGAAAAGGAAGATGGAGGGA ccggaattccggTTACATATTCTTGAAGTGTAAGA	1116
AtMPK14	At4g36450	BamHI EcoRI	cgcgatccgcgATGGCGATGCTAGTTGATCCTCCA ccggaattccggTTAAGCTCGGGGGAGGTAATGAAGCA	1110
AtMPK15	At1g73670	BamHI XhoI	cgcgatccgcgATGGGTGGTGGTGGCAATCTCGTCGA ccgctcgagcggCTAAGAATTGTGTAGAGATGCAACTT	1755
AtMPK16	At5g19010	BamHI BamHI	cgcgatccgcgATGCAGCCTGATCACCGCAAAAAG cgcgatccgcgTTAATACCAGCGACTCATTGCAGTA	1728
AtMPK17	At2g01450	XhoI XhoI	ccgctcgagcggATGTTGGAGAAAGAGTTTTTCACGGA ccgctcgagcggCTATGACACTGCAGAGGAGACACCA	1575
AtMPK18	At1g53510	BamHI EcoRI	cgcgatccgcgATGGAGTTTTTCACAGAGTATGGTGA ccggaattccggCTATGATGCTGCGCTGTAACATAATTG	1836
AtMPK19	At3g14720	BamHI EcoRI	cgcgatccgcgATGGAGTTTTTCACTGAGTATGGTGA ccggaattccggCTAAGACATGCCATACCCAACA	1785
AtMPK20	At2g42880	BamHI XhoI	cgcgatccgcgATGGAGTTCTTTTCTGACTATGGCGA ccgctcgagcggCTAGTACATCTTTGACATACCGTA	1809

2.3 Results and Discussion

2.3.1 Tissue differentiation of the *Arabidopsis* MAPKK/MAPK gene families: Characteristic profiles in mature and developing organs using RT-PCR data

I initially examined whether individual members of the *Arabidopsis* MAPK and MAPKK gene families were expressed in particular organs and tissues by using the RT-PCR approach. My expression results revealed that transcripts for most of the *Arabidopsis* MAPK and MAPKK genes could be detected in all tissues/organs tested, although for a few members expression could only be detected in particular organs (Table 2.3 and Table 2.4), and no signal was detected for a few others. I also include the publicly available MPSS (Massively Parallel Signature Sequencing) dataset of the *AtMPK* and *AtMKK* genes (Meyers *et al.*, 2004a; Meyers *et al.*, 2004b) as presented in Table 2.5 and Table 2.6. My RT-PCR data is generally consistent with the MPSS data except a few genes e.g. *AtMPK1*, *AtMPK8*, *AtMPK14* and *AtMKK7*.

Among the 20 *Arabidopsis* MAPK genes, *AtMPK11*, *AtMPK12* and *AtMPK13* showed the greatest differentiation in expression across organ types. *AtMPK11* expression could not be detected in bolting stems and 4-day seedlings, whereas *AtMPK12* and *AtMPK13* transcripts were found in greatest abundance in tissues that contain actively dividing cells such as callus, flowers and roots, but were barely detected in mature organs such as leaves and secondary hypocotyls (Table 2.3). These data are consistent with the report that NTF6, a putative tobacco ortholog of *AtMPK13*, has a role in cell division (Calderini *et al.*, 1998).

Among the 10 *Arabidopsis* MAPKK genes whose expression was tested by RT-PCR, the *AtMKK6* gene was the only one that showed differentiation of expression across tissue

types (Table 2.4). Its transcripts were detected most readily in tissues that contain young dividing cells such as callus, flowers, roots and seedlings but could barely be detected in mature tissues that were no longer growing (Figure 2.2 A). This expression pattern to a large

Table 2.3 The gene expression profiles in all known *Arabidopsis* MAPK genes

Groups	Genes	CHR_locus	RT-PCR							
			Signal in Different Tissues/Organs							
			Leaves	Callus	Flowers	Roots	Stems	4-d SL	2-w SL	SH
A	AtMPK3	At3g45640	+	+	+	+	+	+	+	+
	AtMPK6	At2g43790	+	+	+	+	+	+	+	+
	AtMPK10	At3g59790	NS	NS	NS	NS	NS	NS	NS	NS
B	AtMPK4	At4g01370	+	+	+	+	+	+	+	+
	AtMPK11	At1g01560	+	+	+	+	-	-	+	+
	AtMPK12	At2g46070	-	+	+	+	+	+	-	-
	AtMPK5	At4g11330	+	+	+	+	+	+	+	+
	AtMPK13	At1g07880	-	+	+	+	-	-	-	-
C	AtMPK1	At1g10210	NS	NS	NS	NS	NS	NS	NS	NS
	AtMPK2	At1g59580	+	+	+	+	+	+	+	+
	AtMPK7	At2g18170	+	+	+	+	+	+	+	+
	AtMPK14	At4g36450	+	+	+	+	+	+	+	+
D	AtMPK8	At1g18150	NS	NS	NS	NS	NS	NS	NS	NS
	AtMPK15	At1g73670	+	+	+	+	+	+	+	+
	AtMPK9	At3g18040	+	+	+	+	+	+	+	+
	AtMPK17	At2g01450	+	+	+	+	+	+	+	+
	AtMPK16	At5g19010	+	+	+	+	+	+	+	+
	AtMPK18	At1g53510	+	+	+	+	+	+	+	+
	AtMPK19	At3g14720	+	+	+	+	+	+	+	+
	AtMPK20	At2g42880	+	+	+	+	+	+	+	+

(-) = not detected or barely detected, (+) = detected and NS = No Signal

4-d SL = 4 days old seedlings, 2-w SL = 2 weeks old seedlings, SH = Secondary hypocotyls

Table 2.4 The gene expression profiles in all known *Arabidopsis* MAPKK genes

Groups	Genes	CHR_locus	RT-PCR							
			Signal in Different Tissues/Organs							
			Leaves	Callus	Flowers	Roots	Stems	4-d SL	2-w SL	SH
A	AtMKK1	At4g26070	+	+	+	+	+	+	+	+
	AtMKK2	At4g29810	+	+	+	+	+	+	+	+
	AtMKK6	At5g56580	-	+	+	+	-	+	+	-
B	AtMKK3	At5g40440	+	+	+	+	+	+	+	+
C	AtMKK4	At1g51660	+	+	+	+	+	+	+	+
	AtMKK5	At3g21220	+	+	+	+	+	+	+	+
D	AtMKK7	At1g18350	+	+	+	+	+	+	+	-
	AtMKK8	At3g06230	NS	NS	NS	NS	NS	NS	NS	NS
	AtMKK9	At1g73500	+	+	+	+	+	+	+	+
	AtMKK10	At1g32320	NS	NS	NS	NS	NS	NS	NS	NS

(-) = not detected or barely detected, (+) = detected and NS = No Signal

4-d SL = 4 days old seedlings, 2-w SL = 2 weeks old seedlings, SH = Secondary hypocotyls

Table 2.5 The MPSS data for the *AtMPK* genes

Groups	Genes	Expression Signal* in Different Tissues/Organs				
		Leaf	Callus	INF	Root	Silique
A	AtMPK3	341	187	151	162	61
	AtMPK6	152	190	113	347	87
	AtMPK10	NS	NS	NS	NS	NS
B	AtMPK4	114	169	119	175	93
	AtMPK11	0	0	0	0	0
	AtMPK12	21	19	0	0	0
		55	63	51	16	3
	AtMPK5	19	6	2	16	12
	AtMPK13	2	4	3	4	16
C	AtMPK1	NS	NS	NS	NS	NS
	AtMPK2	31	30	17	32	4
		15	18	8	31	27
	AtMPK7	10	60	65	32	63
		0	0	0	3	0
		0	0	0	0	0
D	AtMPK14	NS	NS	NS	NS	NS
	AtMPK8	36	26	115	127	114
		23	58	59	2	14
	AtMPK15	33	11	24	20	14
	AtMPK9	28	29	30	15	27
	AtMPK17	63	117	68	1	26
	AtMPK16	45	37	59	35	29
		51	72	164	101	103
		19	2	6	0	25
	AtMPK18	24	38	68	19	10
		18	8	10	6	6
	AtMPK19	23	46	61	97	89
	AtMPK20	22	22	64	120	179
		15	12	51	19	80

MPSS has been described in a publication by Brenner *et al.* (2000). MPSS produces short sequence signatures produced from a defined position within an mRNA, and the relative abundance of these signatures in a given cDNA library (e.g. leaf, callus, inflorescence (INF), root, or silique cDNA library) represents a quantitative estimate of expression of that gene. Numbers in the same column were derived from expression data from the same sequence signature.

* Specific transcripts detected per 1,000,000 total transcripts

Table 2.6 The MPSS data for the *AtMKK* genes

Groups	Genes	Expression Signal In Different Tissues/Organs				
		Leaf	Callus	INF	Root	Silique
A	<i>AtMKK1</i>	72	46	50	4	42
	<i>AtMKK2</i>	0	0	0	10	0
		6	0	0	0	0
	<i>AtMKK6</i>	1	63	16	12	12
B	<i>AtMKK3</i>	10	66	36	20	28
		5	0	0	3	0
C	<i>AtMKK4</i>	5	25	10	0	0
	<i>AtMKK5</i>	17	14	23	14	6
		10	37	25	15	11
D	<i>AtMKK7</i>	NS	NS	NS	NS	NS
	<i>AtMKK8</i>	NS	NS	NS	NS	NS
	<i>AtMKK9</i>	34	75	19	39	21
		1	26	0	2	1
		3	20	0	0	13
	<i>AtMKK10</i>	NS	NS	NS	NS	NS

MPSS has been described in a publication by Brenner *et al.* (2000). MPSS produces short sequence signatures produced from a defined position within an mRNA, and the relative abundance of these signatures in a given cDNA library (e.g. leaf, callus, inflorescence (INF), root, or silique cDNA library) represents a quantitative estimate of expression of that gene. Numbers in the same column were derived from expression data from the same sequence signature.

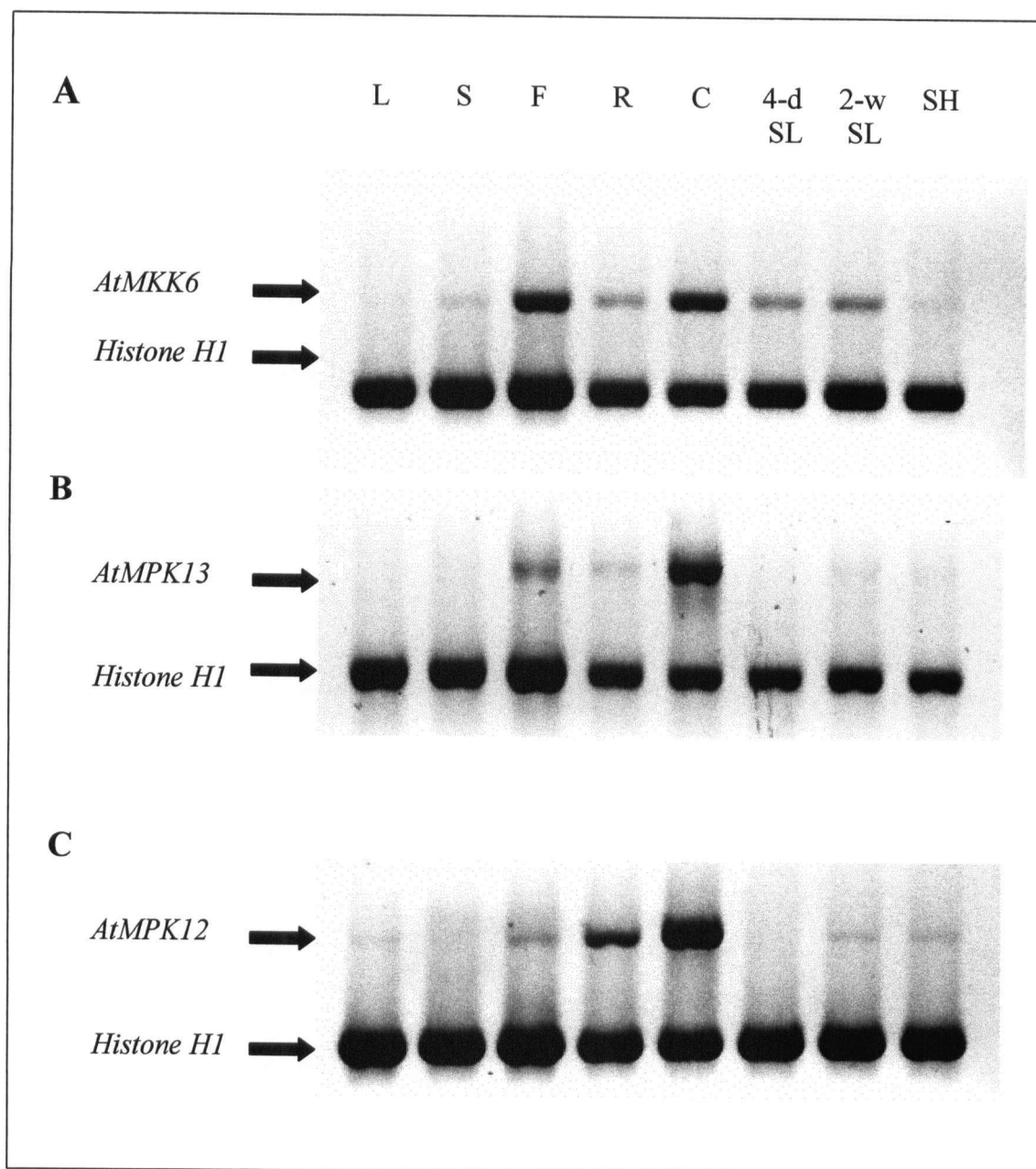


Figure 2.2 RT-PCR analysis of the expression pattern of the *AtMKK6* and *AtMPK13* genes. L = Leaves, S = Bolting stem, F = Flower buds, R = Roots, C = Callus, 4-d SL = 4 days old seedlings, 2-w SL = 2 weeks old seedlings, SH = Secondary hypocotyls. A, B and C show the expression patterns of the *AtMKK6*, *AtMPK13* and *AtMPK12* genes, respectively. *Histone H1* was used as a control gene. The experiments were repeated giving comparable results.

degree parallels that seen with the *AtMPK13* gene (Figure 2.2 B). *NtMEK1* and *NTF6*, the putative tobacco orthologs of *AtMKK6* and *AtMPK13*, respectively, were previously reported to be co-expressed both across plant tissues and following the induction of cell division in leaves (Calderini *et al.*, 2001). In addition, their yeast two-hybrid interaction analysis and *in vitro* kinase assays indicated that AtMEK1 could act as an upstream MAPKK for NTF6, and that their biological functions were involved in cell division. This relationship strongly indicates that AtMKK6 and AtMPK13 could operate in an analogous cascade in *Arabidopsis* and might play a role in cell proliferation. Similar to the *AtMPK13* gene, the *AtMPK12* gene also showed preferential expression in specific tissues/organs, which is, again, similar to *AtMKK6* (Figure 2.2 C). However, very little is known about the biological function of ATMPK12.

In my RT-PCR expression survey, I also found that *AtMKK9* expression was developmentally regulated because it was differentially expressed in different tissues, and its transcriptional level was markedly higher in 2-week-old seedlings as compared with that in 4-day old seedlings (Figure 2.3 A). These results were confirmed by performing an expression time-course experiment with 1-week old to 5-week old *Arabidopsis* leaves. Again, the expression of the *AtMKK9* gene was clearly increased as the leaves became mature (Figure 2.3 B). The possible role of the MAPK pathways in developmental processes has been studied in a variety of plant species. The gene encoding the rice MAPK, OsMAPK4, was predominantly expressed in leaves of the rice plant at a late developmental stage (Fu *et al.*, 2002), while the synthesis of the tobacco MAPK, NTF3, occurred at the late-bi-cellular stage of pollen maturation (Wilson *et al.*, 1997). The transcripts of the *Arabidopsis*

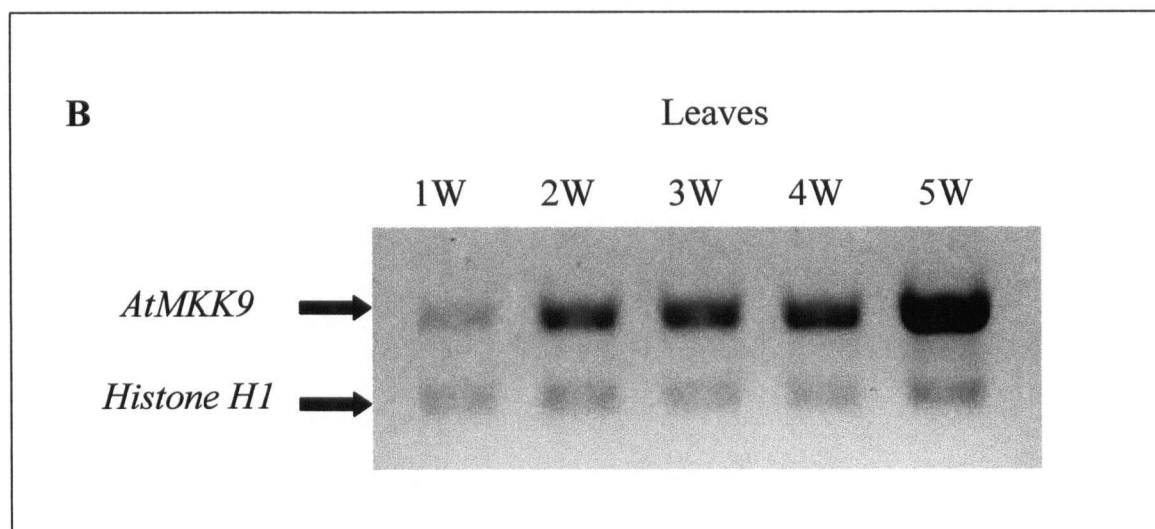
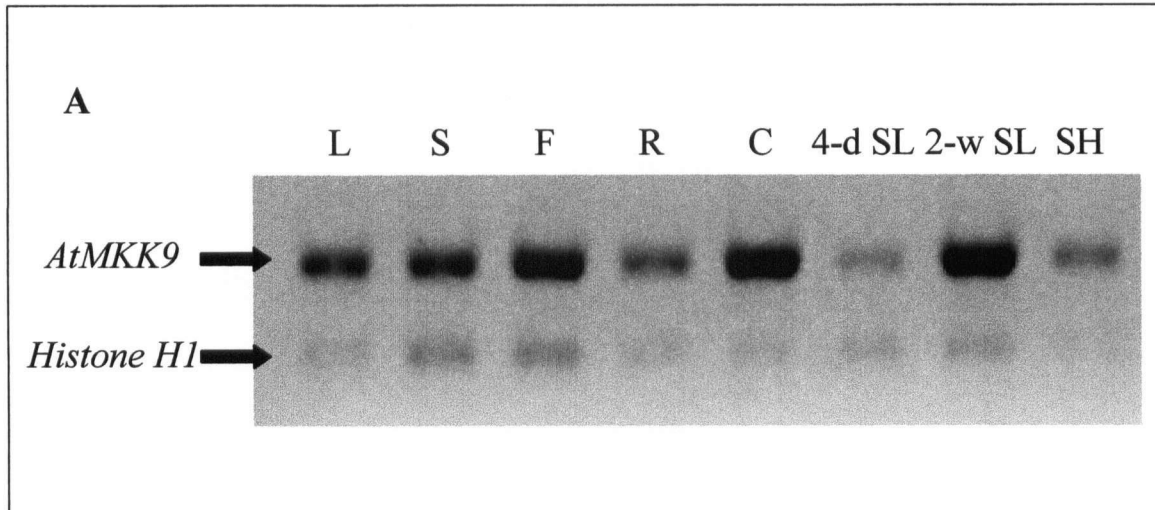


Figure 2.3 The *AtMKK9* gene was differentially expressed in organs and during developmental stages.

L = Leaves, S = Bolting stem, F = Flower buds, R = Roots, C = Callus, 4-d SL = 4 days old seedlings, 2-w SL = 2 weeks old seedlings, SH = Secondary hypocotyls

1W – 5W = One week old plants – Five week old plants

Histone H1 was used as a control gene. These are the RT-PCR results. The experiments were repeated giving comparable results.

MAPKK, MAP2K α (probably ATMKK5) were much more abundant in old leaves than in young leaves (Hamal *et al.*, 1999).

2.3.2 Stress differentiation of the *Arabidopsis* MAPKK/MAPK gene families

Transcription of several genes in the plant MAPK gene family has been reported to be induced by various abiotic stresses (Hirt, 2000; Ichimura *et al.*, 2000; Ligterink and Hirt, 2001; Yuasa *et al.*, 2001; Agrawal *et al.*, 2002; Mayrose *et al.*, 2004). In this RT-PCR survey, I also examined the effects of various abiotic stresses on the expression of all the identified *AtMPK* and *AtMKK* genes in leaves by subjecting three-week old *Arabidopsis* plants to ozone, wounding and chilling stresses.

Among the 20 *AtMPK* gene expression profiles in response to abiotic stresses (Table 2.7), group A *AtMPK3* and *AtMPK6* genes were induced in response to all abiotic stresses tested. *AtMPK10* is classified in the same phylogenetic group as *AtMPK3* and *AtMPK6* but its expression was not detected. This result is consistent with the fact that no mRNA and EST were found for this gene in the MIPS (Munich Information Center for Protein Sequences) database (Table 2.7). Ahlfors *et al.* (2004) demonstrated that *AtMPK3*, but not *AtMPK6* responded transcriptionally and translationally during ozone exposure. Both *AtMPK3* and *AtMPK6* kinases were previously shown to be activated by ozone, wounding, hypoosmolarity, low humidity and touch (Ichimura *et al.*, 2000; Droillard *et al.*, 2002; Ahlfors *et al.*, 2004). In addition, these two proteins were constitutively activated in the *Arabidopsis* *ssi4* mutant that accumulated H₂O₂ and salicylic acid prior to lesion formation (Zhou *et al.*, 2004). H₂O₂, generated by *Arabidopsis* cells in response to challenge with harpin

(a proteinaceous bacterial elicitor) was also shown to activate ATMPK6 (Desikan *et al.*, 2001).

Some members of the group B MAPKs classified in the cell-division module including *AtMPK11*, *AtMPK12* and *AtMPK13* (Figure 2.1), did not change in their expression in response to the applied abiotic stresses (Table 2.7). The fact that these genes were preferentially expressed in organs containing actively dividing cells such as flowers and callus, indicates that they are more likely to encode proteins that function in response to plant growth and development rather than abiotic stresses. However, some other genes in this cell-division module did show a stress response, such as *AtMPK4* and *AtMPK5*. Expression of *AtMPK4* was induced by wounding, and that of *AtMPK5* was up-regulated by chilling (Table 2.7). Additional expression data of the group B MAPKs came from previous work done by Ichimura *et al.* (2000) and Desikan *et al.* (2001). Consistent with my data, low temperature did not affect *AtMPK4* expression or its protein level, but it did respond at the posttranslational level since this environmental stress induced rapid and transient activation of ATMPK4, as assessed by tyrosine phosphorylation on the protein (Ichimura *et al.*, 2000). In contrast to my data, it was previously reported that wounding did not have an effect on *AtMPK4* expression (Ichimura *et al.*, 2000), nor did a bacterial elicitor, harpin and H₂O₂ (Desikan *et al.*, 2001). However, publicly available data showed that the *AtMPK5* gene was transcriptionally induced by chitin oligomers, elicitors that can be released from fungal cell walls by endochitinase (TAIR, <http://www.arabidopsis.org/>).

Table 2.7 The gene expression profiles in all known *Arabidopsis* MAPK genes under different stress conditions

Groups	Genes	CHR_locus	Stress Treatments (Leaves)			mRNA	EST
			Ozone	Wounding	Chilling		
A	AtMPK3	At3g45640	+	+	+	3	25
	AtMPK6	At2g43790	+	+	+	2	7
	AtMPK10	At3g59790	NS	NS	NS	none	none
B	AtMPK4	At4g01370	0	+	0	4	1
	AtMPK11	At1g01560	0	0	0	none	none
	AtMPK12	At2g46070	0	0	0	2	3
	AtMPK5	At4g11330	0	0	+	1	2
	AtMPK13	At1g07880	0	0	0	none	none
C	AtMPK1	At1g10210	NS	NS	NS	3	1
	AtMPK2	At1g59580	0	0	0	4	2
	AtMPK7	At2g18170	+	+	+	1	2
	AtMPK14	At4g36450	+	+	0	none	none
D	AtMPK8	At1g18150	NS	NS	NS	3	11
	AtMPK15	At1g73670	0	0	0	2	2
	AtMPK9	At3g18040	0	0	0	1	2
	AtMPK17	At2g01450	+	+	+	none	21
	AtMPK16	At5g19010	+	+	+	2	9
	AtMPK18	At1g53510	0	0	+	3	7
	AtMPK19	At3g14720	0	0	+	none	6
	AtMPK20	At2g42880	0	0	0	2	16

(+) = Changed compared to non-treated control

(0) = Not changed compared to non-treated control

NS = No signal

mRNA and EST data were taken from MIPS database on January 13, 2004

For group C MAPK genes, I found that *AtMPK2* had no significant change in its expression whereas *AtMPK7* and *AtMPK14* displayed altered transcript levels in response to the applied abiotic stresses (Table 2.7). Although for *AtMPK1*, I obtained no expression signal in the RT-PCR dataset, 3 RNAs and 1 EST derived from this gene were found in the MIPS database (Table 2.7). These observations indicate that *AtMPK1* gene may not be responsive to some abiotic stresses but perhaps is responsive to other specific stimuli. For instance Mizoguchi *et al.* (1996) showed that mRNA of *AtMPK1* was induced by salt-stress treatment, whereas it was transcriptionally unaffected by cold stress.

Among previously uncharacterized group D MAPKs, expression of the *AtMPK17* and *AtMPK16* genes was induced by all the abiotic stresses tested, while *AtMPK18* and *AtMPK19* expression was only induced by chilling stress. Expression of the *AtMPK9*, *AtMPK15* and *AtMPK20*-encoding genes did not change when the abiotic stresses were applied (Table 2.7). I did not detect any expression signal for the *AtMPK8* gene by RT-PCR, but at least 3 RNAs and 11 ESTs for this gene were found in the MIPS database (Table 2.7).

Among the 10 *AtMKK* genes, on one hand, *AtMKK1* and *AtMKK2* expression was induced in response to wounding and chilling stress (Table 2.8). *AtMKK6*, on the other hand, showed no change in its expression in response to the specified stresses, nor did *AtMKK3* (Table 2.8). My results also showed that the structurally similar *AtMKK4* and *AtMKK5* genes appear to have somewhat different roles, because their expression patterns could be distinguished. The *AtMKK4* gene did not change its expression in response to abiotic stresses, but the *AtMKK5* gene did (Table 2.8). It is, of course, possible that genes whose transcript levels were not responsive to these abiotic stresses could respond to other stimuli

Table 2.8 The gene expression profiles in all known *Arabidopsis* MAPKK genes under different stress conditions

Groups	Genes	CHR_locus	Stress Treatments (Leaves)			mRNA	EST
			Ozone	Wounding	Chilling		
A	AtMKK1	At4g26070	0	+	+	5	6
	AtMKK2	At4g29810	0	+	+	4	11
	AtMKK6	At5g56580	0	0	0	1	none
B	AtMKK3	At5g40440	0	0	0	4	2
C	AtMKK4	At1g51660	0	0	0	7	7
	AtMKK5	At3g21220	+	+	+	2	7
D	AtMKK7	At1g18350	+	+	0	none	none
	AtMKK8	At3g06230	NS	NS	NS	none	none
	AtMKK9	At1g73500	0	0	+	6	8
	AtMKK10	At1g32320	NS	NS	NS	none	none

(+) = Changed compared to non-treated control

(0) = Not changed compared to non-treated control

NS = No signal

mRNA and EST data were taken from MIPS database on January 13, 2004

such as biotic stresses, phytohormones and/or other chemicals. For example, a preliminary experiment showed that *AtMKK4* transcription was responsive to infection by *Peronospora* (our unpublished data), suggesting that *AtMKK4* might play a role in biotic stress responses rather than abiotic stress response.

Since H₂O₂ is known to be generated by *Arabidopsis* cells in response to exposure to ozone, my expression data for tissue response to ozone is in agreement with previous data showing that the expression of *AtMKK1* (*AtMEK1*), and *AtMKK2* was not affected by H₂O₂ treatment (Desikan *et al.*, 2001). *AtMKK1* expression in response to wounding observed in my study is consistent with a previous report of its transcriptional up-regulation upon wounding (Morris *et al.*, 1997). However, Matsuo *et al.* (2002) demonstrated that the amounts of the *ATMKK1* protein did not change significantly in response to wounding and

other abiotic stresses including cold, drought, and high salt. At the same time, AtMKK1 did display elevated protein kinase activity. Their data also indicated that the AtMEK1 becomes activated through phosphorylation and activates its downstream target, ATMPK4, during stress response in *Arabidopsis*. Ichimura *et al.* (1998b) showed that ATMKK2/ATMKK1 and ATMPK4 physically interacted with two distinct regions of the upstream MAPKKK, ATMEKK1 (AtMKKK1) protein, the N-terminal regulatory domain and the C-terminal kinase domain, respectively. Co-expression of ATMEKK1 increased the ability of either of the two closely related MAPKKs, ATMKK2 or AtMKK1, to complement a growth defect of the yeast *pbs2* mutant. They suggested that ATMEKK1, ATMKK2/ATMKK1, and ATMPK4 might therefore constitute a plant MAP kinase cascade. Very little is known about the *AtMKK3*, *AtMKK4* and *AtMKK5* gene expression in response to abiotic and biotic stresses.

No information has been published on the function of group D AtMKKs (MAPK Group, 2002). Our data showed that some group D *AtMKK* genes were involved in specific abiotic stress responses. For example, the *AtMKK7* gene, whose expression signal was weak in non-treated leaves, had its expression significantly induced by ozone and by wounding, whereas the expression of the *AtMKK9* gene was induced specifically in response to low temperature stress (Table 2.8). Notably, neither *AtMKK8* nor *AtMKK10* gene expression was detectable by the RT-PCR method, which is consistent with the absence of their mRNA and ESTs from the MIPS database (Table 2.8).

2.3.3 Three candidate genes with interesting expression pattern for further functional characterization

2.3.3.1 The *AtMKK6* and *AtMPK13* genes

From the expression profiling of two classes of genes encoding putative MAPKs and MAPKKs in *Arabidopsis*, I identified a pair of genes, *AtMKK6* and *AtMPK13*, that were co-expressed in various tissues/organs containing actively dividing cells such as flowers, roots and callus under normal growth condition, and had a similar expression pattern under different environmental conditions in leaves (Figure 2.2 A and B). Recently, *AtMKK6* was shown to functionally activate the *AtMPK13* in yeast as the kinase activity of *AtMPK13* is stimulated in the presence of *AtMKK6* in yeast cells (Melikant *et al.*, 2004). In addition, their co-expression data was also consistent with my expression data. Significantly, *NtMEK1* and *NtF6*, tobacco orthologues of *AtMKK6* and *AtMPK13*, respectively, were shown to be involved in cytokinesis (Calderini *et al.*, 1998; Calderini *et al.*, 2001; Soyano *et al.*, 2003).

Based on my expression data together with the available functional information on their orthologues in tobacco and from the *in vitro* and *in vivo* (yeast) kinase assays, I postulated that *AtMKK6* and *AtMPK13* may function in the same cascade involving in cell proliferation in some specific cell- or tissue- types in *Arabidopsis*. Therefore, I further investigated the biological function of these two genes in *planta* as presented in Chapter 3.

2.3.3.2 The *AtMPK12* gene

The *AtMPK12* expression pattern is particularly interesting, because it showed preferential expression in some specific tissues (Figure 2.2 C). In addition, its expression pattern in various organs was somewhat similar to those of *AtMKK6* and *AtMPK13* genes (Figure 2.2

A, B and C). Notably, ATMPK12 and ATMPK13 have been grouped in the same functional module based on their deduced amino acid sequences (MAPK Group, 2002 and Figure 2.1). Therefore, it seemed possible that ATMPK12 could have a function similar to that of ATMPK13 in *planta*. To elucidate the function of AtMPK12 in *planta*, I further characterized the *AtMPK12* gene expression and its function in detail, as presented in Chapter 4.

2.3.4 Perspectives

2.3.4.1 Expression profiling approach is useful to identify developmentally regulated and stress-responsive genes.

I focused my interpretation and discussion based on only positive signals, not negative signals. The positive signal detected in various organs by RT-PCR approach is strong evidence for the actual presence of transcripts in those organs, since the identities of the *Arabidopsis* *MAPK* and *MAPKK* RT-PCR products obtained as positive expression signals were confirmed by sequencing. Similarly, the RT-PCR expression survey of tissues subjected to various abiotic stresses is useful for identification of stress-responsive genes.

As stated in the introduction in this chapter, my goals were to identify functions of the individual members of *Arabidopsis* *MAPKK* and *MAPK* gene families and to detect functional cascades between these two classes of the *MAPK* gene family based on expression profiling. As a result from the expression survey, I found that some previously uncharacterized group C *AtMPK7* and *AtMPK14* genes and group D *AtMPK16* and *AtMPK17* genes are responsive to environmental stresses. In addition, I found that group D *AtMKK9* is

involved in developmental processes. Significantly, I also found one pair of the developmentally regulated genes (*AtMKK6* and *AtMPK13*) that potentially function in the same cascade. This grouping based on the co-expression pattern is consistent with those based on both phylogenetic grouping and the association of their orthologues with a known function (cell-division) (Figure 2.1). However, some other genes with known physical and/or biochemical interactions could not be associated by the expression profiling, including some of the well known pairs: *ATMKK1* and *ATMPK4*; *ATMKK4/ATMKK5* and *ATMPK3/ATMPK6* (Figure 2.1). *ATMKK1* was previously shown to phosphorylate and physically interact with *ATMPK4* *in vitro* (Huang *et al.*, 2000) as did *ATMKK4* and *ATMKK5* with *ATMPK3* and *ATMPK6* (Asai *et al.*, 2002). Notably, the genes encoding these proteins are stress-responsive genes.

Overall, my results demonstrated that expression profiling using various tissues/organs and under various stress stimuli is informative, because it can be used to identify developmentally regulated genes and stress-responsive genes, respectively. However, this approach is limited and not sufficient for grouping the stress-responsive genes into common signaling cascades. This may be due to the fact that most of the stress-responsive *MAPK/MAPKK* genes are expressed ubiquitously across many tissues/organs (Table 2.3 and Table 2.4), so that their co-expression simply cannot be distinguished in tissues/organs. In addition, expression profiling does not provide differentiation between active and inactive forms of proteins. Some MAPKs are not regulated primarily at the transcriptional level, but rather regulated at the post-translational level through phosphorylation (Tena *et al.*, 2001).

Notably, no expression signal from some of the genes, like *AtMPK10*, *AtMKK8* and *AtMKK10*, was detected in any organs and stress conditions tested by the RT-PCR approach, which is consistent with the fact that no RNA and EST records were found in the MIPS database (Table 2.7 and 2.8). It is possible that these genes might respond specifically to certain stimuli or growth conditions or they could represent non-functional genes (pseudogenes).

2.3.4.2 Spatial and temporal expression can infer gene function in

Arabidopsis

It is notable that expression analysis in *Arabidopsis* could detect functional differentiation across different organs despite the fact that the mRNA population reflects a mixture of cell or tissue types in each plant organ. For example, a wild-type root organ is made of five tissue types; the outermost is epidermis, and then inside is cortex, endodermis, pericycle and vascular tissues. The abundance of transcripts of a cell-specific gene observed in an organ with multiple cell types cannot be assumed to demonstrate the presence of more of those mRNAs in every cell in the organ. Rather, it may reflect the absence and presence of mRNAs or proteins in certain cell-types in a given organ/tissue. Knowledge of the expression of a gene in specific cells or tissues in *Arabidopsis*, would therefore help to infer the biological roles of a gene product of unknown function. A useful approach to the more detailed localization of gene expression in *planta* employs transgenic plants carrying a gene-specific promoter fused with the β -glucuronidase (*GUS*) reporter gene. My investigation of this is presented in the Chapters 3 and 4.

CHAPTER 3

***Arabidopsis* MAP kinase kinase 6 (AtMKK6) and MAP kinase 13 (AtMPK13) encode positive regulators of lateral root formation.**

3.1 Introduction

Lateral root formation is an important process for plant growth and development. Root branching greatly increases the zone of substrates that can be exploited by the plant, and also enables re-direction of root growth in response to locally unfavorable rhizosphere conditions. Environmental and developmental signals must be integrated to determine both the frequency of lateral root initiation and the location of the lateral root primordia (LRP) along a parental root (Malamy and Ryan, 2001; Casimiro *et al.*, 2003). In *Arabidopsis*, the primary root consists of four single layers of epidermal, cortical, endodermal and pericycle cells surrounding the vascular tissues (Figure 3.8 B and Dolan *et al.*, 1993). The formation of a new lateral root begins with localized renewal of cell division in pericycle cells. The resulting new lateral root primordia originate specifically from pericycle cells positioned opposite the xylem poles of the vascular cylinder (Dolan *et al.*, 1993). In *Arabidopsis*, the pericycle consists of dissimilar cell files. Those pericycle basal cells located adjacent to protoxylem poles proceed to G2 phase of the cell cycle, whereas other pericycle cells remain in G1 phase (Beeckman *et al.*, 2001; Himanen *et al.*, 2002). However, since LRP develop at discrete positions along the primary root, it appears that even within the file of G2-arrested cells, only a subset is involved in lateral root initiation. It has been proposed that this localized initiation competency is established by two intersecting signals. Pericycle cells across from the protoxylem poles are “primed” by a radially diffusible factor, while a

longitudinally distributed factor subsequently triggers cell division within a subset of the “primed” cells (Skene, 2000).

The phytohormone auxin is known to play an important role in lateral root formation (Boerjan *et al.*, 1995; Celenza *et al.*, 1995; Laskowski *et al.*, 1995; Beeckman *et al.*, 2001; Himanen *et al.*, 2002), and is a compelling candidate as the longitudinally distributed factor that promotes the primed cells to divide. Auxin has profound effects on root growth and development (Casimiro *et al.*, 2001; Bhalerao *et al.*, 2002; Himanen *et al.*, 2002), and on cell cycle activity (Stals and Inze, 2001), and it has been proposed that auxin induces lateral root initiation by cell cycle stimulation (Himanen *et al.*, 2002). Several auxin-responsive mutants have altered lateral root initiation and emergence (Celenza *et al.*, 1995; Casimiro *et al.*, 2003). Normally quiescent pericycle cells in fully developed areas of roots still maintain the ability to generate LRPs in response to exogenously applied auxin (Laskowski *et al.*, 1995; Doerner *et al.*, 1996).

MAPK cascades are involved in many aspects of growth, stress management and cell fate in eukaryotes including yeasts, mammals and plants (Widmann *et al.*, 1999; Ligterink and Hirt, 2001; Tena *et al.*, 2001). In plants, MAPK cascade genes have been implicated in signal transduction associated within plant development and plant hormone responses (See literature review in Chapter 1 and references therein). My RT-PCR survey of the expression patterns of *Arabidopsis* MAPKs and MAPKKs revealed that most *AtMKK* and *AtMPK* genes showed uniform expression during development but *AtMKK6* and *AtMPK13* did not (Chapter 2, Table 2.3 and 2.4). These two genes were preferentially expressed in tissues and organs that contain proliferating cells, including flowers, callus and roots (Chapter 2, Figure 2.2).

Therefore, activity of the products of these genes appears to be associated with active cell-division processes in plants.

Arabidopsis AtMKK6 and its tobacco ortholog, NtMEK1, have recently been reported to be associated with cell plate formation during cytokinesis (Calderini *et al.*, 2001; Soyano *et al.*, 2003), and a MAPK cascade controlling cytokinesis in tobacco cells was proposed to consist of the tobacco NPK1 MAPKKK (Nishihama *et al.*, 2001), the NQK1/NtMEK1 MAPKK and the NRK1 MAPK (Soyano *et al.*, 2003). This “PQR” pathway operates downstream of the kinesin-related proteins, NACK1/2, during the late M phase of the cell cycle in tobacco cells (Takahashi *et al.*, 2004). *Arabidopsis* NACK1 and NACK2 genes are identical to *HINKEL* (*HIK*) and *STUD* (*STD*) / *TETRASPORE* (*TES*) genes, respectively (Strompen *et al.*, 2002; Yang *et al.*, 2003). Loss-of-function mutations in *AtNACK1* / *HIK* result in cytokinesis defects such as abnormally large cells with incomplete cell walls and multiple nuclei (Tanaka *et al.*, 2004; Strompen *et al.*, 2002). Plants with mutations in *AtNACK2* / *STD* / *TES* exhibit cytokinesis defects during the formation of microspores (Yang *et al.*, 2003). The tobacco NRK1 MAPK (earlier identified as the NTF6 MAPK (Calderini *et al.*, 1998) is the apparent ortholog of *Arabidopsis* MPK13 (AtMPK13), and NRK1 was shown to be activated by constitutively active tobacco NQK1/NtMEK1 (Calderini *et al.*, 2001; Soyano *et al.*, 2003). Similarly, recombinant AtMPK13 was recently shown to be phosphorylated by constitutively active recombinant AtMKK6 (Melikant *et al.*, 2004).

In this study, I investigated the hypothesis that AtMKK6 and AtMPK13 activities are restricted to particular cell division phenomena. First, I analyzed the *in vivo* pattern of the promoter activity of *AtMKK6* and *AtMPK13* genes in various tissues/cells during

development. I also analyzed the behavior of these two promoters upon treatments with auxin and with NPA, a polar auxin transport inhibitor. To examine the loss-of-function mutant phenotype, I generated glucocorticoid-inducible AtMKK6RNAi mutant plants and was also able to test AtMPK13RNAi mutant plants (obtained from A.Walia). For this analysis, I focused specifically on lateral root formation.

3.2 Materials and Methods

3.2.1 Plant materials

All plants used were *Arabidopsis thaliana* ecotype Columbia. Unless otherwise noted, seed was planted in 10-cm pots of synthetic potting soil (Redi-earth® or Terra-lite®, W.R. Grace & Co. of Canada Ltd., Ontario, Canada), watered and kept under a mist area for 3 days. The pots were then placed in the greenhouse under supplemental white lights at ambient temperature. They were watered and fertilized as needed.

3.2.2 Genomic DNA isolation

Arabidopsis genomic DNA was isolated from 2-week old leaf tissue using the genomic DNA purification kit (DNeasy Plant Mini Kit, Qiagen) according to the manufacturer's instructions. Leaf tissue (100 mg) was ground to a fine powder under liquid nitrogen using a mortar and pestle. The tissue powder was transferred to a Falcon tube (15 mL) and the liquid nitrogen was allowed to evaporate. To extract the cells, 400 μ L Buffer AP1 and 4 μ L RNase A stock solution (100 mg/mL) were added to the tissue powder and vortexed vigorously. The mixture was incubated for 10 minutes at 65 °C and mixed by inverting the tube 2-3 times during incubation. To precipitate detergent, proteins and polysaccharides, 130 μ L Buffer

AP2 were added to the extract, mixed and incubated for 5 minutes on ice. To remove most precipitates and cell debris, the mixture was centrifuged for 5 minutes at full speed and the supernatant was applied to a QIAshredder spin column sitting in a 2-mL collection tube. This was then centrifuged for 2 minutes at 12000 x g (Eppendorf model 5415 C). Approximate 450 μ L flow-through fraction was transferred to a new tube without disturbing the cell-debris pellet. To precipitate DNA, 1.5 volumes (675 μ L) ethanol-containing Buffer AP3/E were added to the cleared supernatant and mixed by pipetting. A portion of the mixture (650 μ L) was transferred to a DNeasy mini spin column sitting in a 2-mL collection tube and centrifuged for 1 minute at $\geq 5300 \times g$. The flow-through was discarded and the remaining mixture was added to the same spin column, which was centrifuged as before. The flow-through and collection tube were discarded and the DNeasy column was placed in a new 2-mL collection tube. To wash the column, 500 μ L Buffer AW were added to the DNeasy column and centrifuged for 1 minute at $\geq 5300 \times g$. The flow-through was discarded and the column wash was repeated with 500 μ L Buffer AW. This time the DNeasy column was centrifuged for 2 minutes at maximum speed (to dry the DNeasy membrane) before being transferred to a 2-mL microcentrifuge tube. To elute the genomic DNA, 50 μ L preheated (65 °C) Buffer AE was pipetted directly onto the DNeasy membrane, incubated at room temperature for 5 minutes and centrifuged for 1 minute at $\geq 5300 \times g$. The DNA concentration was measured by spectrophotometry. The final yield of genomic DNA obtained from this procedure was 13.5 ng DNA/ μ L.

3.2.3 Molecular cloning of *AtMKK6* or *AtMPK13* promoter::*GUS* DNA construct and generation of GUS reporter plants

To examine cell- and tissues-specific expression of *AtMKK6* and *AtMPK13* genes during plant development, transgenic *Arabidopsis* plants harboring either an the *AtMKK6* or *AtMPK13* promoter:: *β -glucuronidase (GUS)* reporter gene construct were generated through the following procedures.

3.2.3.1 Cloning of promoters

The promoter regions of the *AtMKK6* and *AtMPK13* genes (740 bp and 1534 bp upstream of their translational start ATG codon, respectively) were amplified from *Arabidopsis* genomic DNA (obtained from Section 3.2.2) using the Expand High Fidelity PCR System Kit (Roche Molecular Biochemicals, Catalog No. 1 732 641) through a PCR-mediated method according to the manufacturer's instructions. The promoter fragment of the *AtMKK6* gene was amplified using PKK6F1 and PKK6R1 primers, and the promoter fragment of the *AtMPK13* gene was amplified using PK13F1 and PK13R1 primers. All primer sequences are presented in Table 3.1. The resulting amplicons were cloned into the pCR[®]2.1-TOPO[®] vector using a TOPO TA Cloning[®] Kit (Invitrogen, Carlsbad, USA, and Catalogue No. K4500-01) and sequenced to confirm the identity and sequence accuracy of the promoters.

Table 3.1 Primer sequences for promoter cloning

Primer Name	Restriction Enzyme Site	Sequence (5'-3')	Amplified Promoter Region Length (bp)
PKK6F1	EcoRI	ccggaattcGCTCTCTCTCTCTCTCTACAGCGAG	741
PKK6R1	BamHI	cgcggatccTTTTTCTTTGGTTTCTTCCTTGG	
PK13F1	BamHI	cgcggatccGCAATTGGAGGATACATGCTTCGTGTG	1534
PK13R1	HindIII	cccaagcttCTCTTCTTTGGAAGAAGAACTCGG	

3.2.3.2 Generation of promoter::*GUS* fusion DNA constructs

The amplified PCR product of the 740 bp *AtMKK6* promoter fragment was digested with *EcoRI* and *BamHI*, and ligated in the sense orientation adjacent to the *GUS* coding region in the promoter cloning vector, pCAMBIA1381Z (CSIRO, Canberra, Australia) that had been predigested with *EcoRI* and *BamHI*. The 1534 bp promoter fragment of *AtMPK13* was cloned in a similar way, except that the PCR product was digested with *BamHI* and *HindIII*, and ligated into pCMBIA1381Z that had been predigested with the same enzymes. Uncut pCAMBIA1381Z was used as a promoterless-*GUS* construct (negative control) and pCAMBIA1301 (CSIRO, Canberra, Australia) was used as a 35S promoter-*GUS* fusion construct (positive control). A schematic diagram of the pCAMBIA1381Z vector, showing how a promoter region was integrated into this vector, and of the pCAMBIA1301 vector are presented in Figure 3.1.

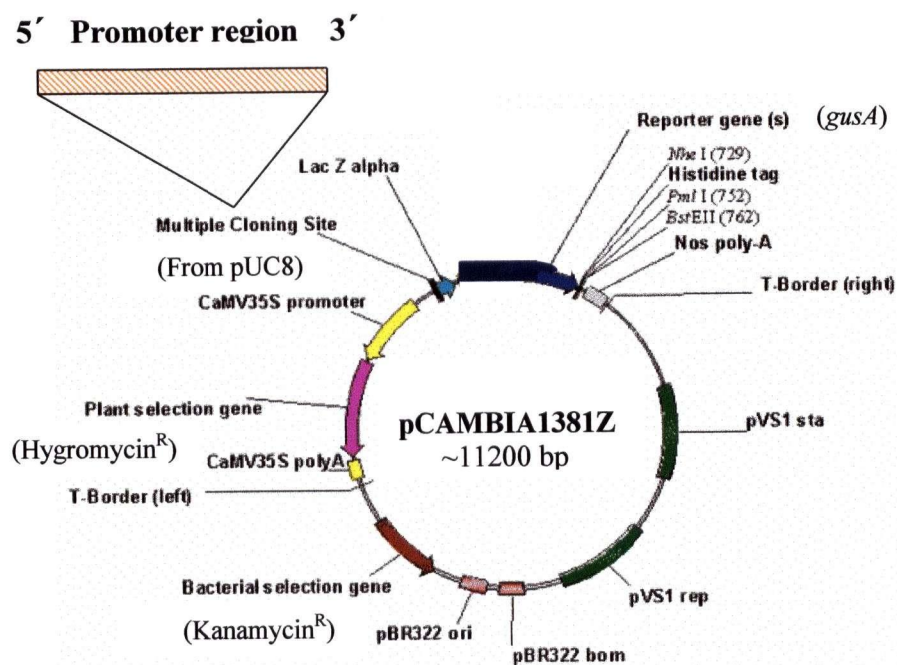
The ligation reactions were performed as follows: digested products were separated on a 0.8 % low-melting point agarose gel. (The amount of DNA loaded on the gel was estimated by running the DNA samples alongside a low DNA mass ladder (Invitrogen, Catalogue No. 10068-013). The digested products were then cut from the gel, the excised bands were melted at 65 °C for 10 minutes, transferred to a 37 °C heating block and the DNA samples were purified using QIAquick Gel Extraction Kit (Qiagen, Catalogue No. 28704)

according to the manufacturer's instructions. The purified, digested promoter fragment was mixed with the purified digested vector in a 3:1 molar ratio and ligase reaction buffer was added to 1X. One to two units of T4 DNA ligase (Invitrogen, Catalog No. 15224-041) was added and the mixture was incubated at 37 °C for 1-2 hours. The mixture was cooled to 4 °C and maintained at this temperature overnight. A portion of the ligation reaction (2 µL) was used to transform 100 µL *E. coli* (DH5α) competent cells (See below in the Section 3.2.7). The cell culture was then spread on kanamycin (50 mg/L)-containing LB agar plates (See below in Section 3.2.10), which had been loaded with 40 µL of 40 mg/mL X-Gal stock half an hour prior to culture plating. Positive white DH5α clones which grew successfully on kanamycin- and X-Gal-containing LB agar plates were screened by PCR and PCR-positive colonies used for plasmid DNA isolation using Wizard® *Plus* SV Miniprep DNA Purification System (Promega Corporation, Catalogue No. A1330). Isolated plasmides were analyzed by restriction enzyme digestion.

3.2.3.3 Transformation of *Agrobacterium*

The *AtMKK6* or *AtMPK13* promoter::*GUS* fusion DNA construct was introduced into *Agrobacterium tumefaciens* strain GV3101 by normal triparental mating (Van Haute *et al.*, 1983). In brief, 10 µL of DNA solution were used to transfect 200 µL *Agrobacterium* competent cells (See below in Section 3.2.9). DNA was added to the frozen *Agrobacterium* competent cells in a microcentrifuge tube that was held in a 37 °C water bath for 5 minutes with occasional mixing during the incubation. To this sample, 1 mL sterile LB broth was added and the tube was shaken at 100 rpm for 3 hours at 28 °C. The cells were pelleted by

(A)



(B)

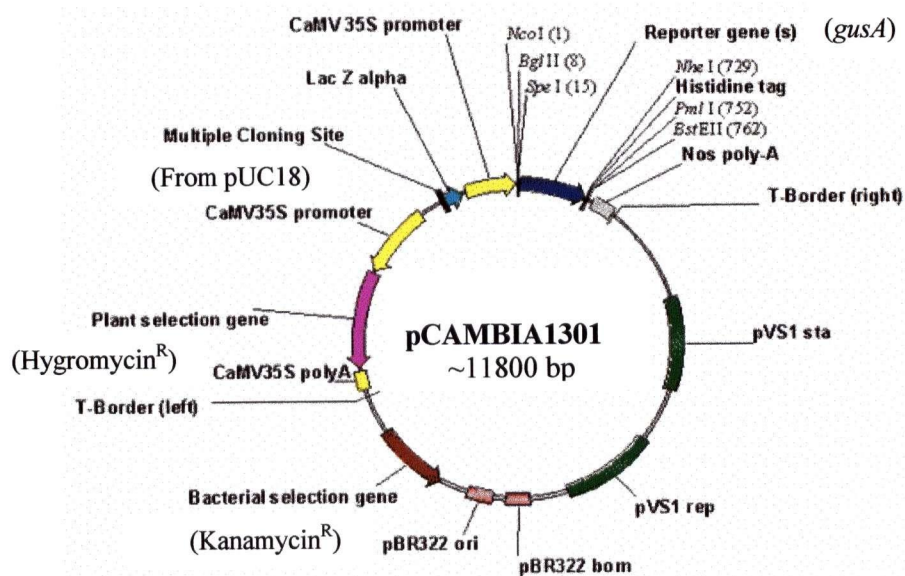


Figure 3.1 Schematic diagrams of pCambia1381Z and pCambia1301 vectors (modified from <http://www.cambia.org.au/daisy/cambia/585>)

centrifugation for 30 seconds and the supernatant was discarded. The cell pellet was re-suspended in 1 mL sterile LB broth and 0.2 mL of this cell suspension were plated on each LB agar plate containing 25 mg/L rifampicin, 25 mg/L gentamycin and 50 mg/L kanamycin. These plates were incubated for 2 and 1/2 days at 28 °C in the dark for 2 and ½ days to allow development of transformant colonies.

3.2.3.4 *In planta* transformation of *Arabidopsis*

The *AtMKK6* or *AtMPK13* promoter::*GUS* fusion construct was delivered into wild-type *Arabidopsis thaliana* ecotype Columbia by the floral dip method (Clough and Bent, 1998). Briefly, six 10-cm pots each with 6-8 *Arabidopsis* plants were used for plant transformation with each genotype. Six days prior to *Agrobacterium* floral dip the developing inflorescences were cut to induce secondary bolting and formation of many immature flower clusters. Two days before floral dip, the appropriate *Agrobacterium* strain was inoculated into 500 mL of LB broth, containing 25 mg/L rifampicin, 25 mg/L gentamycin and 50 mg/L kanamycin. This culture was grown for 24 hours at 28 °C with shaking at 200 rpm. The cells were then pelleted at 4000 x g for 5 minutes. The supernatant was discarded and the cells were re-suspended in 500 mL 5% sucrose containing 0.03% Silwet L-77 (Lehle Seeds, Catalogue No. VIS-01). The cell suspension was poured into an autoclavable plastic container and *Arabidopsis* plants that had been watered a day earlier to wet the soil, were held upside down in the container with their inflorescences submerged in culture suspension for 3 seconds with gentle agitation. The pots were then laid on their side on a plastic tray, covered with a plastic bag, and kept overnight in the dark to maintain high humidity. The plants were then turned upright and returned to normal growing conditions. The dipped plants were not watered once siliques began to mature, and the seeds (T1 generation) were harvested when dry.

3.2.3.5 Selection of transformants

Seeds of the T1 generation were surface-sterilized by vortexing them in a solution containing 1.5 % sodium hypochlorite (Sigma, Catalogue No. 42504-4) and 0.01 % tween-20 (BDH Laboratory Supplies, Catalogue No. P28829) and letting them sit in this solution for 20 minutes in a microcentrifuge tube. The solution was withdrawn and seeds were rinsed with sterile water five times. The surface-sterilized seeds were re-suspended in sterile, viscous 0.1 % agarose (prepared at least one day before use so it became viscous) and spread on agar-solidified MS medium plates containing ½ MS salt mix, 1% sucrose, 1 x B5 vitamins, 0.5 g/L MES, and 0.8 % agar, pH 5.7 plus 50 mg/L hygromycin B (Invitrogen, Catalogue No. 10687-010) and 50 mg/L vancomycin hydrochloride (Sigma, Catalogue No.V2002) (Vancomycin was added to control the *Agrobacterium* growth). All the plates were sealed with 3M Micropore™ tape (Acrona Inc., Catalogue No.1530-0), then wrapped with aluminium foil (dark condition) and kept at 4 °C for 2-4 days to vernalize the seeds. The plates were then placed in the growth room under 16h/8h light-dark cycle conditions at 22-24 °C. This temperature is critical to control the rapid growth of contaminating *Agrobacterium* on the plant agar media.

Approximately 7-10 days post-germination, the positive T1 transformants displaying resistance to hygromycin B (50 mg/L) were transferred to soil for growth to mature plants. Some of the T1 plant tissues were subjected to histochemical GUS staining. Plants positive for *GUS* expression were tagged and allowed to set seeds of the T2 generation. T2 plants were similarly analyzed for *GUS* expression at the young seedling stage. Finally, detailed analysis of *GUS* expression was conducted using T3 homozygous lines (*AtMKK6* promoter::*GUS* lines 1, 2 and 6, and *AtMPK13* promoter::*GUS* lines 1, 2 and 6). *GUS*

activity of T3 transgenic plants was monitored throughout plant development from 3-day to 35-day-old plants by histochemical GUS staining, using independent transformants of each genotype.

3.2.4 Histochemical GUS assay

Histochemical staining for GUS activity was performed as described previously by (Jefferson, 1987), except that all plant materials analyzed were pre-soaked in heptane for 10 minutes. The heptane was removed and the plant materials were air-dried for 5 minutes prior to incubation in a GUS reaction solution. The GUS reaction solution consisted of 0.5 mg/mL X-Gluc (5-bromo-4-chloro-3-indolyl-*beta*-D-glucuronic acid, cyclohexylammonium salt) (BioVectra, Prince Edward Island, Canada) in 50 mM sodium phosphate buffer, pH 7.0, (0.5 mg X-Gluc per 10 μ L N, N-dimethyl formamide was completely dissolved before adding to the sodium phosphate buffer), and 0.5 mM each potassium ferricyanide and ferrocyanide as an oxidation catalyst, and 0.1% Triton® X-100. The heptane-treated plant materials were incubated in the GUS reaction solution at 37 °C for 10-12 hours. The plant materials were then cleared as described previously by (Malamy and Benfey, 1997). In brief, both stained and unstained plant materials were transferred to small Petri dishes containing 0.24 N HCl in 20% methanol and incubated on a 57 °C heat block for 15 minutes. This solution was replaced with 7% NaOH in 60% ethanol for 15 minutes at room temperature. Samples were then re-hydrated for 5 minutes each in 40%, 20% and 10% ethanol, and infiltrated for 15 minutes in 5% ethanol, 25% glycerol. Cleared tissues were mounted in 50% glycerol on glass microscope slides and observed under a dissecting microscope and a light microscope.

Images were recorded with a digital camera (Nikon coolpix 995, Nikon Inc., New York, USA).

3.2.5 Resin embedding and cross-sectioning of root tissue

Ten-day old *Arabidopsis* seedlings harboring the *AtMKK6* promoter::*GUS* fusion or the *AtMPK13* promoter::*GUS* fusion were pre-stained for GUS activity as described in Section 3.2.4 for 10-12 hours, and then rinsed in 0.1 M sodium phosphate buffer pH 6.8. The roots were cut into small pieces, approximately 5 mm in length, on a wax plate and fixed in 2.5 % glutaraldehyde in 0.1 M sodium phosphate buffer, pH 6.8, overnight at 4 °C. The fixed root samples were then subjected to serial dehydration in 10%, 20%, 40% and 80% ethanol (about 15 minutes in each solution), while rotating slowly on a rotary shaker at room temperature, and then subjected to a final dehydration in 100% ethanol for 3 x 25 minutes, still rotating slowly at room temperature. The dehydrated samples were left in 100% ethanol at room temperature overnight. The samples were then infiltrated with Spurr's resin by passing them through a series of resin:ethanol mixtures, 1:3 (25% resin), 1:1 (50% resin), 3:1 (75% resin) and twice with 100% resin solution (1 hour in each mixture). The infiltrated samples were left rotating overnight in 100% resin solution, after which the resin solution was changed with a fresh 100% resin solution. The samples were then transferred to rubber or plastic molds, submerged in resin, and arranged as desired under the dissecting microscope for cross or longitudinal sectioning. The samples were then held at 60 °C for 16 hours to polymerize the resin. The polymerized resin blocks containing embedded root samples were trimmed and sectioned (1 µm thick) and the sections were mounted on glass slides for observation and image recording on a light microscope.

The Spurr resin solution was prepared following a recipe from the Electron Microscopy (EM) facility of the University of British Columbia. For a quantity of 50 mL, the following chemicals were mixed: 30.2 g noneyl succinic anhydride (NSA), 11.7 g vinylcyclohexene dioxide (ERL-4206), 8.2 g diglycidylether of polypropylene glycol DER-736 and 0.5 g dimethylamino ethanol (DMAE). (NSA was purchased from CANEMCO Inc and ERL-4206, DER-736 and DMAE were purchased from J.B.EM Services Inc).

3.2.6 Hormone treatments

Seeds from *AtMKK6* promoter- and *AtMPK13* promoter-*GUS* reporter plants were surface sterilized (see above in the Section 3.2.3.5) and then each individual seed was placed along a line on square agar-solidified MS medium plates containing ½ MS salt mix, 1% sucrose, (without B5 vitamins), 0.5 g/L MES, and 0.8 % agar, pH 5.7. The plates were sealed with 3M Micropore™ tape and the seeds were vernalized at 4 °C in the dark for 2-4 days. The plates were then placed in the growth room, mounted on edge so that the seedlings could grow vertically under 16h/8h light-dark cycle conditions at 22-24 °C for 9 days.

For the auxin transport inhibitor treatment, NPA (5 µM)-containing MS liquid medium (without B5 vitamins) (20 mL) was added to the 9-day old reporter seedlings, which were allowed to sit in the solution for 24 hours. The solution was then decanted from the plates. For the NPA and auxin (IAA) treatment or control, either NPA (5 µM) / IAA (1 µM)-containing liquid MS medium (without B5 vitamins) or the unsupplemented liquid MS medium (without B5 vitamins), respectively, was added to the reporter seedlings for 24 hours and then decanted. Histochemical GUS assays for all control and treatments were performed (24 hours post-treatment) as described in Section 3.2.4.

3.2.7 *E. coli* (DH5 α) competent cells

One mL of overnight culture of *E.coli* strain DH5 α was transferred to a sterile 250-mL flask containing 100 mL LB broth. The culture was grown for ~2.5 - 3 hours at 37 °C, shaking at 250 rpm (O.D.₅₅₀ = 0.45-0.55). The culture was chilled on ice for 30 minutes and centrifuged in sterile Oakridge tubes in a centrifuge rotor at 2500 x g for 10 minutes at 4 °C. The supernatant was then removed and the cell pellet was re-suspended by vortexing in 20 mL cold, filtered sterile Tfb I solution containing 30 mM potassium acetate, 100 mM rubidium chloride, 10 mM calcium chloride, 50 mM manganese chloride and 15 % glycerol, pH 5.8. The suspension was chilled on ice for 10 minutes and centrifuged at 2500 x g for 10 minutes at 4 °C. The supernatant was removed and the cell pellet was gently re-suspended by slowly pipetting up and down several times, in 2 mL cold, filtered sterile Tfb II solution containing 10 mM morpholinepropanesulfonic acid (MOPS), 10 mM rubidium chloride, 75 mM calcium chloride and 15 % glycerol, pH 6.5. The suspension was chilled on ice for 10 minutes and pipetted (100 μ L or 200 μ L aliquots) into sterile screw-cap microcentrifuge tubes. The competent cell suspension was frozen in liquid N₂ for 1-2 minutes and then stored at -80 °C.

3.2.8 *E. coli* transformation

Transformation of *E. coli* was performed according to instructions in (Sambrook *et al.*, 1989). A microcentrifuge tube of *E. coli* (strain DH5 α) competent cells was removed from the -80 °C freezer when needed. The cells were thawed and immediately transferred to an ice bath and stored on ice for 10 minutes. The competent cells were either kept in the same microcentrifuge tube or transferred to chilled, sterile polypropylene tubes (Falcon 2059, 17 mm x 100 mm), using chilled, sterile pipette tips, then stored on ice. DNA was added to the

competent cells and the tubes were swirled gently to mix their contents. The tubes were stored on ice for 30 minutes. The tubes were transferred to a 42°C water bath for exactly 90 seconds without shaking, and were then immediately transferred to ice bath to be chilled for 1-2 minutes. An 800 µL aliquot of LB medium containing appropriate antibiotic(s) was added to each tube and the tubes were incubated at 37 °C with shaking at 200 rpm for 45 minutes. A 200 µL aliquot of transformed competent cells was spread on each 90-mm Petri plate containing agar LB medium supplemented with appropriate antibiotic(s) and the plates were then incubated at 37 °C overnight. Colonies were observed on the plates within 12-16 hours.

3.2.9 *Agrobacterium* competent cells

One mL of overnight culture of *Agrobacterium* strain GV3101 was transferred to a sterile 250-mL flask that contained 50 mL LB broth with 25 mg/L rifampicin, 25 mg/L gentamycin. The culture was shaken for ~2.5 - 3 hours at 28 °C at 250 rpm (O.D.₅₅₀ =0.45-0.55). The culture was chilled on ice and centrifuged in sterile Oakridge tubes at 2500 x g for 5 minutes at 4 °C. The supernatant was removed, the cell pellet was re-suspended in 0.7 mL 20 mM CaCl₂, and 100 µL aliquots were distributed into sterile screw-cap microcentrifuge tubes. The competent cell suspension was frozen in liquid N₂ for 1-2 minutes and then stored at -80 °C.

3.2.10 Bacterial growth media

LB (Luria-Bertani) broth medium contained 10 g/L Tryptone Peptone (DIFCO Laboratories Inc., Catalogue No. 211705), 5 g/L Bacto™ yeast extract (DIFCO Laboratories Inc., Catalogue No. 212750) and 10 g/L NaCl, pH 7.0. LB agar plates consisted of similar

contents as LB broth medium plus 15 g/L Bacto™ agar (DIFCO Laboratories Inc.). All the media were autoclaved for 15-20 minutes at 15 lb / square inch prior to use.

3.2.11 *Arabidopsis* plant growth media

Unless otherwise noted, MS (Murashige and Skoog) liquid or agar-solidified media was used as *Arabidopsis* growth medium. The MS liquid media contains ½ strength MS salt mix (2.15 g/L) (Sigma, Catalogue No.M5524), 1 x MS vitamins (Sigma M3900) or 1 x B5 vitamins (containing 100 mg/L myo-inositol, 10 mg/L thiamine-HCl, 1 mg/L nicotinic acid, 1 mg/L pyridoxine-HCl), 1% sucrose and 0.5 g/L MES (2-[N-morpholino] ethanesulfonic acid (Sigma, Catalogue No. M2933), pH 5.7. The MS agar-solidified media contains half strength MS (2.15g/L), 1x B5 vitamins, 1% sucrose, 0.5 g/L MES and 0.8 % agar (Sigma, Catalogue No. A7002), pH 5.7.

3.2.12 Molecular cloning of glucocorticoid-inducible AtMKK6RNAi and AtMPK13RNAi DNA constructs and screening for the mutant plants

The double-stranded RNA interference (RNAi) constructs were made through a PCR-mediated approach. A minimal intron and the flanking regions (exon parts) of the fifth intron of *AtMPK6* were incorporated into the sense strand reverse primer (M. Samuel and G. Miles, personal communication). For the generation of AtMKK6RNAi, the sense strand was then amplified using a primer combination that generated an *Xho I* cleavage site and *EcoR I*-splice junction loop sequence on the opposite end of the PCR product, whereas the antisense strand was amplified using a primer combination that added *Spe I* and *EcoR I* sites on the opposite end of the PCR product. All primers used for generation of AtMKK6RNAi are presented in Table 3.2. These two PCR products were directionally cloned into *Xho I* / *Spe I*-digested

pTA7002 vector through triple ligation as presented in Figure 3.2, which resulted in an AtMKK6RNAi construct under the control of the glucocorticoid (dexamethasone)-inducible promoter (Figure 3.3 A). A diagram of the inducible RNAi system is presented in Figure 3.3 B. The AtMKK6RNAi construct was introduced into *Agrobacterium* and transformed to *Arabidopsis* plants (See Section 3.2.3.3 and 3.2.3.4).

Seeds of the T1 generation were germinated on MS agar plates containing 50 mg/L hygromycin B (Invitrogen, Catalogue No. 10687-010) and 50 mg/L vancomycin hydrochloride (Sigma, Catalogue No.V2002) (Vancomycin was added to control the *Agrobacterium* growth). The seeds were vernalized at 4 °C in the dark for 2-4 days prior to being grown under 16 h/8 h light-dark cycle conditions, at 22-24 °C (This temperature is critical to delay the growth of contaminating *Agrobacterium* in T1 seeds and it is an optimum temperature for growing *Arabidopsis* plants). Approximately 7-10 days post-germination, the positive T1 transformants that displayed resistance to hygromycin B (50 mg/L) were allowed to set seeds for T2 generation. T2 plants were screened for the seedlings that showed a difference in their phenotypes when grown in the presence or absence of 1 µM dexamethasone (dex) (Sigma, Catalogue No. D4902). Five independent T2 lines were recovered and selfed to produce T3 seeds. Two of the T3 homozygous lines that displayed a strong phenotype (line 13 and line 8) were carried through for detailed phenotypic analysis. Transgenic plants containing the empty vector, pTA7002, (line 4) were used as controls. An overview of the procedures for generating the glucocorticoid-inducible AtMKK6RNAi transgenic plants is presented in Figure 3.4.

In addition to my analysis of these AtMKK6RNAi transgenic plants, I also carried out lateral root analysis on three independent lines of AtMPK13RNAi transgenic plants, which

had been generated by Ankit Walia under my supervision, using the same protocol as I had for AtMKK6RNAi plants. The primers used for generation of the AtMKPK13RNAi construct are also presented in Table 3.2.

Table 3.2 Primers for the AtMKK6RNAi and AtMPK13RNAi constructs. Lower case letters represent the restriction enzyme sites.

Construct	Primer Name	Restriction Enzyme Site	Sequence (5'-3')	PCR Product Length (bp)
AtMKK6RNAi	KK6SF1	XhoI	ccgctcgagATGGTGAAGATCAAATCGAACTTGAAGCA	318
	KK6SR1	EcoRI + Intron	ccggaattcCTATGAGCTGCAAAAACTACTTACCTC (A minimal intron with its flanking exons sequence) TCAGCAGTAATTTCGAAATCAAGCTCC	
	KK6AF1	SpeI	ggactagtATGGTGAAGATCAAATCGAACTTGAAGCA	291
	KK6AR1	EcoRI	ccggaattcTCAGCAGTAATTTCGAAATCAAGCTCC	
AtMPK13RNAi	K13SF1	XhoI	ccgctcgagGAGATACTTAGAAGAGAGACGCTTTTCCC	441
	K13SR1	EcoRI + Intron	ccggaattcCTATGAGCTGCAAAAACTACTTACCTC (A minimal intron with its flanking exons sequence) AGACTCTCTCCAGACAAGCTCCTTG	
	K13AF1	SpeI	ggactagtGAGATACTTAGAAGAGAGACGCTTTTCCC	414
	K13AR1	EcoRI	ccggaattcAGACTCTCTCCAGACAAGCTCCTTG	

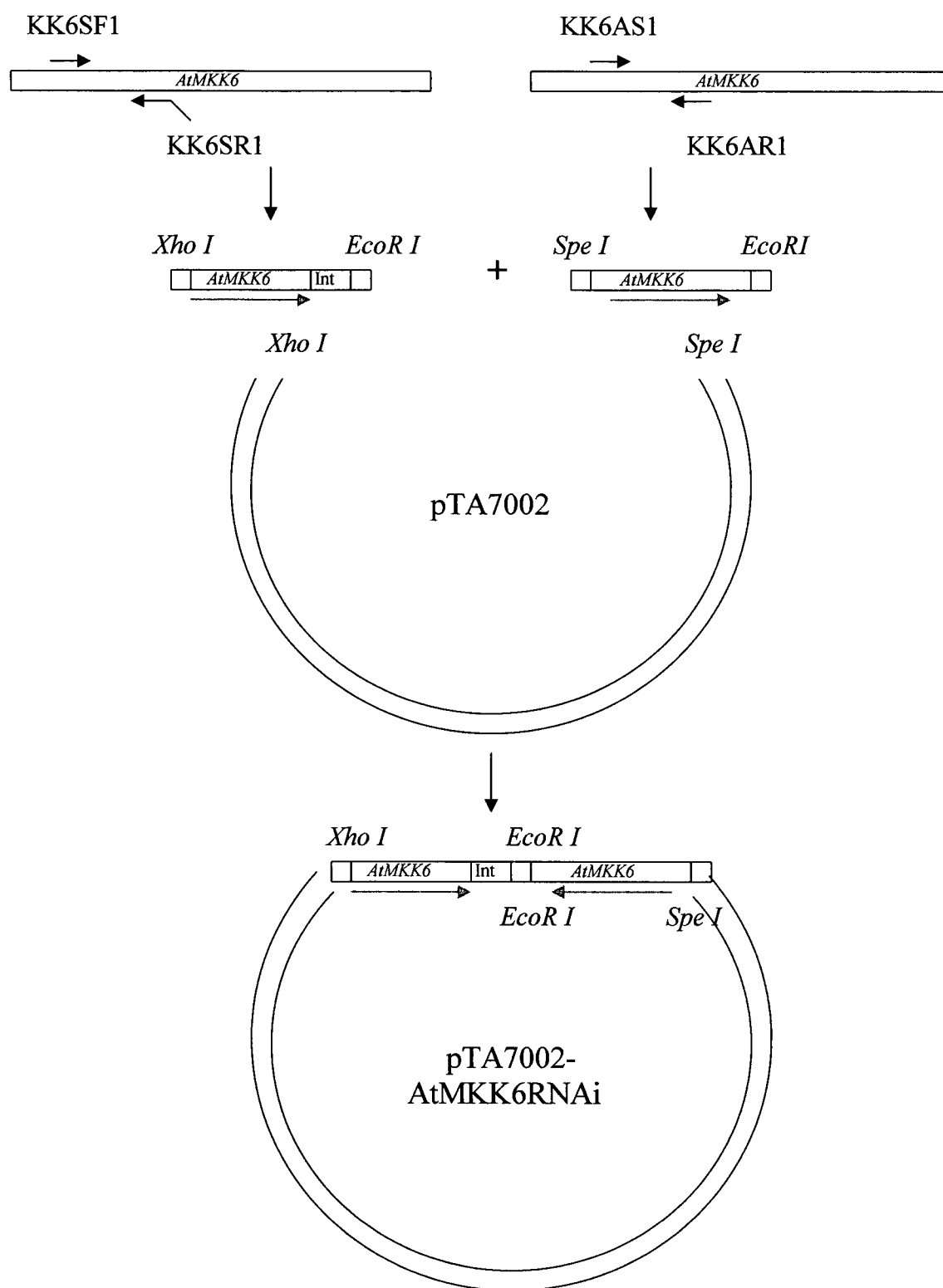
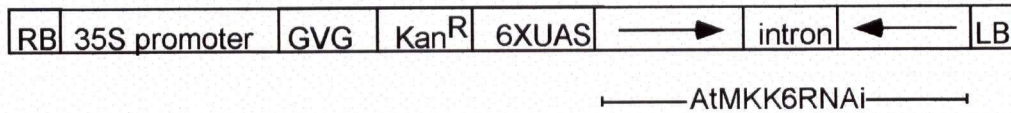


Figure 3.2 Schematic diagram describing construction of the AtMKK6RNAi construct
Int = Intron

A



B

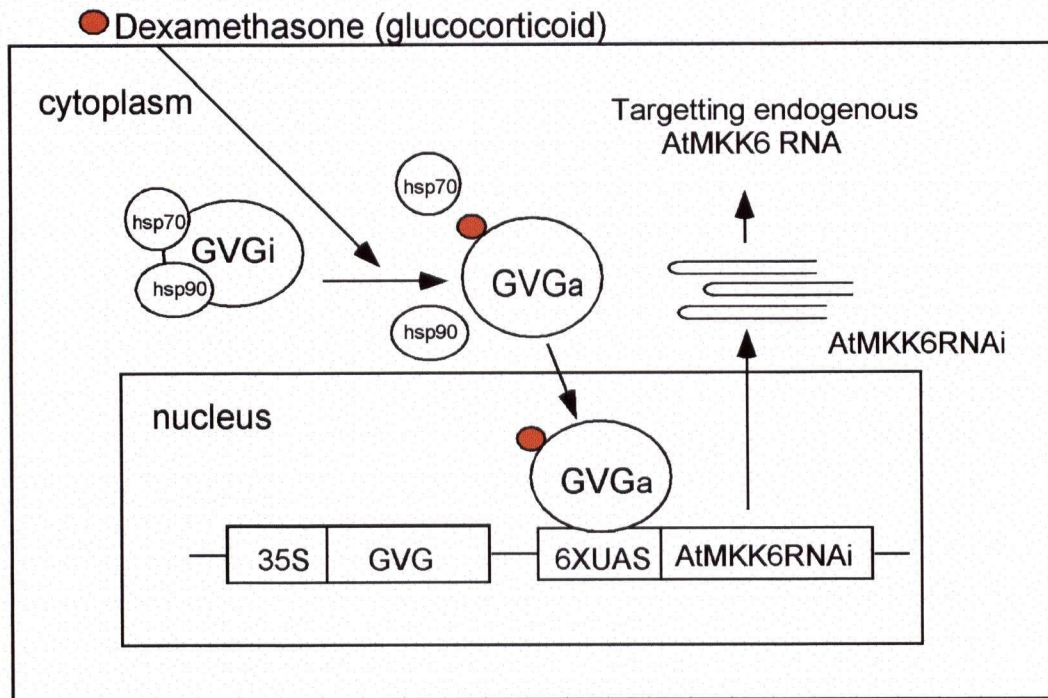


Figure 3.3 Glucocorticoid-inducible AtMKK6RNA interference (AtMKK6RNAi) system

(A) T-DNA region of the glucocorticoid-inducible AtMKK6RNAi DNA construct consisting of RB, right T-DNA border; 35S promoter; GVG, glucocorticoid-inducible transcription factor; Kan^R, kanamycin resistance gene; 6XUAS, GVG-regulated promoter; AtMKK6RNAi DNA construct; LB, left T-DNA border.

(B) A schematic diagram of dexamethasone-inducible AtMKK6RNAi system showing the activation of the AtMKK6RNAi and subsequent targeting of endogenous *AtMKK6* RNA. The T-DNA is shown in the nucleus where it has integrated into the plant nuclear genome. For simplicity, the Kan^R gene is omitted and the genes are shown in the left to right orientation. The GVG protein is made in the cytoplasm and retained there in an inactivated state (GVGi) by interaction with heat shock proteins, including hsp70 and hsp90. The binding of exogenously applied dexamethasone causes the disassociation of hsp proteins from GVGi. GVGi is then converted into an active state (GVGa), enters the nucleus and binds to the target promoter, 6XUAS, allowing the transcription of the AtMKK6RNAi to be initiated, which then silences endogenous *AtMKK6* expression (modified from (McNellis *et al.*, 1998).

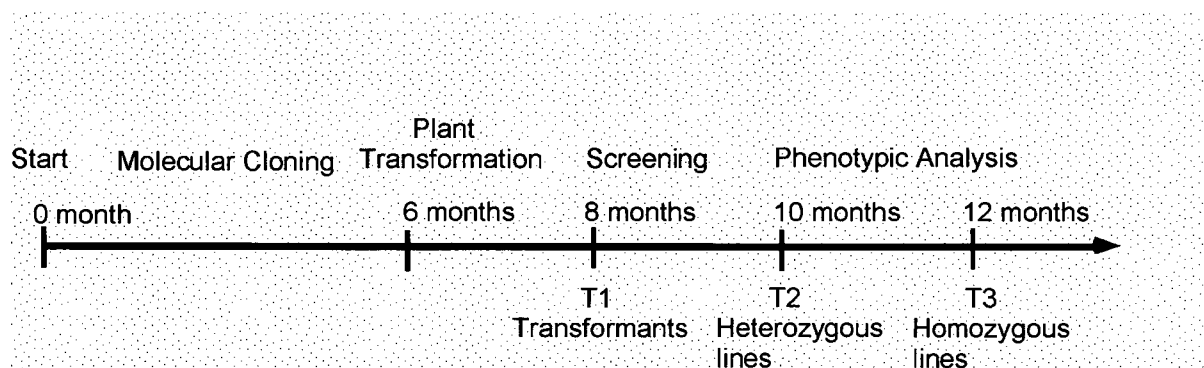


Figure 3.4 Overview of the process for generating *AtMKK6RNAi* transgenic plants

3.2.13 Phenotypic analyses and plant growth conditions

For observation of the plant phenotype in young seedlings, T3 seeds of the *AtMKK6RNAi*, and empty vector (pTA7002) lines were surface-sterilized and germinated on MS agar-solidified medium plates in the absence and presence of 1 μM dexamethasone (dex). The seeds were vernalized at 4 $^{\circ}\text{C}$ in the dark for 2-4 days prior to being grown at 22-24 $^{\circ}\text{C}$, under 16 h/8 h light-dark cycle conditions. On day 7, phenotypes were observed and recorded.

For observation of the *AtMKK6* suppression phenotype during growth and development, five sets of the *AtMKK6RNAi* and empty vector transgenic plants were grown in soil in a growth chamber, under 16 h/8 h light-dark cycle conditions at 22-24 $^{\circ}\text{C}$. For set one to set five, plants were sprayed with a solution containing 25 μM dex and 0.015 % Silwet L-77 at day 7, 14, 21, 28 and 35 post-germination, respectively, and photographs were taken at day 3-7 post-treatment. This phenotypic analysis of *AtMKK6RNAi* transgenic plants grown in soil was performed with two independent T3 lines and the entire process with each set was done in duplicate.

3.2.14 Lateral root analysis

AtMKK6RNAi, AtMPK13RNAi and empty vector (pTA7002) transgenic seeds were surface sterilized and stratified for 4 days at 4 °C in the dark. Four seedlings were grown vertically oriented on each MS agar plate at 22-24 °C under 16 h/8 h light-dark conditions. At day 7 post-germination, each of two sets of the same genotype seedlings were sprayed with either a filtered sterile solution containing 1 µM dex and 0.015 % Silwet L-77 or with a control solution containing only 0.015% Silwet L-77 (no dex). Photographs were taken at day 14 post-germination. These experiments were carried out in triplicate.

3.2.15 Total RNA extraction and RT-PCR analysis

Total RNA was extracted from one AtMKK6RNAi transgenic line (line 13, with strongest phenotype) and one empty vector line (line 4) using 10 days old seedlings, as described in Chapter 2, Section 2.2.3. For RT-PCR reactions, cDNA was synthesized from total RNA using a First-Strand cDNA Synthesis Kit (Amersham Biosciences, Catalogue No. 27-9261-01) according to the manufacturer's instructions. A total of 1 µg RNA was added to RNase-free water to produce a final volume of 8 µL. The RNA solution was heated for 10 minutes at 65 °C and then placed on ice. Bulk first-stand reaction mix (5 µL) containing reverse transcriptase, RNA guard, RNase/DNase-free BSA, dATP, dCTP, dGTP and dTTP in aqueous buffer, was added to the tube containing the heat-denatured RNA. One µL DTT solution (200 mM) and 1 µL oligo dT primers (Not I-d(T)₁₈) (0.2 µg) were added to the reaction mix, which was mixed by pipetting up and down several times. The reaction was then incubated at 37 °C for 1 hour.

The resulting cDNA was employed as the amplification template. PCR was performed using JumpStart™ REDTaq™ ReadyMix™ (Sigma, Catalogue No. P0982) and gene-specific primers designed to target the *AtMKK6*, *AtMKK1* or *AtMKK2* gene (the last two genes are closely related to *AtMKK6* gene), and a control gene, *Arabidopsis Histone H1* (*AtH1*). The primers used are presented in Table 3.3. Twenty microliters of PCR mixture (a final concentration of 0.6 units (10 µL) JumpStart™ REDTaq™ ReadyMix™, 1 µL first-stand cDNA, 0.1 µM each forward and reverse gene-specific primers, and forward and reverse *AtH1* primers) was cycled in a Biometra T-gradient thermo cycler as follows: denaturation (4 minutes, at 95°C), 32 cycles (30 seconds, at 95°C, 30 seconds at 57 °C, 2 minutes at 72 °C). The reaction was held for 10 minutes at 72°C after cycling and then maintained at 4 °C. The PCR amplification product was analyzed by 0.8 % agarose gel electrophoresis.

Table 3.3 Primers used for checking gene expression of the *AtMKK6*RNAi (line13) and empty vector (line 4) plants

Primer Name	Sequence (5'-3')	PCR product size (bp)
MKK1F	ccgctcgagcggATGAACAGAGGAAGCTTATGCCCTA	1079
MKK1R	ccgctcgagcggCTAGTTAGCAAGTGGGGGAATCAAAG	
MKK2F	ccgctcgagcggATGAAGAAAGGTGGATTCAGCAATAA	1116
MKK2R	ccgctcgagcggATGGTGATATTATGTCTCCCTTGTAG	
MKK6F	cgcgatccgagATGGTGAAGATCAAATCGAACTTG	1095
MKK6R	ccgctcgagcggTTATCTAAGGTAGTTAACAGGTGG	
AtH1F	ccggaattccggGGTTAAAGTCAAAGCTTCTTTTAAGA	726
AtH1R	ccgctcgagcggGAGTGAAGAAACCATCACATTATA	

3.3 Results

3.3.1 Histochemical localization of GUS activities driven by *AtMKK6* and *AtMPK13* promoters during plant growth and development

The 5'-upstream regions of the *AtMKK6* and *AtMPK13* genes were fused to the β -glucuronidase (*GUS*) reporter gene and the resulting constructs were transformed into *Arabidopsis* plants. The patterns of *GUS* activity were surveyed in 3-day, 5-day, 10-day, 15-day, 27-day, and 35-day plants derived from three independent transformation events for each construct. Transgenic plants harboring pCAMBIA1381Z, a promoterless::*GUS* fusion construct, were used as a negative control (Figure 3.5), and transgenic plants harboring pCAMBIA1301, a 35S promoter::*GUS* fusion construct were used as a positive control (Figure 3.6).

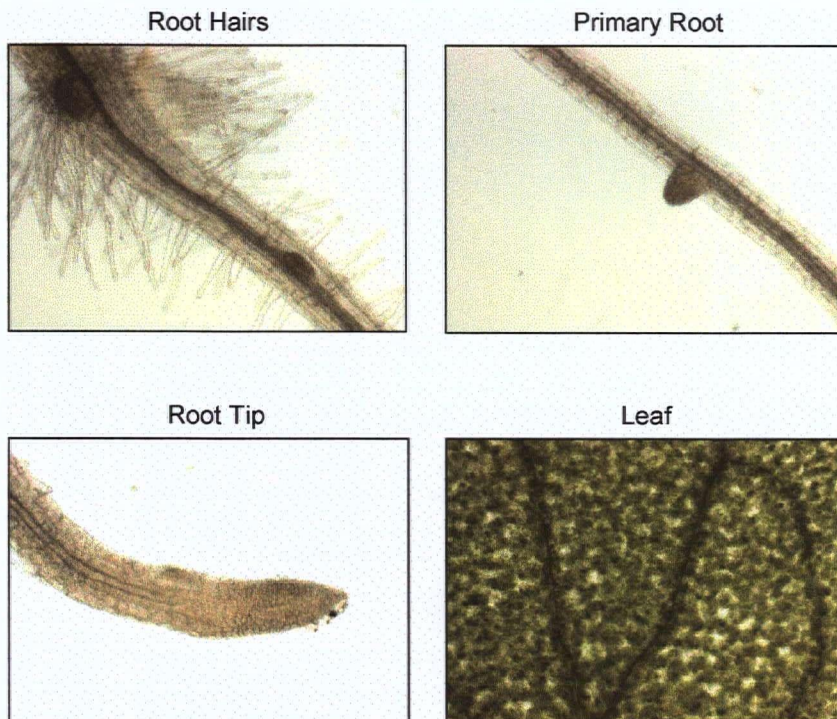


Figure 3.5 Promoterless-GUS activity as a negative control for GUS assay. pCAMBIA1381Z-containing plants showed no blue GUS staining in any plant tissues.

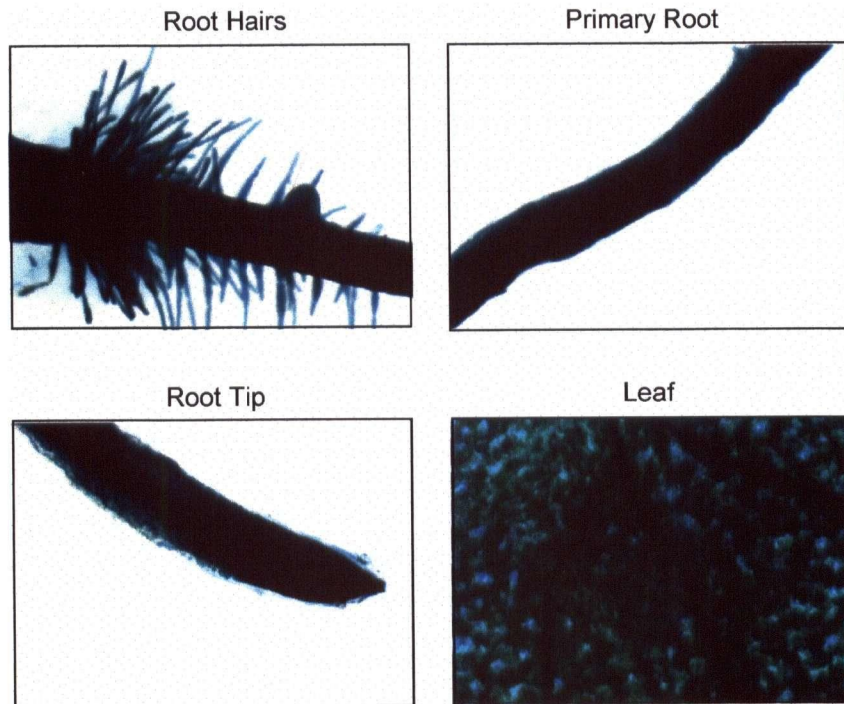


Figure 3.6 35S promoter-GUS activity as a positive control for GUS assay
pCAMBIA1301-containing plants showed strong GUS staining in almost
all plant tissues.

3.3.2 *AtMKK6* promoter::*GUS* activity distribution during plant growth and development

The spatial and temporal patterns of histochemical GUS activity during plant growth and development in transgenic *Arabidopsis* carrying the *AtMKK6* promoter::*GUS* fusion gene, are shown in Figure 3.7. Overall, GUS activity was observed most strongly in the vascular tissue of many tissues/organs including cotyledons, hypocotyls, leaves, roots and inflorescence (Figure 3.7). No GUS staining was observed in the roots of the 3-day-old seedling (not shown) or 5-day-old seedlings (Figure 3.7 A). However, GUS activity appeared

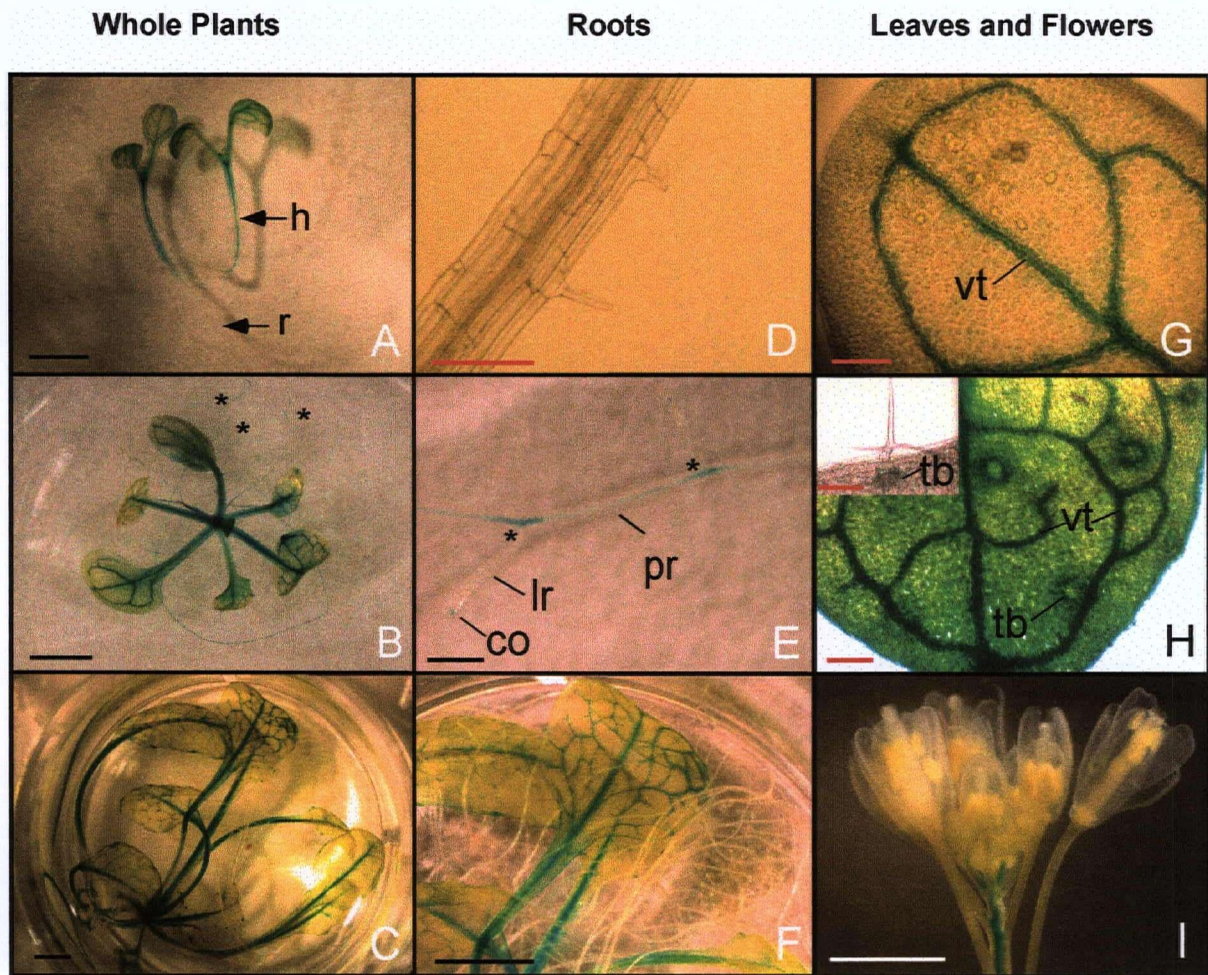


Figure 3.7 Histochemical localization of GUS activity in *AtMKK6* promoter::*GUS* reporter plants through development from 3 days to 35 days.

(A) 5-day-old seedlings, blue GUS staining was detected in hypocotyls (h), but was barely detected in young roots (r); (B) A 15-day-old plant, GUS staining was detected in both shoots and roots; (C) A 27-day-old plant, GUS staining was mainly detected in shoots, not roots; (D) A primary root from a 5-day-old seedling showing no GUS staining; (E) Lateral roots (lr) emerged from a primary root (pr) from a 10-day-old plant, GUS staining was detected along the primary root region where lateral roots emerged and also at columella cell area (co); (F) Roots and leaves from a 27-day-old plant; (G) Light microscopic view of a cotyledon from a 5-day old seedling showing GUS staining in vascular tissue (vt); (H) Light microscopic view of a leaf from a 10-day-old seedling showing GUS staining in trichome bases (tb) and in vascular tissue (vt); (I) A cluster of flowers from a 35-day-old plant; GUS staining is shown in blue. In B and E, asterisks indicate adventitious root primordia or emerged lateral roots from a primary root. Scale bars are located at the bottom left of each picture. Black and white bars = 2 mm, red bars = 0.2 mm.

in the vascular cylinders of the older roots of 10- and 15-day-old seedlings (Figure 3.7 E and B, respectively). GUS staining in the roots was most prominent at the sites of lateral root emergence in 10-day- and 15-day-old seedlings (Figure 3.7 E and B, respectively). In addition, strong GUS activity was observed in the bases of trichomes on leaves from 10-day-old seedlings (Figure 3.7 H). By 27 days, the GUS activity in primary roots had almost entirely disappeared (Figure 3.7 F). However, in leaves, strong GUS activity still remained in the vascular tissue after 27 days (Figure 3.7 F). At 35 days, only weak GUS activity could be detected, restricted to the floral tissues (Figure 3.7 I) and siliques (not shown).

3.3.3 The *AtMKK6* promoter activity and lateral root formation

Histochemical GUS staining of root cross-sections from 10-day-old seedlings confirmed the vascular-specific expression pattern of the *AtMKK6* promoter in roots (Figure 3.8 A). In primary roots, GUS staining was highest at sites along primary roots where new lateral roots were formed (Figure 3.8 A), and was also detected in the vascular tissue of newly emerged lateral roots. Transverse sections of roots revealed that the *AtMKK6* promoter drove GUS activity not only in the central vascular cylinder, but also in the layer of pericycle cells surrounding the vascular cylinder in primary roots (Figure 3.8 B and C). No GUS activity was detected in other cell types, such as the epidermal, cortical and endodermal cells in roots (Figure 3.8 B and C).

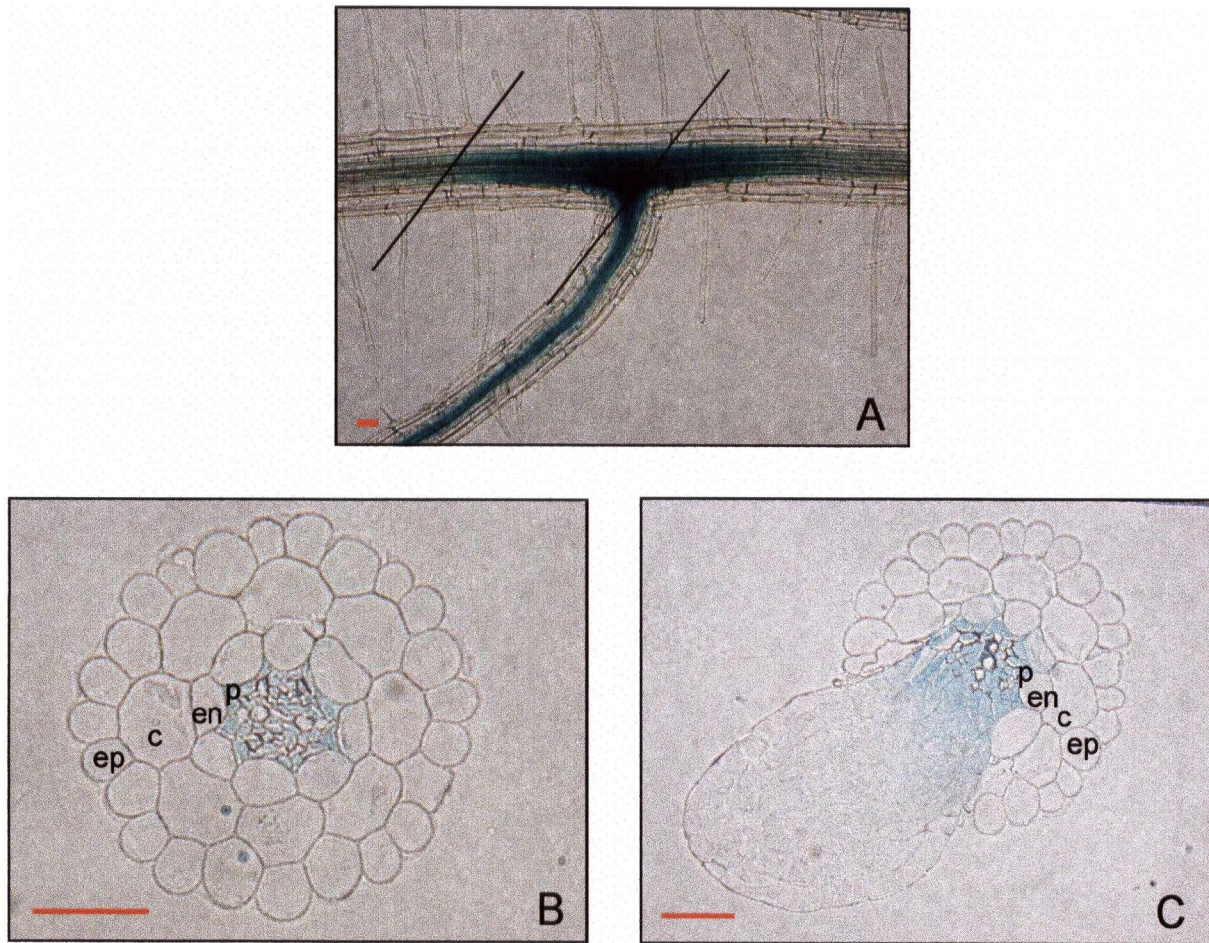


Figure 3.8 Detailed examination of 10-day old seedlings of *AtMKK6* promoter::*GUS* reporter plants.

(A) A root; (B) A transverse section of a primary root at the vicinity of lateral root formation and (C) A transverse section of a primary root at the site where a lateral root emerged, ep = an epidermal cell layer, c = a cortical cell layer, en = an endodermal cell layer, p = a pericycle cell layer. GUS staining is shown as blue. Red bars = 0.02 mm

3.3.4 *AtMPK13* promoter::*GUS* activity throughout plant growth and development

The spatial and temporal patterns of histochemical GUS activity during plant growth and development in transgenic *Arabidopsis* carrying the *AtMPK13* promoter::*GUS* fusion gene are shown in Figure 3.9. GUS activity appeared strongly in vascular tissue of shoots of 3-day-old seedlings (not shown) as well as in seedlings from 5-day-old to 35-day-old (Figure 3.9 A-E). In the root tips, GUS staining was confined to the collumella cells of the root cap and elongation zone, but was not observed in the apical meristem zone in which cell division occurs (Figure 3.9 K and L). As in the shoots, strong GUS staining was also observed in vascular tissue of roots of almost all ages (Figure 3.9 A-D, F, H, I, and K). In 35-day-old plants, *AtMPK13* expression was clearly associated with lateral root formation, although overall GUS staining in roots was substantially diminished at this point (Figure 3.9 E and J). Similar to the GUS activity pattern observed in the *AtMKK6* promoter::*GUS* reporter plants (Figure 3.7 E), GUS activity in the *AtMPK13* promoter::*GUS* reporter plants appeared most strongly at sites along primary roots where lateral root primordia were formed in 10-day-old seedlings (Figure 3.9 G), 15-day old seedlings (not shown) and 27-day-old seedlings (Figure 3.9 I). In addition, the GUS staining was detected in the trichomes of both leaves and stems (Figure 3.9 O) and was observed in a ring of cells at the bases of leaf trichomes (Figure 3.9 N). In flowers, GUS staining was clearly observed in the pistil (Figure 3.9 Q), and in the vascular tissue of inflorescence stems and sepals, but not in the vasculature of the petals (Figure 3.9 P). GUS staining was also found in stamen filaments but not in anthers (Figure 3.9 R). In siliques (fruits), GUS staining was detected in the placenta (Figure 3.9 S and T).

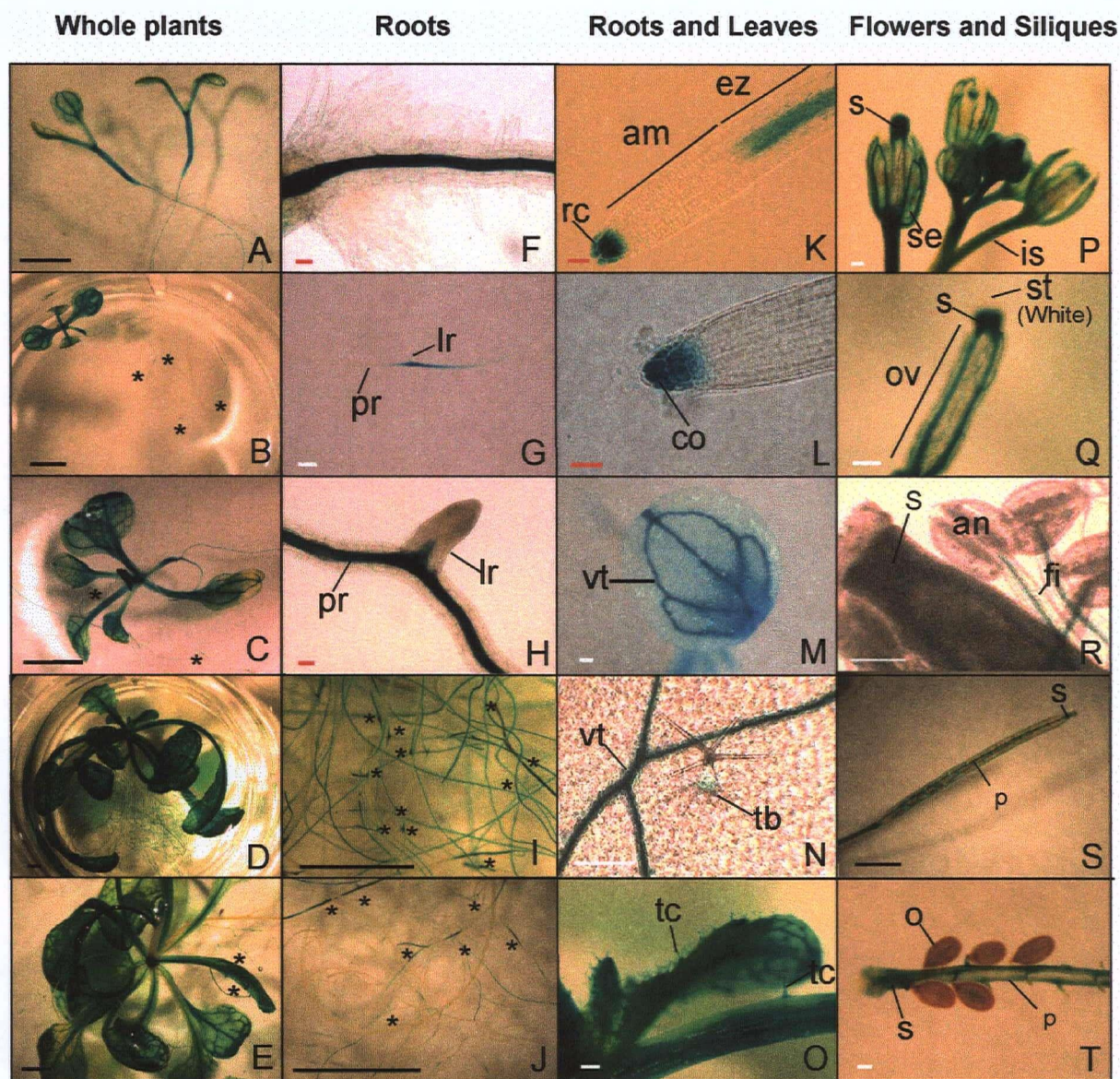


Figure 3.9 Histochemical localization of GUS activity in *AtMPK13* promoter::*GUS* reporter plants through development from 3 days to 35 days.

(A) 5-day-old seedlings; (B) A 10-day-old seedling; (C) A 15-day-old plant; (D) A 27-day-old plant; (E) A 35-day-old plant; (F) A primary root from a 10-day-old seedling; (G) A lateral root (lr) emerged from a primary root (pr) from a 10-day-old seedling; (H) Light microscopic view of an emerged lateral root (lr) from a primary root (pr); (I) Roots from a 27-day-old plant; (J) Roots from a 35-day-old plant; (K) A root tip including root cap (rc), apical meristem (am) and elongation zone (ez); (L) GUS staining at columella cells (co) of a root tip from a 27-day-old plant; (M) A view of the vascular tissue (vt) of a cotyledon from a 10-day-old seedling; (N) A view of a trichome on a leaf from a 10-day old seedling, GUS staining is shown in a trichome base (tb) and vascular tissue (vt); (O) Trichomes (tc) of leaves and of leaf stems from a 27-day-old plant; (P) A cluster of flowers showing GUS

3.3.5 AtMKK6, auxin and lateral root formation

Auxin is known to affect lateral root formation, probably by establishing a population of rapidly dividing pericycle cells (Laskowski *et al.*, 1995). Developing lateral root primordia are thought to receive the endogenous auxin indole-3-acetic acid (IAA) through directed (polar) auxin transport (Reed *et al.*, 1998). Polar auxin transport depends on the asymmetric localization in plant cell membranes of a protein called PIN-FORMED (PIN), which is an auxin transport facilitator (Galweiler *et al.*, 1998). The direction of polar auxin transport varies depending on where PIN proteins are localized in plant cell membranes. For example, in the central part of roots, PIN proteins are localized in the cellular basal membranes and auxin flow is directed downward. There is contradictory evidence concerning the direction of the polar auxin transport associated with lateral root formation. In roots, it has been proposed that plants use the polar auxin transport to move IAA from the base of root toward the root tip via the central cylinder (acropetal) and from the root tip toward the root-shoot junction via the epidermal and cortical cells (basipetal) (Rashotte *et al.*, 2000). N-1-naphthylphthalamic acid (NPA), a polar auxin transport inhibitor, blocks acropetal polar transport of shoot-derived IAA, causing a reduction in IAA level in root and the arrest of lateral root emergence (Reed *et al.*, 1998). In contrast to the conclusions of Reed *et al.*, 1998, it has also been shown that NPA blocks basipetal IAA movement from root tip, while also arresting lateral root formation (Casimiro *et al.*, 2001). I confirmed that NPA caused diminished lateral root formation (Figure 3.11). I also observed that the *AtMKK6* promoter contains a putative auxin-responsive element, AuxREPSIAA4 (KGTCCCAT) (Ballas *et al.*, 1993) at nucleotide position -490, (+ strand) (Figure 3.10), suggesting that auxin might be a regulator of *AtMKK6* expression. To clarify *AtMKK6*/auxin/lateral root formation relationship, I

performed two experiments; blocking and adding auxin to the *AtMKK6* promoter::*GUS* seedlings.



Figure 3.11 NPA effect on lateral root formation in 17-day-old wild-type *Arabidopsis* seedlings

- (A) Lateral roots of plants grown on the unsupplemented MS agar medium
- (B) Diminished lateral root formation in plants grown on MS agar medium containing 5 μ M NPA. White bars = 10 mm.

3.3.6 Blocking polar auxin transport with NPA reduces *AtMKK6* promoter::*GUS* activity.

I grew *AtMKK6* promoter::*GUS* seedlings for 10 days and treated them with and without NPA for 24 hours, before analyzing them for GUS activity. As observed previously, plants grown in the absence of NPA showed strong GUS activity in the vascular tissue of the primary roots, with the most intense staining at the sites where lateral roots were formed (Figure 3.12). In contrast, roots on plants grown in the presence of NPA showed a substantial reduction in GUS activity, accompanied by lower numbers of lateral roots (Figure 3.12).

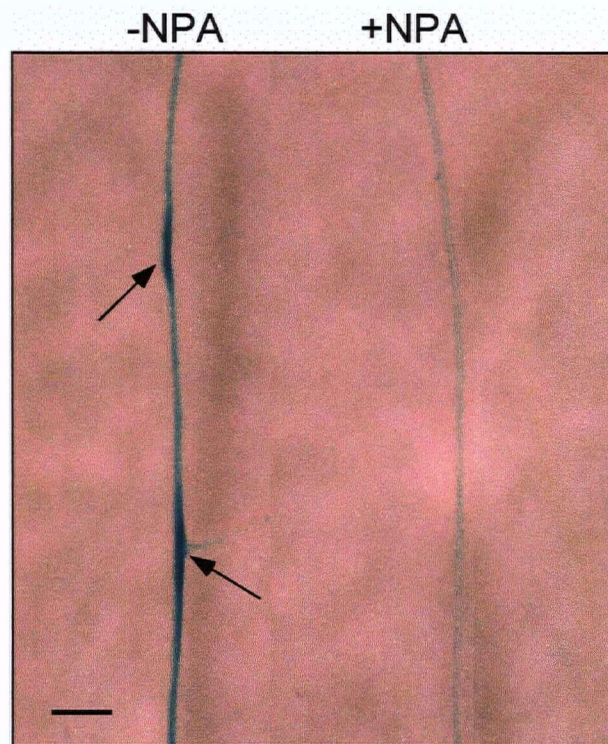


Figure 3.12 NPA (5 μ M) effect on GUS activity in 10-day-old *AtMKK6* promoter::*GUS* reporter seedlings.

Arrows indicate primary root sites from which lateral roots emerged.
A black bar = 0.2 mm.

3.3.7 Auxin can reverse the block of *AtMKK6* promoter::*GUS* activity by NPA in both vascular tissue and pericycle cells.

I have demonstrated in the previous sections that the pattern of GUS activity driven by *AtMKK6* promoter is associated with lateral root formation and that application of NPA, an auxin transport inhibitor, produces a reduction in the *AtMKK6* promoter activity. I hypothesized that optimal levels of auxin could positively regulate the transcriptional control of the *AtMKK6* gene and that optimal levels of AtMKK6, in turn, could control lateral root development. This hypothesis predicted that co-treatment with NPA and IAA would restore both GUS activity in roots and lateral root development of *AtMKK6* promoter::*GUS* reporter plants. To test this hypothesis, I grew *AtMKK6* promoter::*GUS* seedlings for 9 days and treated them with NPA alone and NPA together with IAA for 24 hours before subjecting to GUS activity assay. Roots of plants grown in the presence of NPA alone showed only weak GUS activity in vascular tissue. Strikingly, GUS staining was absent from the pericycle cell layer in primary roots and diminished in almost all dividing pericycle cells of LRP. This pattern was associated with the contribution of fewer pericycle cells to the LRP, leading to an abnormal LRP shape (Figure 3.13 A and B). By contrast, roots of plants grown in the presence of both NPA and IAA showed a substantial level of GUS activity in vascular tissue, and in both inactive pericycle cells and actively dividing pericycle cells of LRP, which also had a normal LRP shape (Figure 3.13 C-F). Closer examination of the *AtMKK6* promoter::*GUS* activity in NPA/IAA-treated roots revealed that the restored GUS activity was localized not only in the root vascular tissue, but also in the pericycle cell layer of primary roots (Figure 3.13 C, D and E). Moreover, GUS staining in the LRP was concentrated in the actively dividing pericycle cells in LRP at the early stage of the lateral

root initiation (Figure 3.13 E, C and D in stages V, VI and VIII, respectively, according to Malamy and Benfey 1997 and Casimiro *et al.*, 2003). These results indicate that exogenous auxin can overcome the block of *AtMKK6* promoter::*GUS* activity by NPA in vascular tissue, and in both inactive pericycle cells and actively-dividing pericycle cells. The increased GUS activity in the NPA/IAA-treated roots was correlated with a substantial increase in lateral root numbers. Roots treated with NPA alone had 3-4 primordia per seedling but roots treated with NPA and IAA had 10-22 primordia/lateral roots per seedling. Notably, only early stage primordia were detected in the NPA-treated roots (Figure 3.13 A and B), whereas both early stage primordia and fully developed lateral roots were detected in the NPA/IAA-treated roots (Figure 3.13 C-F).

The expression pattern of the *GUS* gene directed by the *AtMKK6* promoter changed dramatically when the young primordia continued to form fully developed lateral root organs (Figure 3.13 F). This observation is consistent with the known organization of specialized cells and tissues during lateral root development (Malamy and Benfey, 1997). In fully developed lateral roots, GUS staining was localized in vascular tissue and in the root cap cells, but not in the meristematic zone of lateral roots, even though this is also a site of frequent cell-division (Figure 3.13 F). Notably, the GUS staining pattern in mature lateral roots of *AtMKK6* promoter::*GUS* seedlings (Figure 3.13 F) was similar to that in mature lateral roots of *AtMPK13* promoter::*GUS* seedlings (Figure 3.9 K). Together, these data indicate that *AtMKK6* and *AtMPK13* are likely to be specifically involved in cell-division of pericycle cells during LRP initiation in lateral root formation.

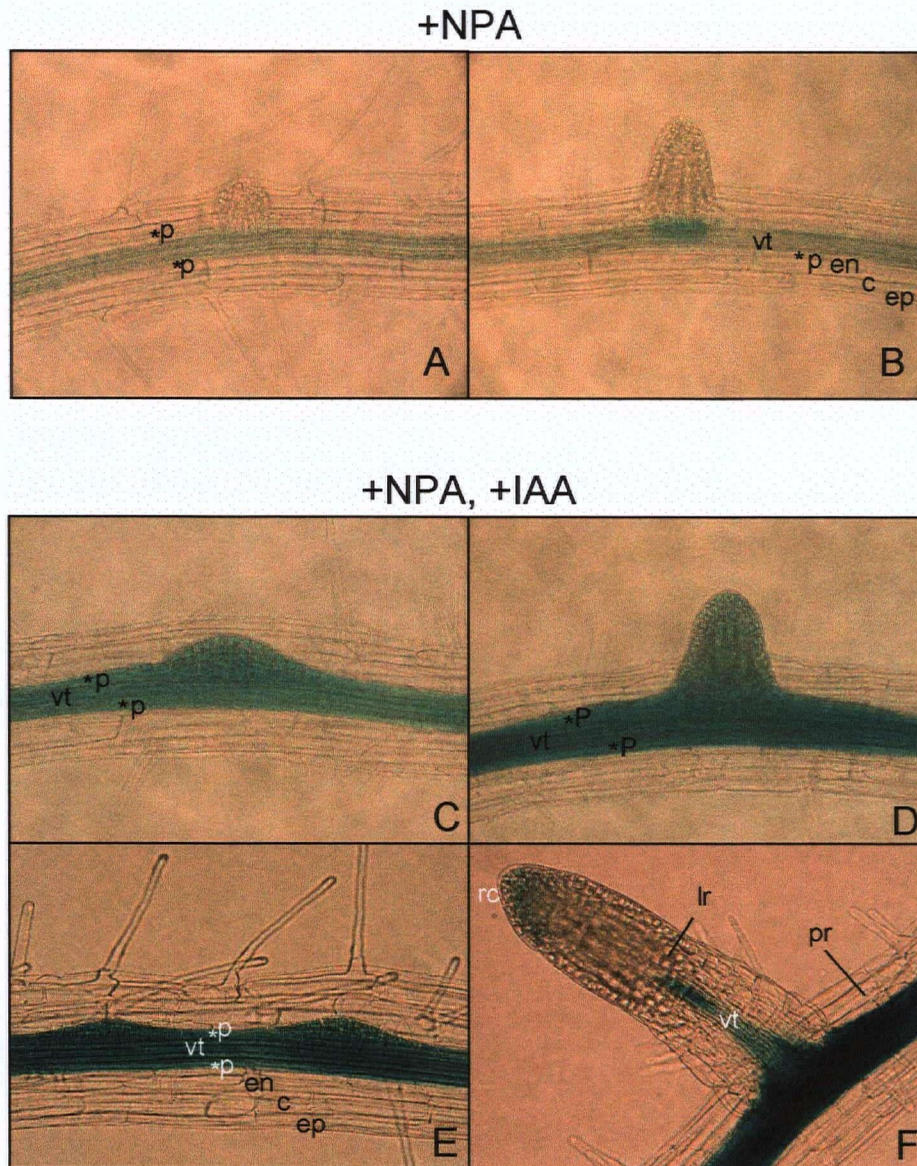


Figure 3.13 Histochemical localization of GUS activity in lateral root primordia (LRP) and lateral roots of AtMKK6 promoter::*GUS* reporter seedlings, upon NPA (5 μ M) treatment and co-treatment of NPA (5 μ M) and IAA (1 μ M).

(A) and (B) LRP in the presence of NPA alone, GUS staining is shown to be faint in vascular tissue (vt) and absent in pericycle cell layer (p) of the primary roots; (C), (D), (E) LRP in the presence of both NPA and IAA. GUS staining is shown in vascular tissue, in pericycle cell layer (p) of primary roots and in actively dividing pericycle cells of LRP; (F) A fully developed lateral root (lr) emerged from a primary root (pr). GUS staining is shown in cells of root cap and in vascular tissue (vt) of both lateral and primary roots; vt = vascular tissue, ep = epidermis, c = cortex, en = endodermis and p = pericycle; Asterisks indicate location of pericycle cell layer. GUS staining is shown as green/blue.

3.3.8 AtMPK13 and auxin

The *AtMPK13* promoter was found to contain two putative auxin-responsive elements, AuxRR-core (GGTCctt and GGTCcct) (Sakai *et al.*, 1996) at nucleotide position -893, (+) strand and -330, (-) strand, respectively (Figure 3.14). Similar to the pattern observed in the *AtMKK6* promoter::*GUS* seedlings, the *AtMPK13* promoter::*GUS* seedlings showed a dramatic decrease in GUS activity in actively-dividing pericycle cells of LRP upon NPA treatment (Figure 3.15 A). However, in contrast to *AtMKK6* promoter::*GUS* seedlings, GUS staining of *AtMPK13* promoter::*GUS* seedlings remained strong in inactive cells of pericycle layer upon NPA treatment (Figure 3.15 A), indicating that NPA cannot block the activity of *AtMPK13* promoter in these non-dividing cells. The diminished GUS activity resulting from NPA treatment was associated with abnormal growth of LRPs, which contained fewer cells (Figure 3.15 A). *AtMPK13* promoter::*GUS* staining was restored in actively dividing pericycle cells when the seedlings were co-treated with both NPA and IAA. (Figure 3.15 B to E), and an increased number of new lateral root primordia were also observed (Figure 3.15 C).

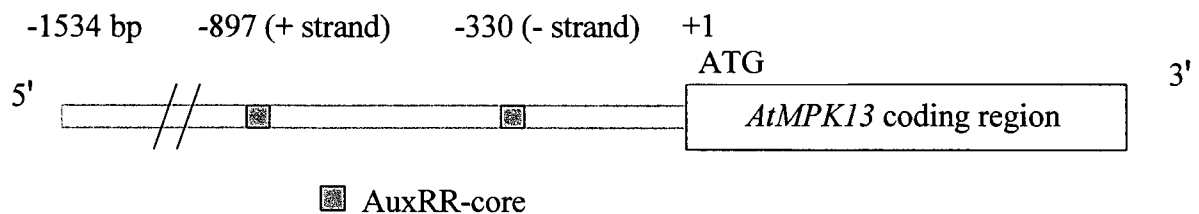


Figure 3.14 Schematic illustration showing the location of two putative auxin-responsive sequences AuxRR-core in the AtMPK13 promoter region (1534 bp).

The AtMPK13 promoter sequence analysis (Lescot et al., 2002) revealed the presence of a putative auxin-responsive element, AuxRR-core (GGTCctt and GGTCcct) (Sakai et al., 1996) at nucleotide position -893, (+) strand and -330, (-) strand, respectively -490.

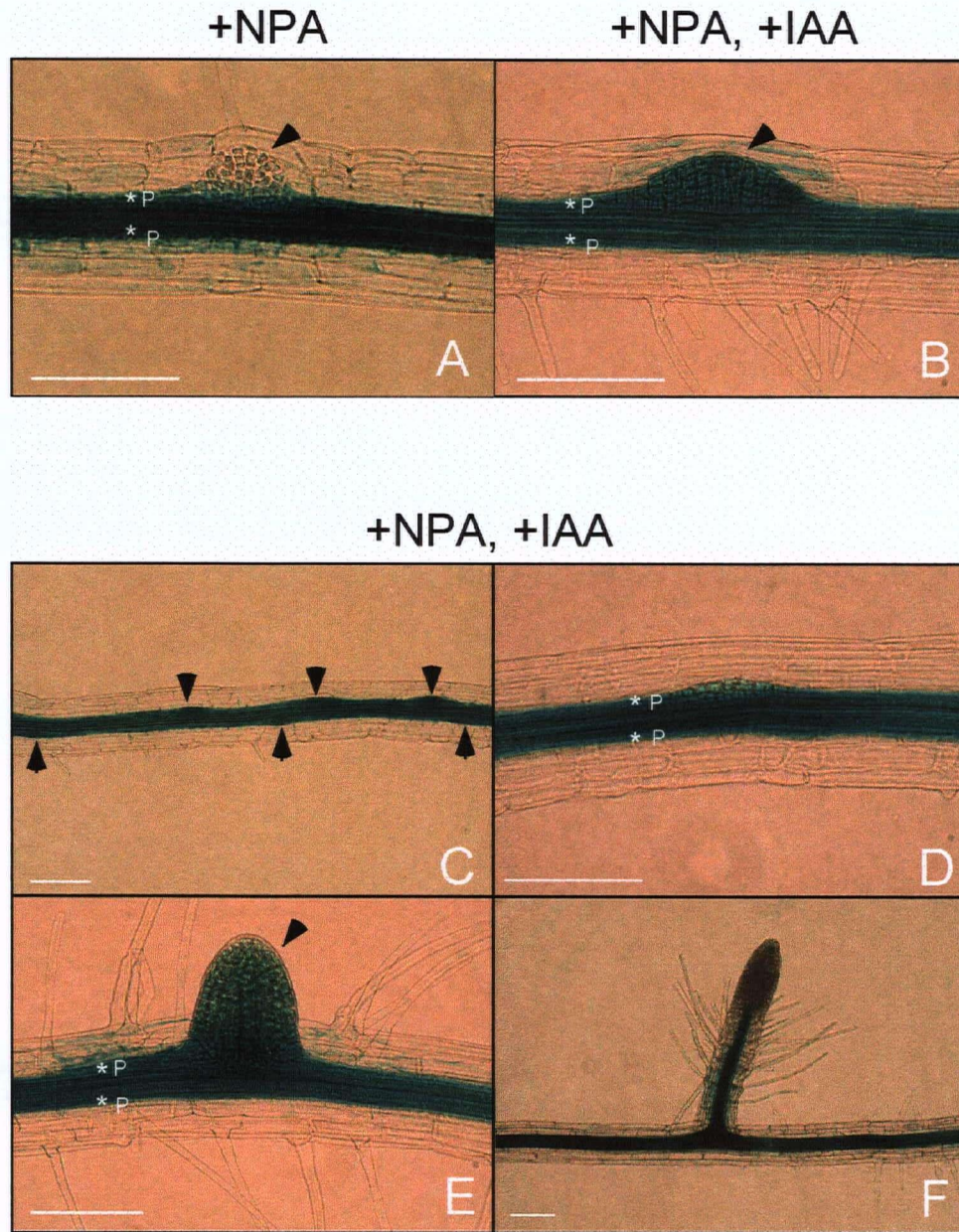


Figure 3.15 Histochemical localization of *AtMPK13* promoter::*GUS* activity in LRPs and lateral roots from 13-day-old reporter seedlings, upon treatment of NPA alone (5 μ M) and co-treatment of NPA (5 μ M) and IAA (1 μ M).

(A) and (B) A lateral root primordium in the presence of NPA alone and in the presence of both NPA and IAA, respectively.

(C) to (F) Different stages of lateral root development emerged from a NPA/IAA-treated roots. Arrowheads indicate LRP. White bars = 0.2 mm. GUS staining is shown as green/blue.

3.3.9 Phenotypic analysis of *AtMKK6*RNAi transgenic plants

To further investigate the biological function of *AtMKK6* in plants, and to specifically ask whether the *AtMKK6* gene product is required for lateral root development, I generated loss-of-function *AtMKK6* mutant plants using a glucocorticoid-inducible RNA interference (RNAi) system. In this inducible RNAi system, the silencing mechanism can be induced by application of low levels of dexamethasone, a glucocorticoid hormone analogue (Figure 3.3 B). Transgenic seedlings of the T2 generation were screened for positive transformants by growing them in the absence and presence of 1 μ M dexamethasone (dex). Positive transformants displayed an abnormal phenotype on dex-containing media, whereas the same genotypes grown in the absence of dex showed a phenotype similar to that of empty vector lines grown in the same growth conditions. Five *AtMKK6*RNAi lines were recovered in this process, all of which showed a similar “hairy” phenotype with various degrees of abnormality when induced with dex. Two lines with the strong abnormal phenotype were used for further detailed analysis.

I used RT-PCR to examine *AtMKK6* transcript levels in the *AtMKK6*RNAi mutant (line 13) that displayed strongest phenotype to determine the specificity of the gene silencing. The abundance of the *AtMKK6* transcripts in the *AtMKK6*RNAi plants was ~23% decreased when the RNA silencing was induced by dexamethasone (Figure 3.16), whereas the abundance of the transcripts of *AtMKK1* and *AtMKK2*, which share high sequence homology to *AtMKK6*, was not significantly changed by dex treatments (data not shown).

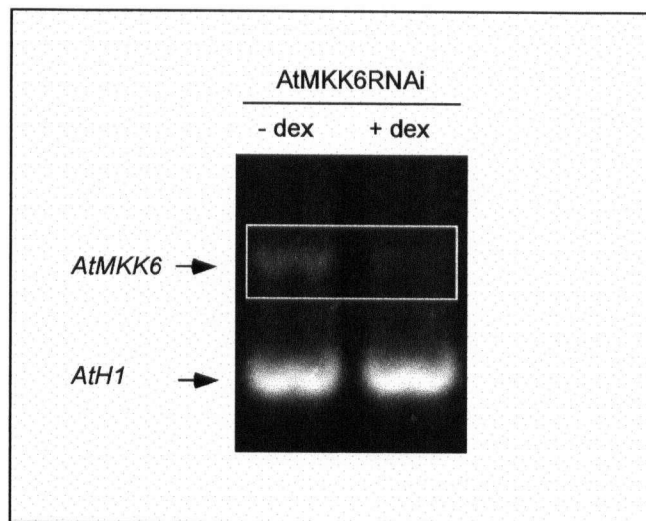


Figure 3.16 RT-PCR analysis showing a ~23% reduction in the *AtMKK6* transcript level in 10-day-old *AtMKK6RNAi* seedlings (line 13) when the gene silencing was induced by 1 μ M dexamethasone (dex) treatment as compared to that without dex treatment (control).

AtMKK6 gene-specific primers and *Arabidopsis* histone H1 (*AtH1*) primers, a control for equal sample loading, were used. The experiments were done in duplicate. The expression signals for both *AtMKK6* and *AtH1* genes were quantified and *AtH1* expression signals were used for normalization.

As expected, lateral root development was negatively affected in dex-inducible *AtMKK6RNAi* plants. *AtMKK6RNAi*-suppressed seedlings showed a 82 % reduction in lateral root numbers (Figure 3.20). Interestingly, root hair development was also strongly affected in dex-inducible *AtMKK6RNAi* plants. *AtMKK6RNAi* seedlings grown on plant growth media in the presence of 1 μ M dex for 7-10 days showed a “hairy” phenotype (Figure 3.17 A, 3.18 A and 3.19 B) with far more root hairs compared to control seedlings from empty vector line (Figure 3.19 A and B). Thus, *AtMKK6* may normally be a negative regulator of root hair development. In mature plants, *AtMKK6* suppression resulted in early senescence in leaf, stem and floral tissues (Figure 3.17 C and Figure 3.18 C).

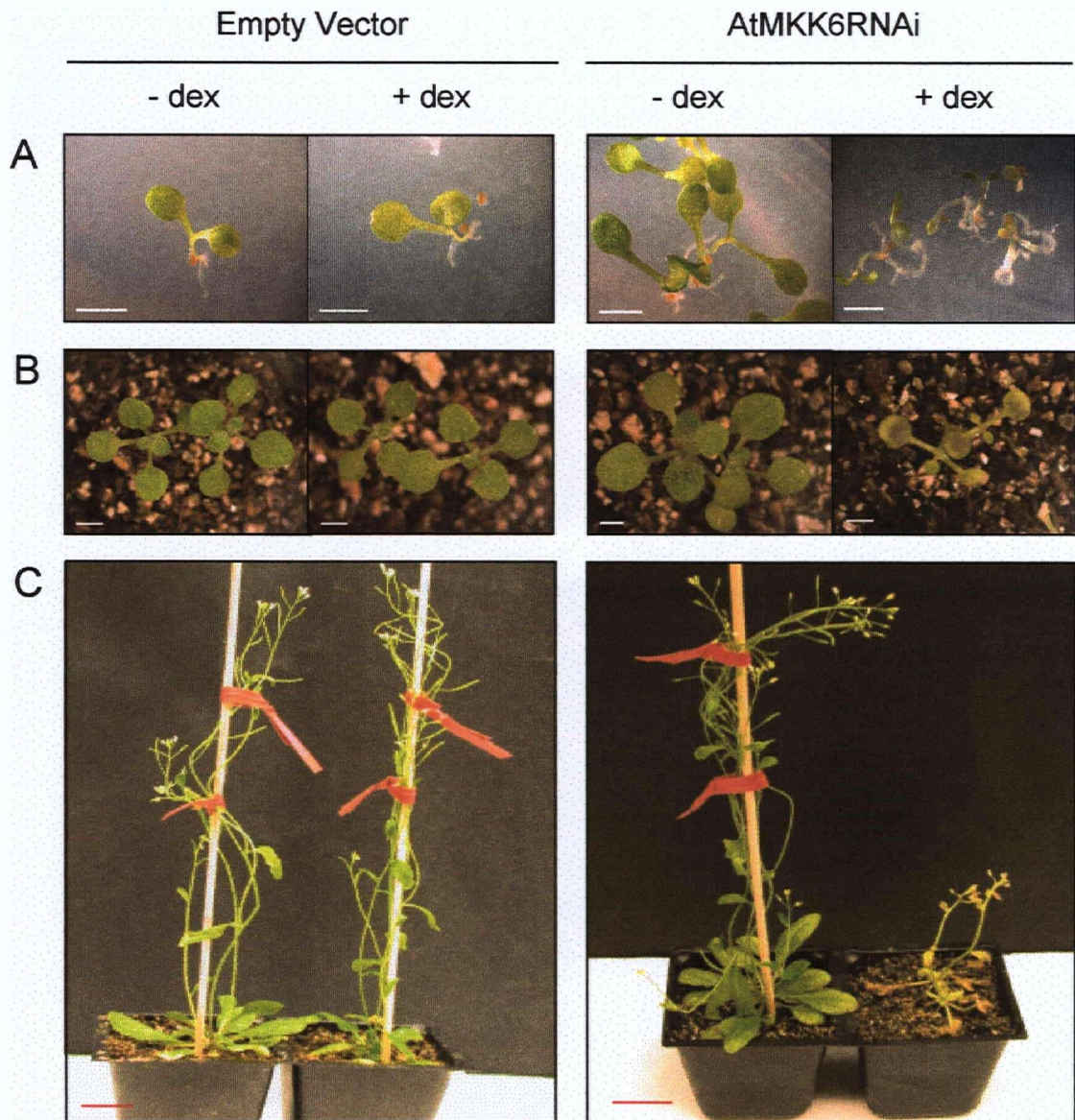


Figure 3.17 Phenotypic analyses revealed growth defects of AtMKK6RNAi plants during plant growth and development. AtMKK6RNAi plants displayed growth defects when gene silencing was induced by dexamethasone (dex) treatment. (A) 7-day-old empty vector and AtMKK6RNAi seedlings grown in $\pm 1 \mu\text{M}$ dex-containing media (B) 10-day-old empty vector and AtMKK6RNAi seedlings grown in soil. Seedlings were treated with $25 \mu\text{M}$ dex at day 7 post-germination. This picture was taken at day 3 post-treatment. (C) 35-day-old empty vector and AtMKK6RNAi plants grown in soil; Plants were treated with $25 \mu\text{M}$ dex at day 28 post-germination. This picture was taken at day 7 post-treatment. White bars = 2 mm, red bars = 20 mm.

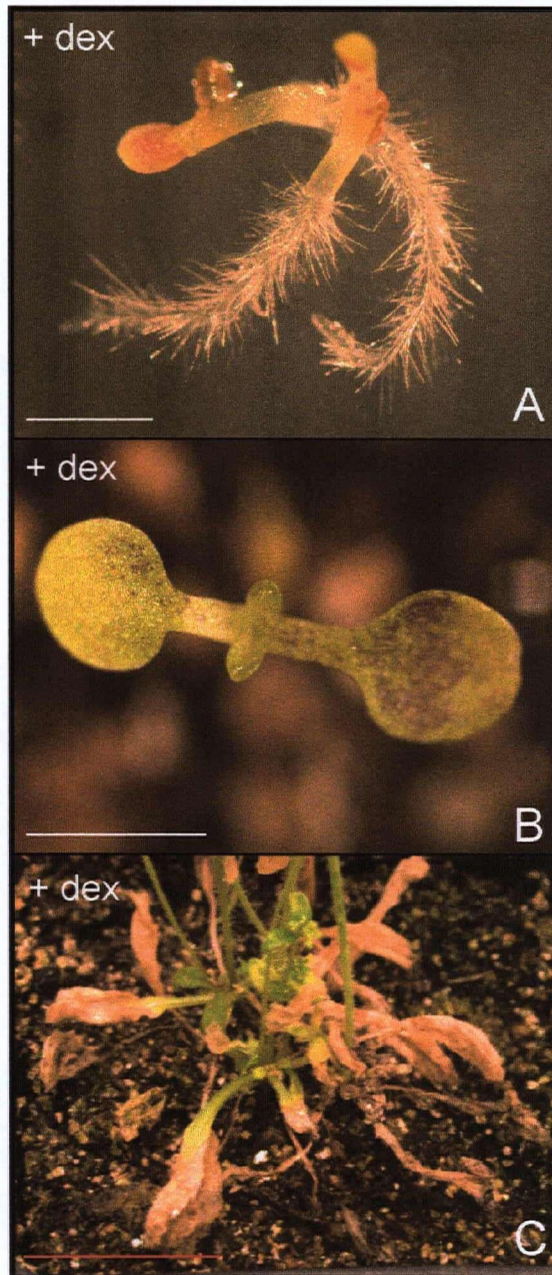


Figure 3.18 Close-up views of phenotypes from *AtMKK6RNAi* plants when induced by dexamethasone (dex).

(A) 7-day-old *AtMKK6RNAi* seedlings grown in 1 μ M dex-containing media
 (B) 10-day-old *AtMKK6RNAi* seedlings grown in soil; Seedlings were treated with 25 μ M dex at day 7 post-germination. This picture was taken after 3 days of dex treatment.

(C) 35-day-old *AtMKK6RNAi* plants grown in soil; Plants were treated with 25 μ M dex at day 28 post-germination. This picture was taken after 7 days of dex treatment. White bars = 2 mm, Red bar = 20 mm.

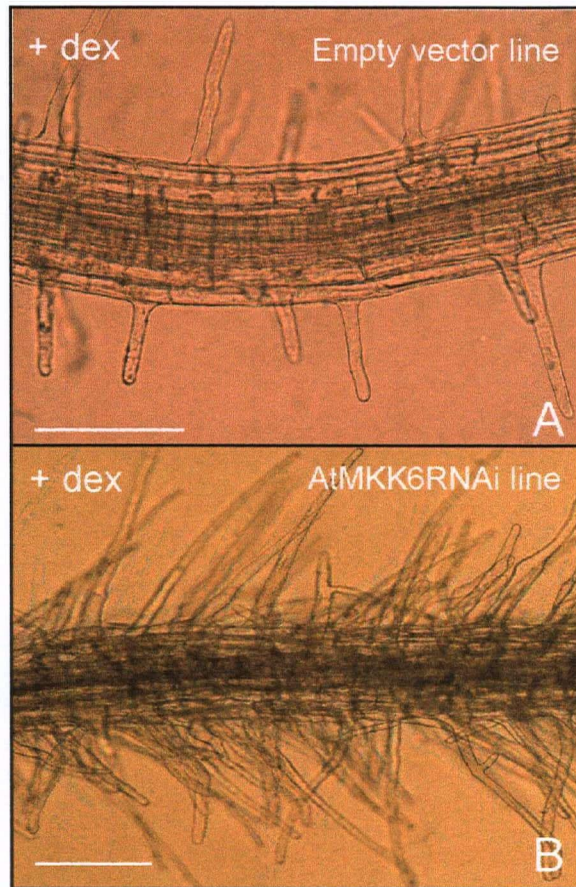


Figure 3.19 AtMKK6RNAi showed ectopic root hairs, when induced by 1 μ M dex

- (A) Root hairs from a 10-day-old seedling of an empty vector (pTA7002) plant (line 4)
 - (B) Root hairs from a 10-day-old seedling of the AtMKK6RNAi plant (line 13)
- White bars = 0.2 mm.

3.3.10 Lateral root analysis of AtMPK13RNAi transgenic plants

To investigate whether AtMPK13 is required in the lateral root formation, three positive T2 AtMPK13RNAi transgenic independent lines were recovered and assessed for lateral root formation, as with AtMKK6RNAi transgenic plants. The AtMPK13RNAi mutant plants, grown in the presence of 1 μ M dex showed a marked reduction (80 %) in lateral root numbers (Figure 3.20).

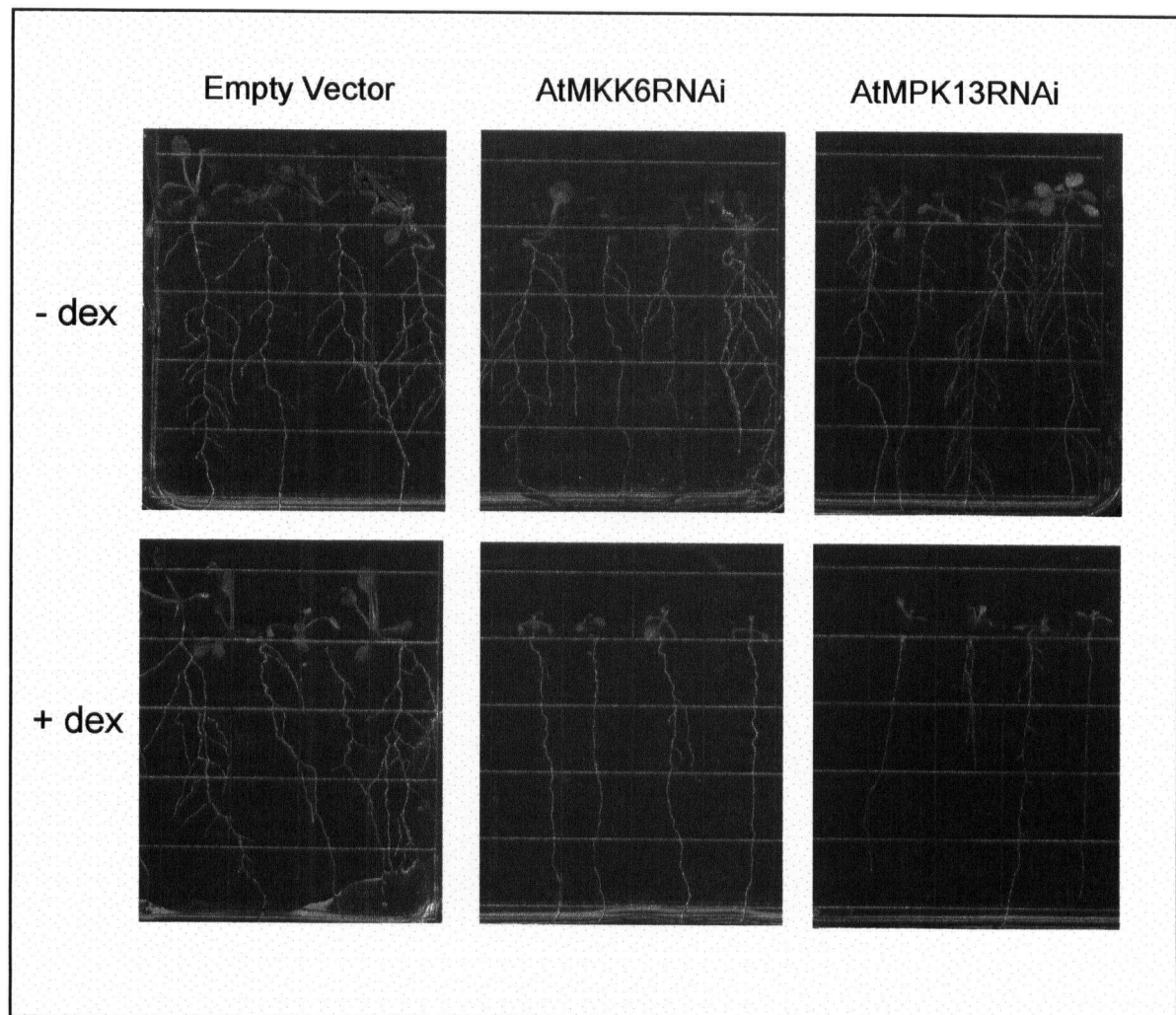


Figure 3.20 AtMKK6RNAi and AtMPK13RNAi showed reduction of lateral root number when RNAi silencing was induced by 1 μ M dex.

Lateral root phenotype of 14-day-old empty vector seedlings, AtMKK6RNAi and AtMPK13RNAi seedlings were grown on MS agar medium and subjected to \pm 1 μ M dex treatments at day 7 post-germination. When compared to the non-treated seedling of the same genotype, the dex-treated AtMKK6RNAi and AtMPK13RNAi seedlings exhibited 82 % and 80 % reduction in the number of lateral roots, respectively, while the dex-treated empty vector line showed no significant change in the lateral root formation. Pictures were taken at day 14 post-germination.

3.4 Discussion

3.4.1 AtMKK6 is required for lateral root initiation

The localization of promoter activity of the *AtMKK6* gene to cell types with well-defined functions in *Arabidopsis* provides an initial indication of the biological process(es) in which the gene may play a role. One of the most fascinating features of plant pericycle cells is their ability to re-initiate cell division and generate a new localized meristem capable of producing all root organ-specific cell types and eventually forming a new lateral root. The *AtMKK6* promoter::*GUS* data reveal that, within the primary roots, *AtMKK6* is specifically expressed in vascular tissue and particularly in non-dividing cells of the pericycle layer surrounding the vascular tissue. Strikingly, GUS-positive cells were observed in the actively dividing pericycle at the site of the lateral root primordia (LRP) initiation. This localization pattern means that the most intense *AtMKK6* expression occurs at sites along the primary root where lateral root formation is taking place, which implicates the possible involvement of AtMKK6 in initiating and/or sustaining pericycle cell division during lateral root initiation. This model is supported by the results obtained with AtMKK6-suppressed plants, where reduction in *AtMKK6* gene expression resulted in the formation of far fewer lateral roots.

In addition to the defect in lateral root development observed in older AtMKK6-suppressed seedlings, AtMKK6RNAi seedlings grown in growth media in the presence of the inducer showed a “hairy” phenotype, marked by inhibition of shoot development and massive formation of ectopic root hairs on elongated primary roots. AtMKK6RNAi plants treated with dexamethasone also displayed growth defects during later stages of plant development. Together, these observations reveal a requirement for the *AtMKK6* gene product activity during lateral root, root hair and whole plant development.

3.4.2 Pericycle-specific expression of the *AtMKK6* promoter is regulated by auxin.

The control of LRP initiation during lateral root formation is not well understood. It has been suggested that there are two possible growth control points for LRP initiation (Dubrovsky *et al.*, 2000). The first control point is developmentally regulated for early lateral root initiation, and is defined after pericycle cells pass from the meristem to the differentiation zone where LRP founder cells are established. The second growth control point is developmentally unrelated to the root apical meristem, and involves LRP initiation as a response to tissue damage or environmental changes, or to being exogenously stimulated with auxin (Laskowski *et al.*, 1995; Doerner *et al.*, 1996). Since *AtMKK6* promoter::*GUS* activity was observed both during LRP initiation in untreated roots, and in exogenously auxin-stimulated roots of *AtMKK6* promoter::*GUS* seedlings, the *AtMKK6* gene product may be required during both growth control points for LRP initiation of the lateral root formation process.

Furthermore, treatment with NPA, a polar auxin transport inhibitor, markedly diminished *AtMKK6* promoter::*GUS* activity in pericycle cells of roots, both in non-dividing and actively dividing cells (Figure 3.13 A and B), indicating that auxin is a positive regulator of transcription of the *AtMKK6* gene in the root pericycle cells. The block of *AtMKK6* promoter activity caused by NPA could be reversed by supplying exogenous IAA (Figure 3.13 C to E), which indicates that supply of an optimal amount of endogenous auxin is likely an important regulator of the pericycle-specific activity pattern of the *AtMKK6* promoter. It has been proposed that inhibition of auxin transport results in accumulation of levels of IAA that are sub-optimal for lateral root initiation in *Arabidopsis* (Casimiro *et al.*, 2001). Notably, in contrast to roots co-treated with the NPA and IAA, roots treated with NPA alone had both

fewer and poorly developed lateral roots. The presence of these residual lateral roots may result from LRP that had formed in roots of 9-day old seedlings prior to the NPA treatment. However, their further development was then blocked by NPA. The failure of LRP to develop further in NPA-treated reporter plants, associated with the reduction of GUS activity in LRPs, might indicate that AtMKK6 activity is also required for outgrowth of lateral roots, but this possibility would need to be tested more directly.

In conclusion, my data show that auxin controls *AtMKK6* gene expression and that the *AtMKK6* gene product is probably required for lateral root formation. Furthermore, during initiation of lateral root formation, AtMKK6 is likely involved in regulating the active cell-division of pericycle cells in both development-related and environment-related scenarios. However, it is unclear about the mechanism of the AtMKK6 regulation in root pericycle cell-division. Recent reports have indicated that protein phosphorylation plays an important role in regulating auxin polar transport. PINOID (PID), a protein serine-threonine kinase, regulates cellular localization of the PIN proteins, auxin transport facilitators (Friml *et al.*, 2004). Ectopic expression of the *pid* gene in roots resulted in mislocalization of PIN proteins to the root cell apical membranes, whereas in wild-type plants PIN proteins are normally localized to the root cell basal membranes. The mechanism of the PID-PIN interaction e.g. what proteins are the downstream target of the PID kinase remains unanswered. Based on this information, it would clearly be of interest to determine whether AtMKK6 is involved in auxin polar transport in *Arabidopsis* roots.

3.4.3 AtMKK6 and AtMPK13 relationship

Besides the gene expression and cellular localization levels of regulation, the *AtMKK6* gene product is likely to be regulated at other levels such as post-translational phosphorylation by its upstream MAPKKK, and interaction with other proteins such as its downstream MAPK. AtMPK13 is a prime candidate as a downstream substrate for AtMKK6 in the context of lateral root formation in *Arabidopsis*, since (1) the activity of the *AtMPK13* promoter and *AtMKK6* promoter were both detected in the primary roots at sites of lateral root formation and in actively dividing pericycle cells of LRP, and (2) AtMKK6 has been shown to be capable of phosphorylating AtMPK13 *in vitro* (Melikant *et al.*, 2004). AtMPK13 might therefore also be involved in regulating the cell-division process in the pericycle, associated with LRP initiation. This model is supported by the observation that dex-induced AtMPK13-suppressed plants showed reduced lateral root formation. Beyond this inferred function in lateral root formation, the tissue/cell-specific expression of the *AtMPK13* promoter::*GUS* activity in floral and silique organs indicates additional involvement of the *AtMPK13* gene product in other developmental transitions. (Figure 3.9 P to T).

The NACK-PQR pathway controlling cytokinesis in tobacco cells was proposed to consist of NACK1/2 kinesin-like proteins (Takahashi *et al.*, 2004), NPK1 MAPKKK (Nishihama *et al.*, 2001), the NQK1/NtMEK1 MAPKK and the NRK1 MAPK (Soyano *et al.*, 2003). This pathway operates during the late M phase of the cell cycle in tobacco cells. NtMEK1/NQK1 (the tobacco orthologues of *Arabidopsis* AtMKK6) has previously been shown to be capable of phosphorylating and activating NtNTF6/NRK1 (the tobacco orthologue of AtMPK13) *in vitro* (Calderini *et al.*, 2001; Soyano *et al.*, 2003). Localization studies have also determined that NTF6 and MMK3, tobacco and alfalfa orthologues,

respectively, of *Arabidopsis* MPK13 can be detected at developing cell plates (Calderini *et al.*, 1998; Bogre *et al.*, 1999). Interestingly, my results indicate that NPA blocked the activities of both the *AtMKK6* and *AtMPK13* promoters in actively dividing pericycle cells during LRP initiation, whereas this treatment failed to block *AtMPK13* promoter::*GUS* activity in non-dividing pericycle cells. It is possible that the *AtMKK6/AtMPK13* signaling interplay is subject to a 'matrix effect' in which certain functions or interactions only occur under specific conditions defined by cell-types or developmental conditions (Coruzzi and Zhou, 2001). Such context-dependent interactions between *AtMKK6*, *AtMPK13* and other auxin-regulated components might give rise to a situation where *AtMPK13* interacts with *AtMKK6* only in actively dividing pericycle cells during LRP initiation but not in pericycle cells during the inactive stage. This possibility could perhaps be explored by using a technique like FRET (Fluorescence Resonance Energy Transfer) for measuring interactions between two proteins *in vivo* (Pollok and Heim, 1999).

CHAPTER 4

AtMPK12, an *Arabidopsis* mitogen-activated protein kinase is guard cell-specific and induced by salt and osmotic stresses.

4.1 Introduction

As discussed in Chapter 2, my examination of *MAPK* gene expression profiles in *Arabidopsis* revealed an interesting expression pattern for *AtMPK12*. In this chapter, I have explored the tissue and cell distribution of *AtMPK12* expression during development through use of *AtMPK12* promoter::*GUS* reporter plants. My results show that the *AtMPK12* promoter directs the *GUS* reporter gene expression specifically to stomatal guard cells of many *Arabidopsis* tissues. This expression is intensified in plants subjected to salt stress and other osmotic stress. In addition, I report the results of phenotypic analysis of a *AtMPK12* loss-of-function mutant recovered from the SALK collection of T-DNA insertional mutants.

4.1.1 Stomatal development

Stomata are specialized structures located in the epidermis of plant aerial tissues. Each stoma is comprised of two opposing guard cells that surround the stomatal pore, an opening which allows exchange of gases and water vapor between the intercellular spaces of the plant and the surrounding atmosphere (Figure 4.1; Nadeau and Sack 2002). Stomata are distributed in the epidermis in a pattern that leaves individual stomata separated by at least one intervening pavement cell (Bergmann, 2004). Little is known about the developmental mechanisms that regulate stomata formation and patterning, but it has been proposed that all *Arabidopsis* stomata form through at least one asymmetric and one symmetric division (Figure 4.2 and Nadeau and Sack 2003). In brief, during stomatal development, the first division occurs in

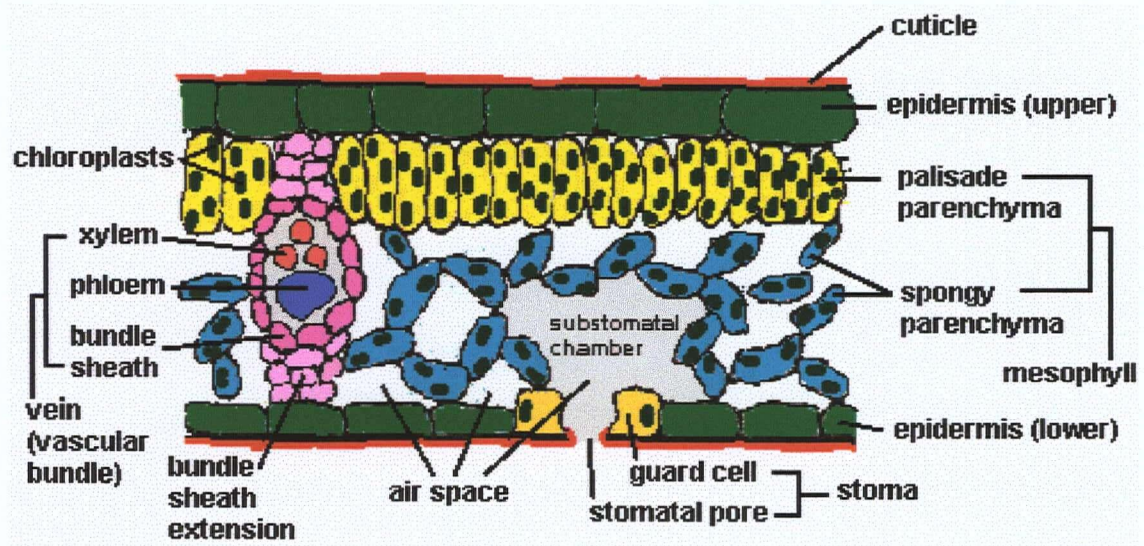


Figure 4.1 Dicot leaf anatomy

(<http://generalhorticulture.tamu.edu/lectsupl/anatomy/anatomy.html>)

a presumed stem cell, the meristemoid mother cell, (MMC) that has become committed to the stomatal pathway (Figure 4.2). The MMC undergoes an asymmetric division, producing a smaller triangular precursor called a meristemoid (M) and a larger sister cell called a neighbor cell (NC). The M can either differentiate immediately into an oval-shape guard mother cell (GMC), which in turn undergoes a symmetric division, producing the two guard cells that form the stoma, or it can continue to divide asymmetrically, producing another M at each division. At each division, the sister cell (NC) may become an MMC and divide asymmetrically to produce a new meristemoid called a satellite meristemoid (SM) (Figure 4.2).

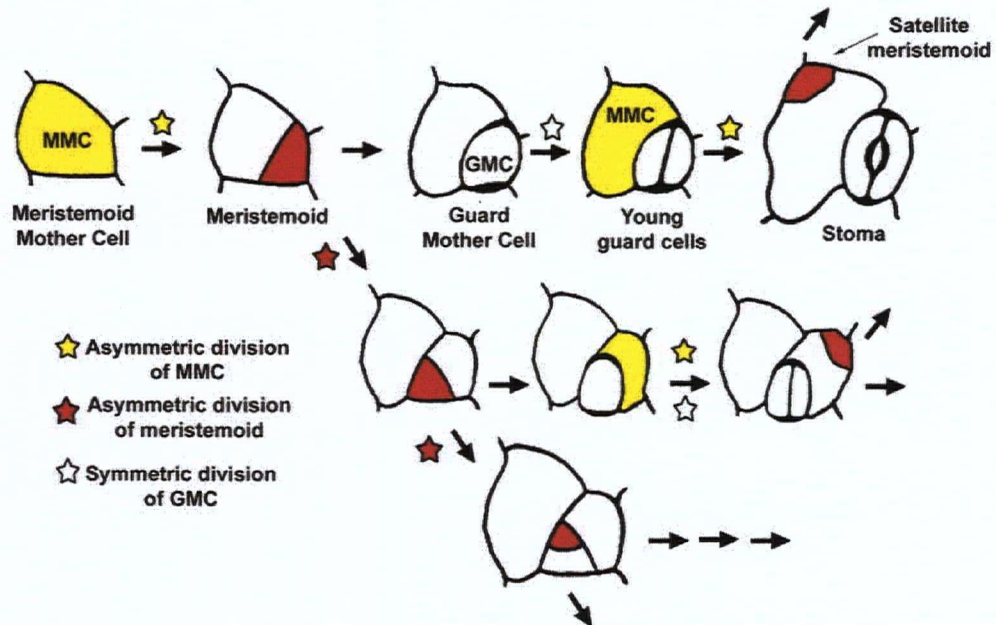


Figure 4.2 *Arabidopsis* stomatal development (Nadeau and Sack, 2002b)

Mutations in several loci are known to disrupt stomatal development and patterning in *Arabidopsis*. The best characterized of these loci are *TOO MANY MOUTHS* (*TMM*), *ERECTA* (*ER*), *STOMATAL DENSITY AND DISTRIBUTION 1* (*SDD1*), *YODA* (*YDA*) and *FOUR LIPS* (*FLP*). The *tmm*, *er er1 er2 triple*, *sdd1* and *yda* mutants display similar phenotypes in that they have an excessive number of stomata compared to wild-type leaves (Berger and Altmann, 2000; Shpak *et al.*, 2005; Geisler *et al.*, 2000; Bergmann *et al.*, 2004), while the *flp* mutants display a paired stomata phenotype (Yang and Sack, 1995).

TMM, which encodes a leucine-rich receptor-like protein has been proposed to play an essential role in the intercellular communication of positional signaling and in establishment of stomatal patterning (Yang and Sack, 1995; Geisler *et al.*, 2000; Nadeau and Sack, 2002a; Larkin *et al.*, 2003). Several spacing mechanisms appear to be disrupted in leaves of *tmm* mutants (Geisler *et al.*, 2000). These mutants have division in cells that

normally would not divide, and TMM is required for the correct orientation of the plane of the asymmetric division that patterns *Arabidopsis* leaf stomata (Geisler *et al.*, 2000; Nadeau and Sack, 2003). In addition to this randomized division phenotype, *tmm* plants possess an altered stomatal distribution pattern where stomata form clusters rather than being distributed properly (Figure 4.3 and Geisler *et al.*, 2000). Stomatal cluster formation in *tmm* plants is partly an outcome of an increase in the number of asymmetric divisions of neighbor cells, compared to the wild-type patterns, and an increase in the number of asymmetric divisions of meristemoids, many of which are misplaced to remain in contact with pre-existing stomata or precursors. Thus, TMM acts as a negative regulator of asymmetric division in neighbour cells and a positive regulator of asymmetric divisions in meristemoids (Geisler *et al.*, 2000; Nadeau and Sack, 2003).

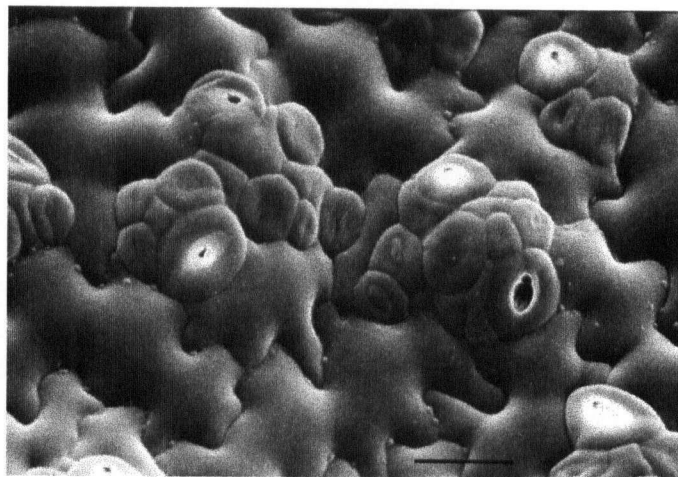


Figure 4.3 Stomatal clusters in *too many mouths*
Cryo-scanning electron micrograph of *tmm* abaxial cotyledon epidermis.
Bar = 15 μ m (Nadeau and Sack, 2002b)

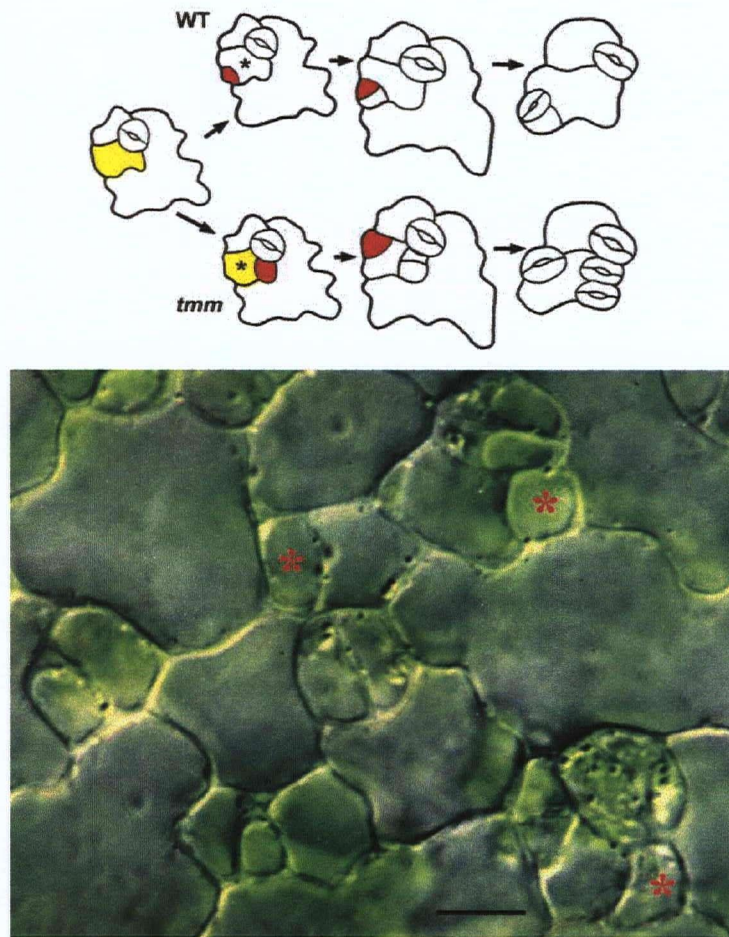


Figure 4.4 Developmental basis of stomatal cluster formation in *tmm* (Nadeau and Sack, 2002b)

(Top) Schematic drawing of *tmm* leaf epidermal surface (bottom row) illustrating that stomatal clusters result from several defects including (1) the randomization of the orientation of asymmetric division, (2) cells (*) next to stomata and/or precursors normally do not divide but do in *tmm*, and (3) sometimes both products of division develop into GMCs (lower right). Top row shows cartoon of what would have happened in wild type.

(Bottom) Differential interference contrast micrograph of *tmm* epidermis showing new meristemoids (red asterisks) that are in contact with developing stomata. Bar = 10 μ m.

Arabidopsis *ER ERL1* and *ERL2*, three *ER*-family leucine-rich repeat-receptor like kinases (LRR-RLKs) together control stomatal patterning (Shpak *et al.*, 2005). Loss-of-function mutations in all three *ER*-family genes cause stomatal clustering and over proliferation of stomata, indicating that the three ER proteins may act as negative regulators of stomatal development. Promoter activity pattern of *ERL1* and *ERL2* are high in stomatal-lineage cells in developing leaves including meristemoids, guard mother cells and immature guard cells. Their promoter activity pattern supports the proposed function these proteins in stomatal development.

SDD1, which encodes a subtilisin-like serine protease, has been proposed to function as a processing protease in developmental signaling (Berger and Altmann, 2000; von Groll and Altmann, 2001). The *sdd1* mutant phenotypes are similar to those of *tmm* in that both have many more stomata than wild-type leaves do. However, *sdd1* has fewer and smaller clusters than *tmm* does, meaning that *sdd1* has many more correctly patterned stomata than *tmm* (Berger and Altmann, 2000).

YODA (YDA), a *MAPKKK* gene, appears to have a central role in stomatal cell fate determination. It controls both stomatal development and formation (Bergmann *et al.*, 2004). Plants containing mutations in *YODA* have an excessive number of stomata, many of which are misplaced, leading to stomatal clusters, while plants containing two copies of a permanently active version of *YODA* completely lack stomata (Bergmann *et al.*, 2004). These authors have proposed that *YODA* acts downstream of *SDD1* and *TMM* because the introduction of a single copy of the constitutively active version of *YODA* into *TMM*- or *SDD*-loss of function plants restores the correct distribution of stomata. It has been

established that YODA also plays a role in cell fate determination in plant embryonic development (Lukowitz *et al.*, 2004).

Four lips (FLP), a MYB transcription factor gene, may function as a negative regulator of cell division at the guard mother cell (GMC) to guard cell transition (Yang and Sack, 1995; Larkin *et al.*, 2003). FLP normally limits the number of symmetrical divisions of the GMC to one, whereas the *flp-1* mutants produce many pairs of laterally-aligned stomata in direct contact with each other (Figure 4.5; Yang and Sack, 1995; Larkin *et al.*, 1997). While stomatal clusters in *tmm* result partly from excess asymmetric divisions, *flp* clusters develop mostly from excess symmetric divisions from a single guard mother cell (GMC). The *flp-1* allele does not appear to affect the total number of meristemoids or pavement cells that are produced (Yang and Sack, 1995; Geisler *et al.*, 1998). The *flp* stomatal cluster phenotype indicates that FLP does not act in stomatal initiation but rather acts later in the stomatal pathway than TMM.

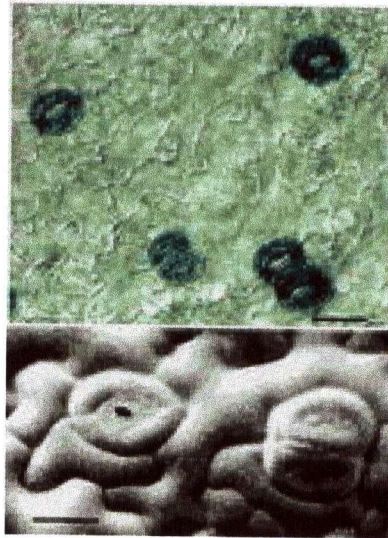


Figure 4.5 Paired stomata in *four lips* (Nadeau and Sack, 2002b)

(Top) *flp-1* displays both unclustered and clustered stomata. Stomata visualized using KAT::GUS staining (promoter from Rebecca Hirsch and Michael Sussman, methods as in Larkin *et al.*, (1997) Bars = 200 μm .

(Bottom) Cryo-scanning electron micrograph showing paired stomata at right. Bar = 10 μm .

4.1.2 Stomatal function and their regulation through ion channels

Stomata regulate CO_2 diffusion into the mesophyll tissue for photosynthetic carbon fixation, water vapor loss via transpiration and O_2 diffusion out to the environment, through the control of the stomatal aperture. Stomatal opening and closing are affected by a number of environmental conditions. For example, high humidity, high CO_2 and light induce stomatal opening (Outlaw, 2003), whereas low humidity, cold, drought and soil salinity induce

stomatal closure, which reduces water loss from the plant (Luan, 2002). From external signals to stomatal movements, many signal transduction mechanisms within the guard cells integrate the input stimuli and link them to the response (Schroeder *et al.*, 2001b; Outlaw, 2003).

Both stomatal opening and closing are known to be regulated by various ion channels. Stomatal opening is initiated by H^+ extrusion from guard cells via the H^+ -ATPase, leading to hyperpolarization of the plasma membrane. This is then followed by rapid uptake of potassium ions (K^+) via the K^+ -in channel (Outlaw, 1983; Outlaw, 2003) and rapid uptake of sucrose via a H^+ -sucrose symporter (Talbott and Zeiger, 1998). As a consequence of this organic solute accumulation, the water potential of the guard cells drops and water enters the guard cells, leading to increased guard cell turgor and swelling/curving of the cells (Figure 4.6 A).

Stomatal closure is caused by plasma-membrane depolarization, resulting from the efflux of anions via an anion channel and consequent K^+ efflux via a K^+ -out channel (Outlaw, 2003). The associated loss of water from the guard cells results in their straightening, and the squeezing together of their opposing surfaces (Figure 4.6 B). This stomatal closure generally occurs daily at the point when light levels drop and the use of CO_2 in photosynthesis decreases. However, it can also occur at any point when plants have lost an excessive amount of water. Such a water deficit induces an accumulation of ABA in plant cells and it has been established that ABA accumulation in guard cells can trigger stomatal closure (Schroeder *et al.*, 2001a), as can application of exogenous ABA (Roelfsema *et al.*, 2004).

ABA regulates ion channel activity in guard cells (MacRobbie, 1997), inhibiting the K^+ -in and activating the K^+ -out channels, thereby decreasing K^+ influx and increasing K^+ efflux. These effects are consistent with ABA's observed ability to inhibit stomatal opening and induce stomatal closure (Luan, 2002). Besides regulation through K^+ -in and -out channels, ABA causes a depolarization of the plasma membranes (Thiel *et al.*, 1992) through activation of anion channels (Grabov *et al.*, 1997; Pei *et al.*, 1997). ABA activates the slow anion channels of the plasma membrane through positive regulation of a protein kinase (Li *et al.*, 2000) and through negative regulation of a different protein kinase (Pei *et al.*, 1997), which highlights the central role of phosphorylation in the signal network that regulates the anion channels of guard cells.

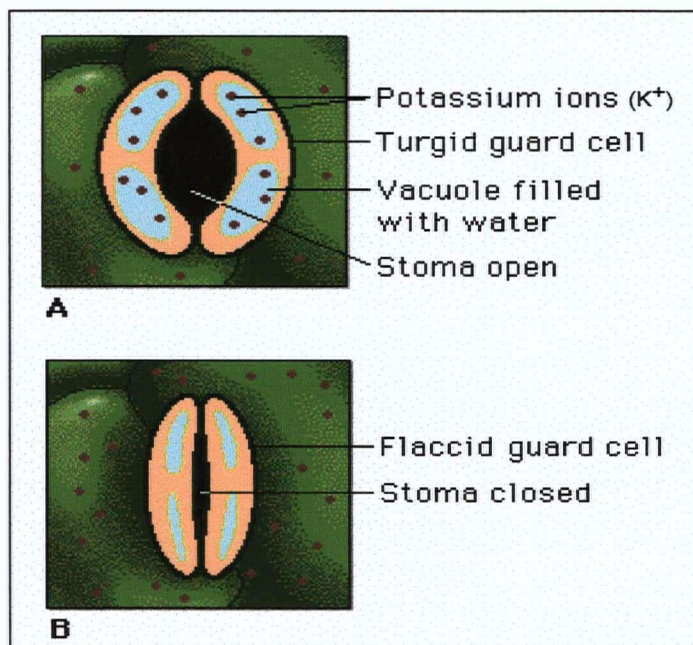


Figure 4.6 Guard cell function: stomatal opening and closing

4.1.3 Involvement of protein phosphorylation in stomatal regulation

Protein phosphorylation has been implicated in ABA signaling in plant guard cells at several points. At least three protein kinases and two protein phosphatases involved in this process have been identified and characterized. The three kinases are AAPK (ABA-activated protein kinase), OST 1 (Open Stomata 1) and AMBPK. AAPK was identified from guard cells of *Vicia faba* through a biochemical approach (Li and Assmann, 1996) and has been shown to be involved in modulating the activity of the ABA-regulated slow-anion channel (Li *et al.*, 2000). OST1 is an *Arabidopsis* ABA-activated protein kinase that is closely related to AAPK from *Vicia faba*. Recessive *ost1* mutations disrupt both ABA induction of stomatal closing and ABA inhibition of light-induced stomatal opening (Mustilli *et al.*, 2002). AMBPK, identified as a MAP kinase, positively controls ABA-induced stomatal closure in *Pisum sativum* (Burnett *et al.*, 2000).

Two phosphatases shown to be involved in ABA signaling in guard cells are ABI1 and ABI2 (ABA-insensitive 1 and ABA-insensitive 2, respectively). They have been identified as type 2C protein phosphatases that are involved in ABA regulation of ion channel activity in *Arabidopsis* guard cells (Leung *et al.*, 1994; Meyer *et al.*, 1994; Leung *et al.*, 1997; Leung and Giraudat, 1998). ABA activation of the slow anion is responsible for the membrane depolarization and prolonged anion efflux required for ABA-mediated stomatal closure. In *abi* mutants, the anion channels remain inactive even in the presence of accumulating ABA, which results in constantly open stomata (Pei *et al.*, 1997). This implies that protein phosphorylation is required to hold the anion channels in a quiescent state, from which they can be released through the action of the ABI1 and ABI2 phosphatases.

Other mutations can also affect ABA signaling in stomata. For example, a mutation in the *GPA1* gene, which encodes a heterotrimeric GTP binding protein α -subunit (GTP α), also diminishes ABA-induced stomatal closure (insensitive to ABA) (Wang *et al.*, 2001). GPA1 has been shown to interact with the *Arabidopsis* putative G protein-coupled receptor GCR1 (Pandey and Assmann, 2004). However, in guard cells, the *gcr1* mutant exhibited the opposite phenotype from *gpa1* (hypersensitive to ABA). Therefore, it has been proposed that GCR1 may be a negative regulator of GPA1 in guard cells (Pandey and Assmann, 2004).

4.1.4 Salt stress signaling

Excessive Na⁺ in the soil, often referred to as high salinity, is a major environmental stress that affects plant growth and development, and can limit crop production (Epstein *et al.*, 1980). When grown in high concentration of salts, plants exhibit a variety of responses at the molecular, cellular and whole plant levels (Zhu, 2001a). These include developmental changes, ion transport adjustment, and shifts in metabolite accumulation. Some of these responses to salt stress are triggered by ion imbalance and osmotic stress signals, whereas others may be caused by secondary signals generated downstream of the primary signals, such as phytohormones (e.g. ABA), reactive oxygen species and intracellular Ca⁺ fluxes. A common primary outcome of salt, drought and cold stresses is associated osmotic stress, whereas a primary outcome uniquely associated with salt stress is ion imbalance or ionic stress. Plants under salt stress therefore have to restore ionic homeostasis as well as water or osmotic homeostasis (Figure 4.7).

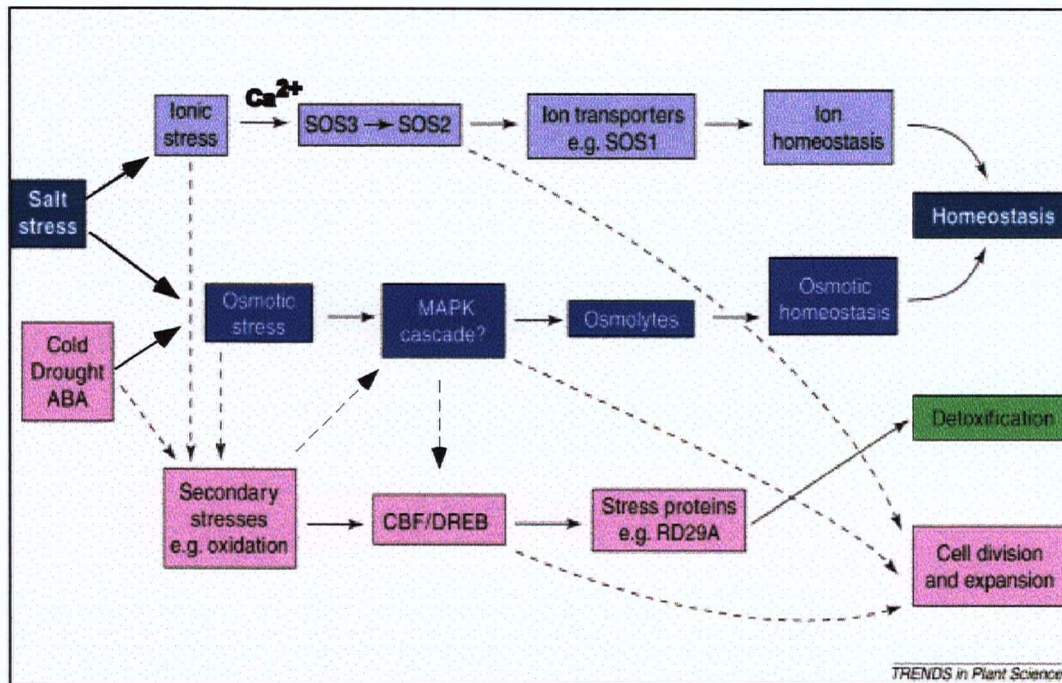


Figure 4.7 Salt stress responses in plants and pathways that interconnect them. Homeostasis can be regarded as consisting of ionic and osmotic homeostasis Components. The SOS pathway is proposed to mediate ionic homeostasis and the MAPK pathway is proposed to mediate osmotic homeostasis (Zhu, 2001b). The two primary stresses, ionic and osmotic stresses cause secondary stresses such as ROS accumulation. This diagram is modified, from Zhu (2001b).

4.1.5 Ionic stress signaling: the “salt overly sensitive” (SOS) pathway

Salt stress disrupts ionic homeostasis in plants, causing a build-up of excess toxic Na^+ in the cell cytosol and a deficiency of essential ions such as K^+ as a result of the negative impact of Na^+ on intracellular K^+ influx (Hasegawa *et al.*, 2000). The signaling pathway components controlling Na^+ homeostasis and salt tolerance have been identified through genetic screens to recover mutants in *Arabidopsis* that are hypersensitive to NaCl stress. These mutants are

designated as *SOS* (*salt overly sensitive*) (Wu *et al.*, 1996; Liu and Zhu, 1997, 1998), several of which have been cloned and characterized. *SOS1* encodes a putative Na^+/H^+ antiport protein whose biological function may be removal of Na^+ from the cytoplasm with export to the extracellular space. The steady-state level of *SOS1* transcripts is up-regulated by NaCl stress (Shi *et al.*, 2000). *SOS2* encodes a serine/threonine protein kinase and is required for salt tolerance (Liu *et al.*, 2000) while *SOS3* encodes a myristoylated Ca^{2+} -binding protein (Liu and Zhu, 1998). These SOS proteins are proposed to constitute a pathway that regulates Na^+ balance in the plant cells.

In the proposed SOS pathway, the sequence of signaling events starts with transient elevation of intracellular Ca^{2+} in response to salt stress. As a consequence, the Ca^{2+} -binding protein, SOS3, is activated (Liu and Zhu, 1998; Ishitani *et al.*, 2000). This activation results in SOS3 recruiting and activating protein kinase SOS2 (Halfter *et al.*, 2000; Ishitani *et al.*, 2000; Liu *et al.*, 2000). The SOS3-SOS2 kinase complex regulates the activity of the plasma membrane-localized Na^+/H^+ antiporter, SOS1, and also activates the transcription of the *SOS1* gene. The complex may also modulate the activity of other ion transporters (Zhu, 2000), which act together to restore ion homeostasis (Figure 4.8).

In addition to ion transporters like SOS1 that directly control Na^+ influx into and efflux out of plant cells through the plasma membrane, there are other ion transporters such as AtNHX1 that regulate Na^+ compartmentation in the vacuole (Figure 4.8). Transport of Na^+ to the vacuole helps prevent Na^+ toxicity in the cytosol; Na^+ can also be utilized in the vacuole as an osmolyte to help restore osmotic homeostasis (Zhu, 2001b).

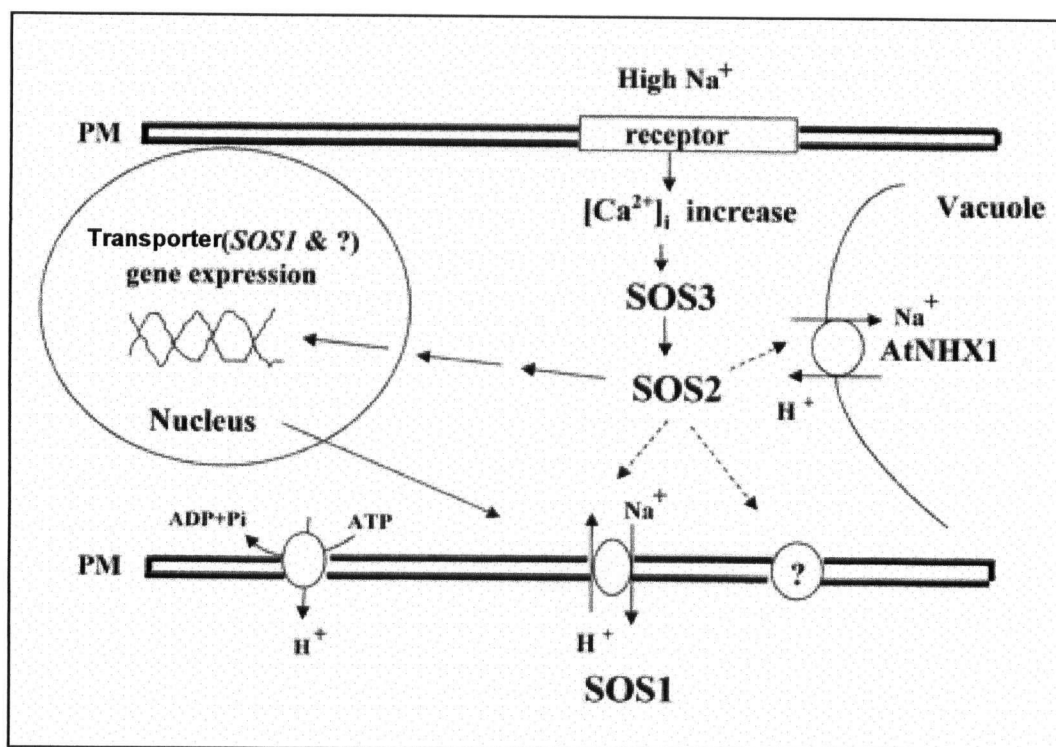


Figure 4.8 Diagram of the SOS pathway for plant Na⁺ response, from Zhu, J-K (2000)

4.1.6 Osmotic stress signaling: SOS-independent protein kinases

In addition to the physiological challenges associated with ionic imbalance, high salinity in soil is a major cause of osmotic stress in plants because of associated changes in water-generated turgor pressure. Several plant MAPK components have been implicated in osmotic stress responses, mainly based on up-regulation of their transcripts and/or kinase activation in response to salt, drought and cold stresses (Mizoguchi *et al.*, 1996; Kiegerl *et al.*, 2000; Teige *et al.*, 2004). The plant MAPKs identified in this fashion include AtMEKK1, MEK1/MKK2 and MPK4/MPK6 in *Arabidopsis* (Ichimura *et al.*, 2000; Teige *et al.*, 2004), SIMKK and SIMK in alfalfa (Kiegerl *et al.*, 2000) and NtMEK2, SIPK and WIPK in tobacco (Yang *et al.*, 2001; Zhang and Klessig, 2001) (Figure 4.9).

In *Arabidopsis*, the MAPKK, MKK2, was specifically activated by salt and cold stresses (Teige *et al.*, 2004). *In vivo* protein kinase assays showed that activated MKK2 phosphorylated MPK4 and MPK6. *mkk2* null plants were impaired in MPK4 and MPK6 activation and were hypersensitive to both salt and cold stresses (Teige *et al.*, 2004). AtMPK6 can also be activated by low temperature and osmotic stresses in *Arabidopsis* cell cultures (Ichimura *et al.*, 2000). In alfalfa, activation of SIMK, a salt stress-induced MAPK, is posttranscriptionally mediated by the MAPKK, SIMKK (Kiegerl *et al.*, 2000).

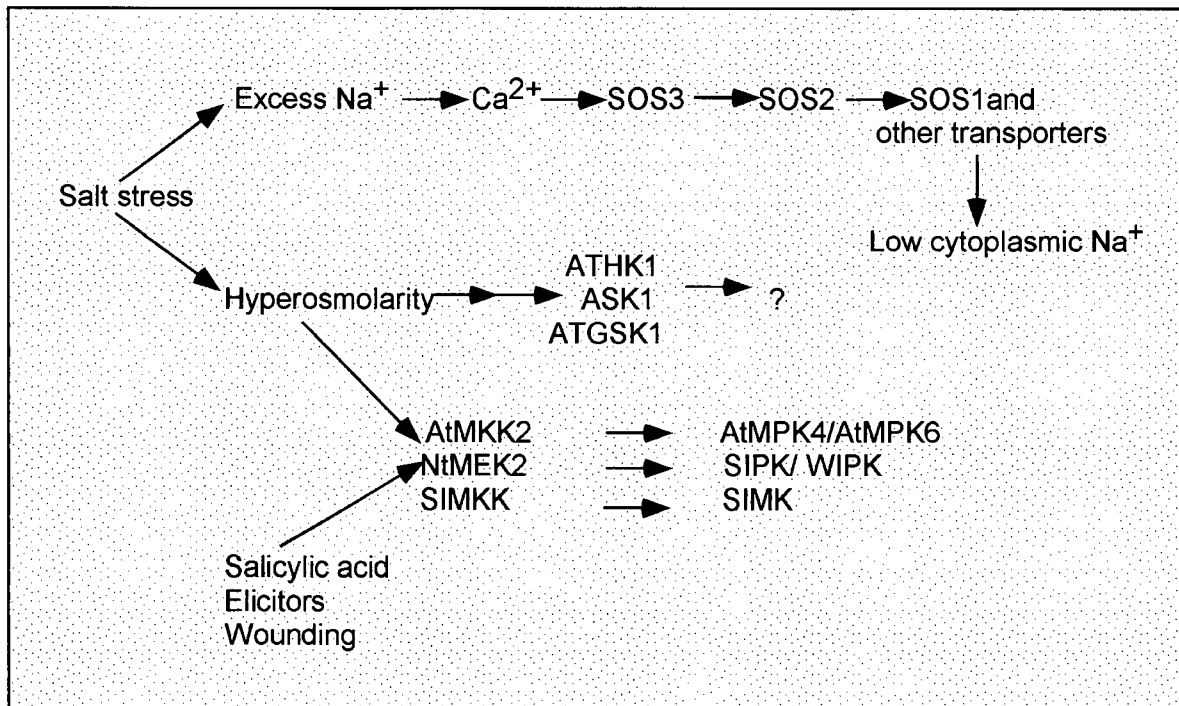


Figure 4.9 Salt stress activates several protein kinase pathways, the SOS3-SOS2 kinase pathway, multiple MAPK pathways and other protein kinases e.g. ATHK1, ASK1 and ATGSK1. Modified from (Zhu, 2001a).

Similarly, in tobacco, SIPK (the orthologue of AtMKK6) becomes activated upon hyperosmotic stress (Mikolajczyk *et al.*, 2000), while WIPK (the orthologue of AtMPK3) is activated by cold, drought, wounding and biotic stimuli (Seo *et al.*, 1995). In tobacco, NtMEK2 is a MAPKK capable of activating both SIPK and WIPK (Yang *et al.*, 2001; Zhang and Klessig, 2001).

Beyond MAPK pathway proteins, additional kinases and other proteins are also involved in responding to salt or osmotic stresses (Figure 4.9). These include *Arabidopsis* ATHK1, a two-component histidine kinase homologous to the yeast osmosensor, SLN1 (Urao *et al.*, 2000), a tobacco homologue of *Arabidopsis* serine/threonine kinase 1 (*ASK1*) (Mikolajczyk *et al.*, 2000) and ATGSK1 (Piao *et al.*, 2001).

4.2 Materials and Methods

4.2.1 Plant materials

Plant materials were prepared as described in Chapter 3, Section 3.2.1.

4.2.2 Genomic DNA isolation

Genomic DNA isolation was performed in the same manner as in Chapter 3, Section 3.2.2.

4.2.3 Molecular cloning of *AtMPK12* promoter::*GUS* DNA constructs and generating the GUS reporter plants

To examine cell- and tissues-specific expression of *AtMPK12* genes during plant development, transgenic *Arabidopsis* plants harboring the *AtMPK12* promoter:: β -glucuronidase (*GUS*) reporter gene construct were generated through the following processes.

4.2.3.1 Cloning of the *AtMPK12* promoter

The promoter region of the *AtMPK12* gene (the 1300 bp region immediately upstream of its translational start ATG codon) was amplified from *Arabidopsis* genomic DNA (obtained from section 3.2.2) using the Expand High Fidelity PCR System Kit (Roche Molecular Biochemicals, Catalog No. 1 732 641). PCR was carried out according to the manufacturer 's instructions, using PK12F1 and PK12R1 primers (Table 4.1). The resulting amplicon was cloned into the pCR[®]2.1-TOPO[®] vector using a TOPO TA Cloning[®] Kit (Invitrogen, Carlsbad, USA, and Catalogue No. K4500-01) and the insert was sequenced to confirm its identity.

Table 4.1 Primer sequences for *AtMPK12* promoter cloning

Primer Name	Restriction Enzyme Site	Sequence (5'-3')	Amplified Promoter Region Length (bp)
PK12F1	BamHI	cgcgaaatccGTGAAGAGAGAAGCTTTTTTCAACTG	1300
PK12R1	BamHI	cgcggaatccGATGAAGCTAGCTATGGAGTCACTCTG	

4.2.3.2 Generation of promoter::*GUS* fusion DNA constructs and transgenic plants

The amplified *AtMPK12* promoter fragment was digested with *Bam*HI and ligated into the *GUS* coding region of the promoter cloning vector, pCAMBIA1381Z (CSIRO, Canberra, Australia) that has been predigested with *Bam*HI. Clones carrying the construct with the promoter in the sense orientation adjacent to the *GUS* ORF were identified by double restriction enzyme digestion. Uncut pCAMBIA1381Z was used as a promoterless-*GUS* construct (negative control) and pCAMBIA1301 (CSIRO, Canberra, Australia) was used as a 35S promoter-*GUS* fusion construct (positive control). Schematic diagrams of the pCAMBIA1381Z and pCAMBIA1301 vectors are presented in Chapter 3, Figure 3.1. The ligation reactions and *E.coli* transformation were performed as previously described in Chapter 3, Section 3.2.3.2. *Agrobacterium* transformation, *in planta* transformation of *Arabidopsis* and selection of transformants were performed as previously described in Sections 3.2.3.3, 3.2.3.4 and 3.2.3.5, respectively.

4.2.4 Histochemical GUS analysis

Three independent transformants of the *AtMPK12* promoter::*GUS* reporter plants (lines 1, 2 and 8) were subjected to detailed histochemical GUS analysis using the methods previously described in Chapter 3, Section 3.2.4.

4.2.5 Resin embedding and cross-sectioning of leaf tissue

Resin embedding of leaf tissue of 10-day-old seedlings harboring the *AtMPK12* promoter::*GUS* fusion construct, and cross-sectioning were performed as previously described in Chapter 3, Section 3.2.5.

4.2.6 NaCl and mannitol treatments

AtMPK12 promoter::*GUS* reporter seeds were surface sterilized as previously described in Chapter 3, Section 3.2.3.5) and then individual seeds were arranged on square agar-solidified MS medium plates containing ½ MS salt mix, 1% sucrose, 0.5 g/L MES, and 0.8 % agar, pH 5.7 (without B5 vitamins). The plates were sealed with 3M Micropore™ tape and the seeds were vernalized at 4 °C in the dark for 2-4 days. The plates were then placed in the growth room, mounted vertically under 16 h/8 h light-dark cycle conditions at 22-24 °C for 9 days.

For the NaCl treatment, sufficient 100 mM NaCl in liquid MS was added to flood 12-day old reporter seedlings for 24 hours. For the control, unsupplemented MS solution was used.

For the mannitol treatment, seedlings were grown on agar-solidified MS medium containing 5% mannitol for 10 days. For the control, seedlings were grown on the normal unsupplemented medium.

4.2.7 Verification of the *AtMPK12* SALK transfer-DNA (T-DNA) insertional homozygous line

4.2.7.1 Genomic DNA extraction of the *AtMPK12* SALK T-DNA insertional plants

Leaves of 4-week-old plants, (the *AtMPK12* T-DNA insertional plants, SALK_074849) were used for genomic DNA extraction, using an adaptation of a protocol described in (Edwards *et al.*, 1991) and Western T. L. (personal communication). The leaf sample from each individual plant was ground in a microfuge tube for 15-30 seconds using an electronic drill at room temperature. To each ground sample, was added 400 μ L extraction buffer (containing 200 mM Tris-HCl, pH 7.5, 250 mM NaCl, 25 mM EDTA, pH 8.0 and 0.5% SDS) and the mixture was vortexed for 5 seconds. The sample was then centrifuged for 3 minutes at 10,000 x g. Without disturbing the pellet, 300 μ L supernatant was transferred to a fresh microfuge tube, and DNA was precipitated by adding 300 μ L isopropanol and mixing by inverting the tube 5 times. The sample was incubated at room temperature for 2 minutes and then centrifuged for 5 minutes at 10,000 x g. The supernatant was discarded, and the pellet was then washed with 500 μ L 70% ethanol and air-dried for 10 minutes. The DNA pellet was re-suspended in 100 μ L TE, pH 8.0, and the genomic DNA-containing solution was stored at 4 °C. A 2 μ L aliquot of the genomic DNA was used for each PCR reaction.

4.2.7.2 Identification of a homozygous SALK T-DNA insertional line

To identify homozygous *AtMPK12* T-DNA insertional line(s), Seed were obtained from the Arabidopsis Stock Centre (ABRC accessed through <http://www.Arabidopsis.org>). PCR was performed using genomic DNA obtained from individual *AtMPK12* SALK T-DNA insertional plants at the T3 generation (section 4.2.7.1). This screen employed three SALK T-DNA primers: the left genomic primer, K12LP; the right genomic primer, K12RP and the left border primer, LBa1. These primers were designed by the SALK iSECT online tools (<http://signal.salk.edu/isects.html>) and the sequences are presented in Table 4.2. A diagram describing the SALK T-DNA primer design is present in Figure 4.10 (Alonso *et al.*, 2003). The expected amplicon sizes for the various primer combinations used are 900 bps and 410+N bps (N = 0-300 bps).

Table 4.2 Primers for verification of the *AtMPK12* T-DNA insertional homozygous line(s) (SALK_074849)

Primer Name	Sequence (5'-3')
K12LP	TCACGTAGCGTTCTCTTAGCATCG
K12RP	TGGCAATGCAGTTGGAGAAGA
LBa1	TGGTTCACGTAGTGGGCCATCG

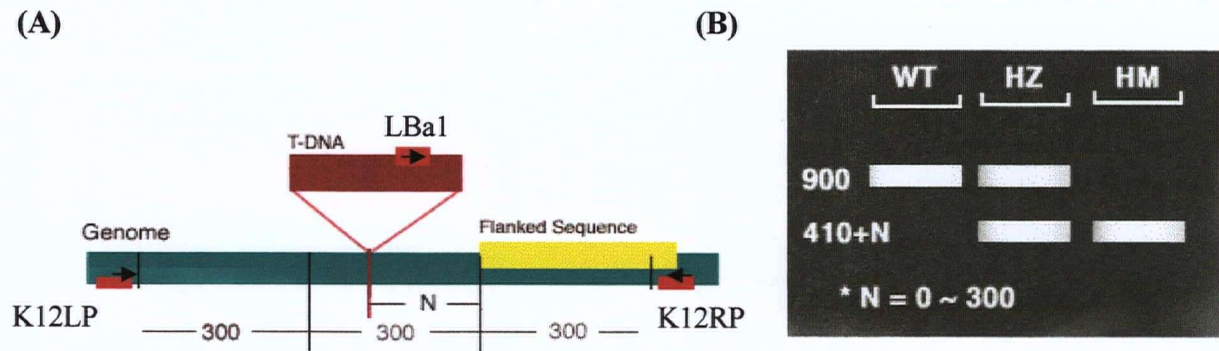


Figure 4.10 Diagram of SALK T-DNA verification primer design and PCR product size
(Modified from <http://signal.salk.edu/tdnaprimers.html> and Alonso *et al.* (2003))

(A) SALK T-DNA verification primer design

K12LP and K12RP = Left and right genomic primers for *AtMPK12* T-DNA insertional lines, respectively

N= Difference of the actual insertion site and the flanked sequence position, usually 0 - 300 bases

LBa1 = Left border primer of the T-DNA insertion

(B) Amplicon sizes expected from using the three primers (LBa1+K12LP+K12RP)

for screening *AtMPK12* SALK_074849 plants, WT (Wild Type - no insertion) plants should yield a product of about 900 bps (from K12LP to K12RP), HM (Homozygous lines - insertions in both chromosomes) plants will yield a band of 410+N bps, and HZ (Heterozygous lines - one of the pair chromosomes with insertion) plants should yield both bands.

4.2.8 Phenotypic analyses of the homozygous *AtMPK12* T-DNA insertional mutant (*atmpk12*) in normal growth conditions

The phenotypic analyses of young seedlings were performed on the MS agar-solidified medium plates. The *atmpk12* mutant and wild-type seeds were surface sterilized and placed on MS agar-solidified media containing ½ MS salt mix, 3% sucrose, 0.5 g/L MES and 1.2 % agar, pH 5.7 (without B5 vitamins). The seeds were vernalized at 4 °C in the dark for 2-4 days prior to being grown at 22-24 °C, under 16 h/8 h light-dark cycle conditions. ~50-100 seeds were sown per plate and five replicate plates were used. Up to 12 days, morphological phenotypes were monitored and photographed.

4.3 Results

4.3.1 Histochemical localization of GUS activity driven by *AtMPK12* promoter during plant development

In Chapter 2, reverse transcriptase polymerase chain reaction (RT-PCR) analysis of the expression of all *Arabidopsis* MAPK genes showed that the *AtMPK12* gene was differentially expressed in *Arabidopsis* tissues and the highest expression was detected in callus (Chapter 2, Figure 2.2). To investigate the cell- or tissue-specific expression of *AtMPK12* gene more closely during plant development, I performed a promoter-GUS activity analysis. A 1.3 kb-promoter region upstream of the *AtMPK12* ATG start codon was fused with the β -glucuronidase (*GUS*) reporter gene and the resulting construct was introduced into wild-type *Arabidopsis* plants. GUS activity was monitored throughout plant development, from 3 days to 35 days, by histochemical staining in three independent transgenic lines.

GUS staining in all three lines was highly localized, appearing as dark blue spots in cotyledons, rosette leaves and hypocotyls (Figure 4.11 A-C). This pattern resulted from strong *GUS* expression in guard cells in these tissues in plants of all ages tested. In contrast to the RT-PCR results, GUS staining was barely detectable in roots (Figure 4.11 A-C, E and F), appearing sporadically in the upper parts (adjacent to the hypocotyls) of the primary roots. No GUS staining was observed in trichomes (Figure 4.11 D). GUS activity was also observed in the guard cells in the inflorescence stems and cauline leaves (Figure 4.11 G). In young flowers and mature flowers, strong GUS staining was observed in guard cells in sepals and anthers, but not in guard cells in petals (Figure 4.11 H). In the pistil of young flowers, GUS activity was barely detected in the styler region of young pistils (not shown), whereas

strong GUS activity was detectable in guard cells of the style in mature flowers (not shown) and in guard cells of the stylar region at the base of developing siliques (Figure 4.11 J). In addition, strong GUS activity was observed in guard cells along the pedicel and body of the siliques (Figure 4.11 I and J). By contrast, no GUS activity was observed in stigma of flowers or the distal end of siliques at either young and mature stages (Figure 4.11 H and J). Overall, the *AtMPK12* promoter drove *GUS* expression specifically in guard cells of most aerial tissues throughout plant development.

Whole plants and leaf guard cells

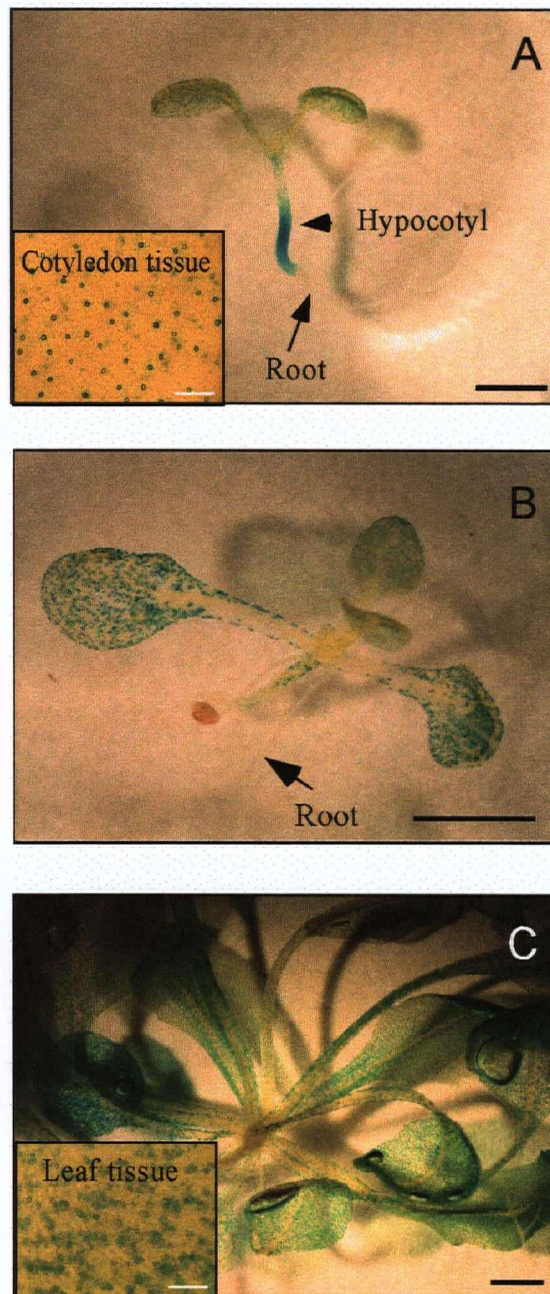


Figure 4.11 *AtMPK12* promoter-GUS activity survey throughout plant development (A, B and C) 5-day, 10-day and 35-day old seedlings or plants are shown, respectively. Black bars = 2 mm and white bars = 0.2 mm.

Trichomes and Roots

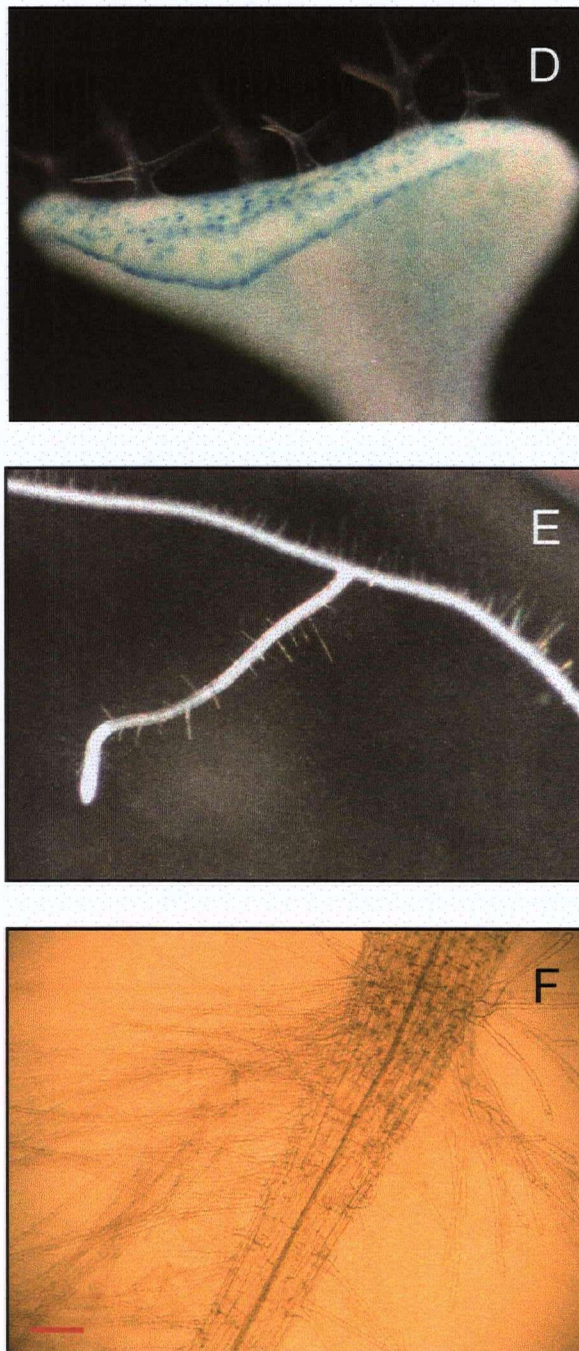


Figure 4.11 (continued) *AtMPK12* promoter-GUS activity survey of leaf trichomes and roots. Red bar = 0.02 mm

Inflorescence, flowers and silique

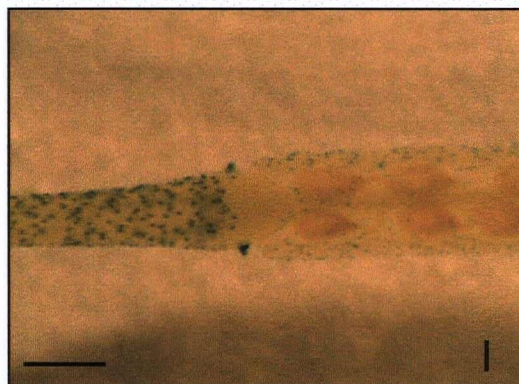
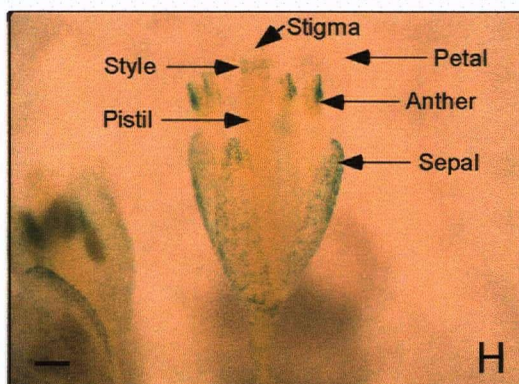
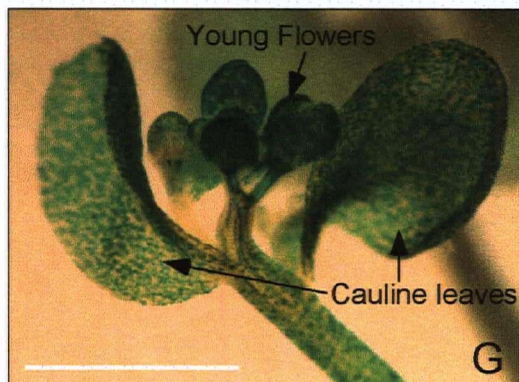


Figure 4.11 (continued) *AtMPK12* promoter-GUS activity survey of inflorescence, flowers and silique

White bar = 2 mm and black bars = 0.4 mm.

A pistil of a fertilized mature flower

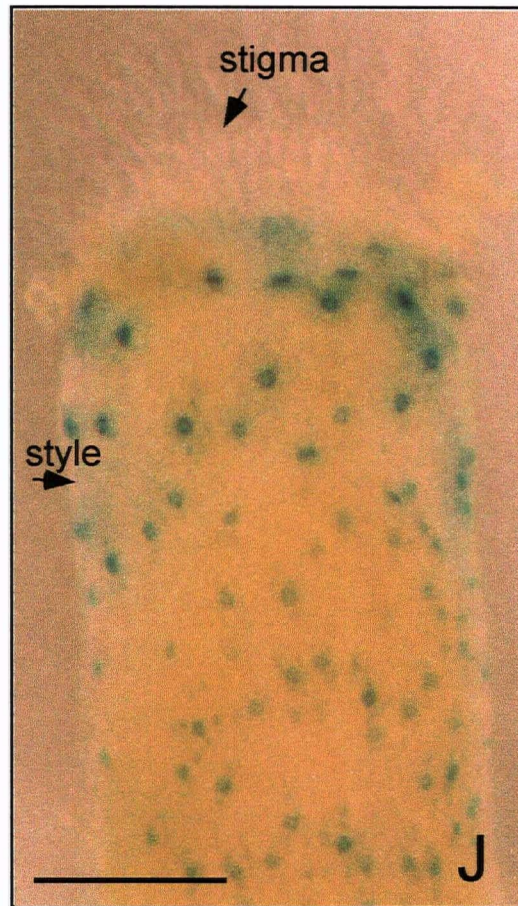


Figure 4.11 (continued) *AtMPK12* promoter-GUS activity survey of floral pistils

(J) A pistil from a fertilized mature flower.

GUS-expression guard cells was clearly detected in the guard cells of mature style tissue. Arrows indicate stigma and style region of a pistil. Black bar = 0.1 mm.

Higher magnification of leaves from 10-day-old *AtMPK12* promoter::*GUS* seedlings revealed GUS activity in leaf guard cells (Figure 4.12 A). However, strong GUS activity was not detected in all leaf guard cells. Strong GUS staining was restricted to the large guard cells, whereas relatively weak GUS staining was observed in the smaller cells (Figure 4.12 B). Weak GUS staining was detectable in many (not all) guard mother cells, which are precursor cells of stomata development, but GUS staining was not detectable in other types of stomatal precursor cells (data not shown). No GUS activity was detected in epidermal pavement cells (Figure 4.12 B), although it was observed in some parts of the leaf vascular tissues (Figure 4.12 A). Finally, examination of leaf cross-sections from 10-day-old seedlings confirmed the guard cell-specific *GUS* expression pattern seen in whole tissue mounts (Figure 4.13 A and B).

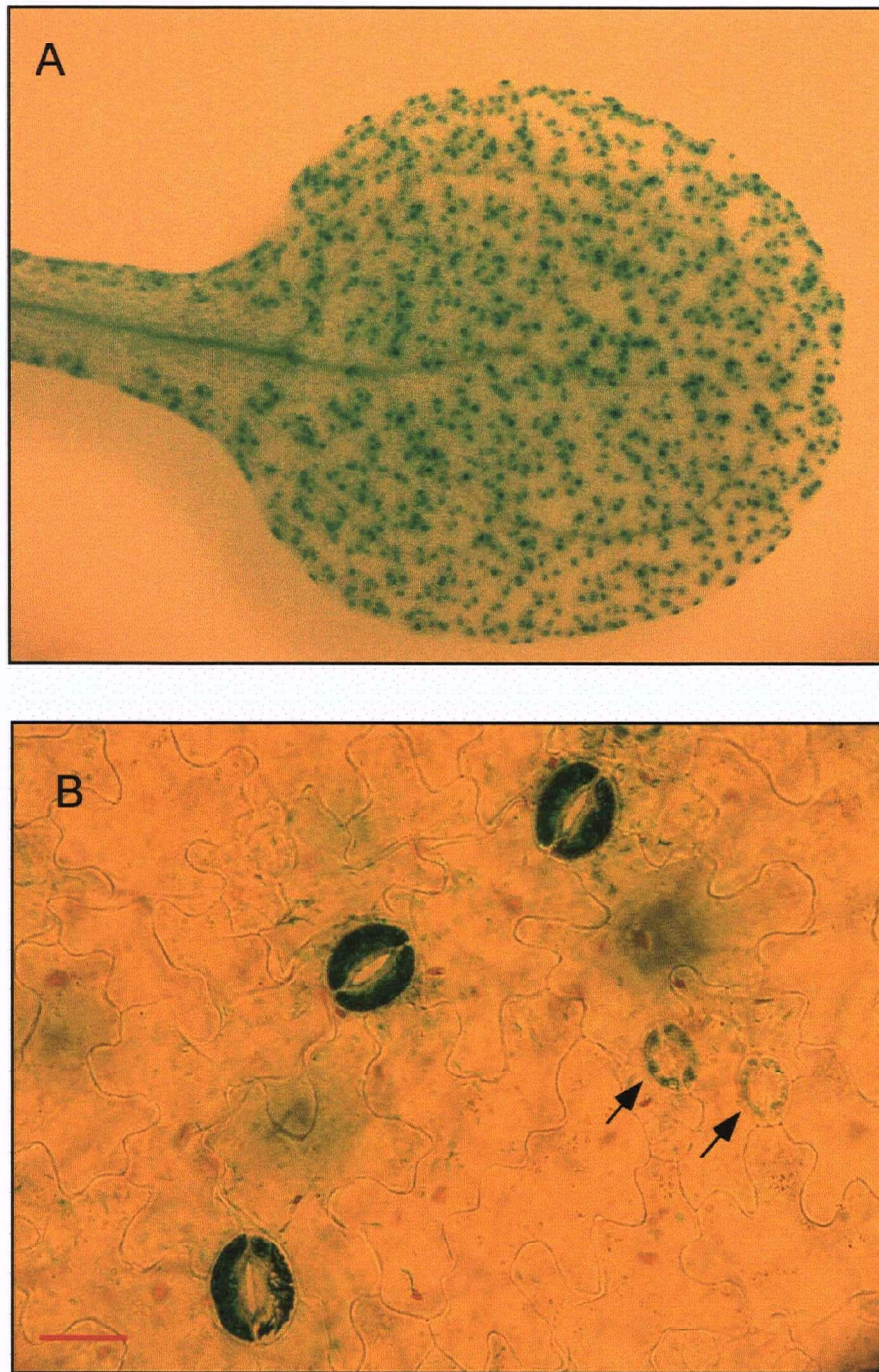


Figure 4.12 Histochemical localization of GUS activity in *AtMPK12* promoter::*GUS* reporter plants.

Arrows indicate smaller guard cells expressing relatively weak GUS activity, compared to the larger ones. A red bar = 20 μm. GUS staining is shown as blue.

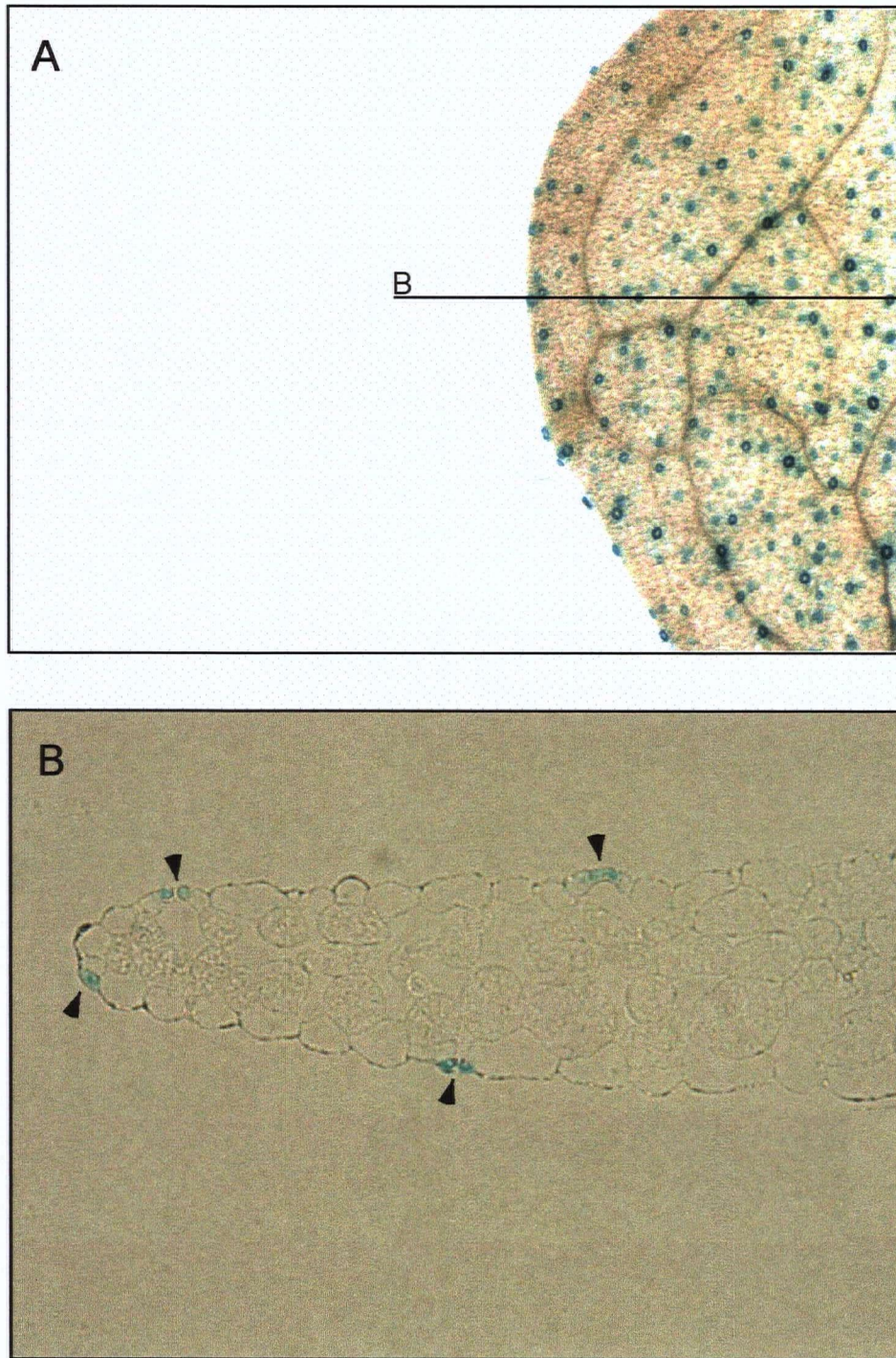


Figure 4.13 Transverse section of leaf from the *AtMPK12* promoter::GUS reporter plant. Arrowheads indicate guard cells where GUS staining is localized as blue.

4.3.2 *AtMPK12* promoter activity was enhanced by NaCl and mannitol treatments.

AtMPK12 promoter::*GUS* activity in both shoots and roots was increased by exposure of the plants to NaCl (100 mM) for 24 hours (Figure 4.14). Normally, GUS staining is barely detectable in roots at different stages of development (Figure 4.11 E-F), but the activity was dramatically increased upon NaCl treatment, as compared to the control, particularly in the vascular tissue of the roots (Figure 4.14 B). Higher magnification revealed that, upon NaCl treatment, a substantial increase in GUS activity could also be induced in leaf stomatal guard cells (Figure 4.15 A and B).

In addition to NaCl stress, I tested the effect of a direct osmotic stress stimulus, using mannitol. In reporter plants grown on MS agar medium containing 5% w/v mannitol, GUS activity was markedly increased in leaf stomata (Figure 4.16). Notably, the seedlings grown in the presence of mannitol also displayed growth defects, as their leaves were smaller and their roots were shorter, compared to the control where the same genotypes were grown on the unsupplemented media.

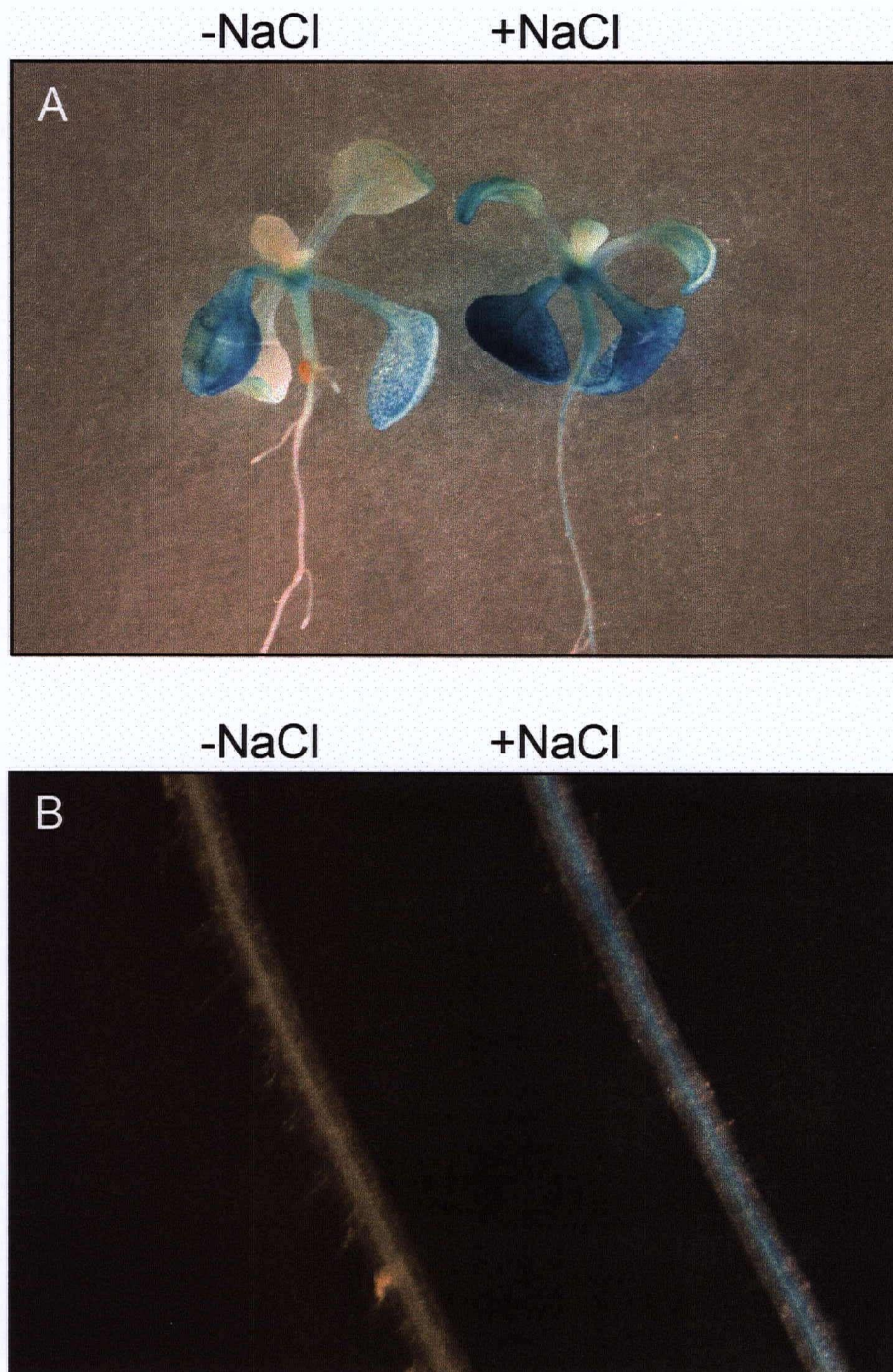


Figure 4.14 NaCl causes an increase in GUS activity of the *AtMPK12* promoter::GUS reporter seedlings. GUS staining is shown as blue.

(A) Shoot and roots from 13-day old seedlings treated without and with NaCl (100 mM)

(B) Roots from 13-day old seedlings treated without and with NaCl (100 mM)

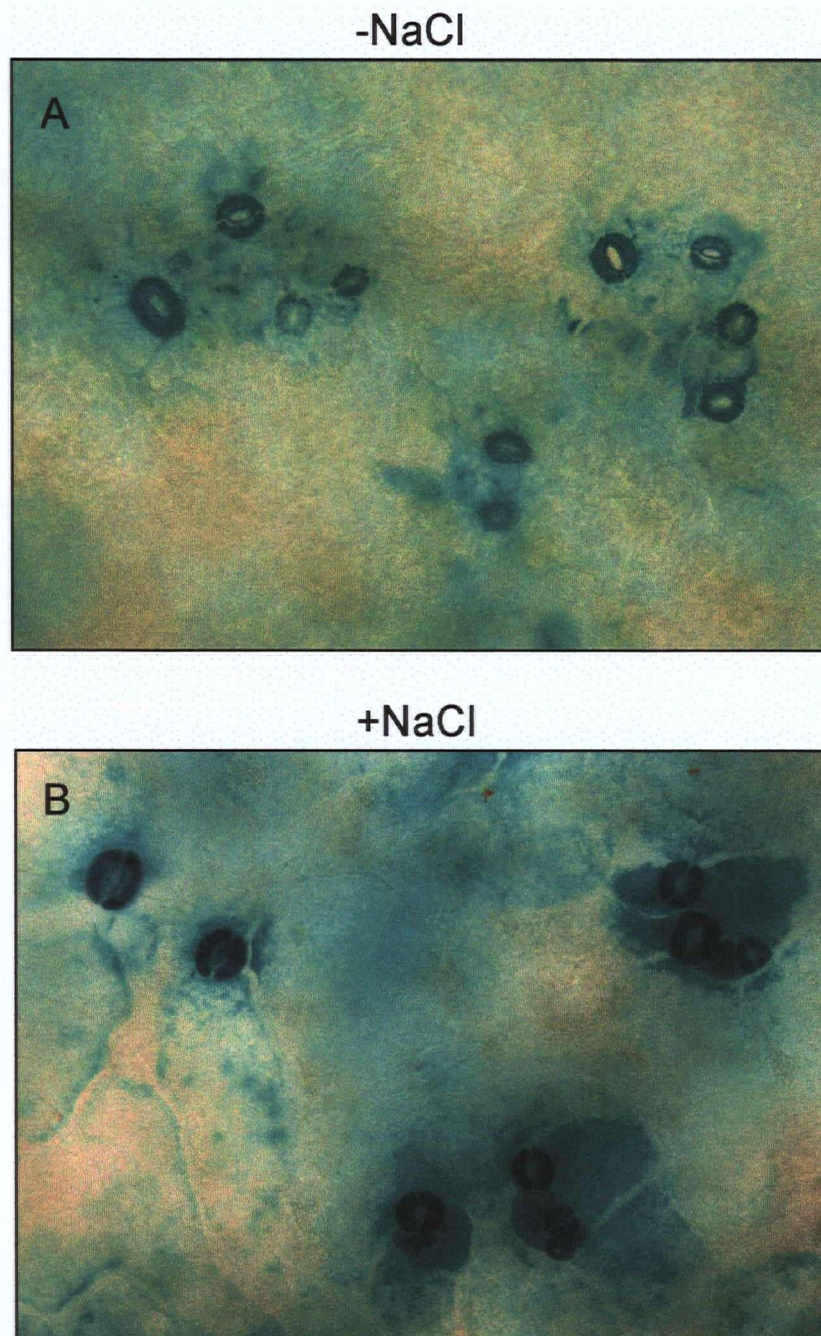


Figure 4.15 NaCl causes an increase in GUS activity in leaf guard cells of *AtMPK12* promoter::*GUS* reporter seedlings.

(A) and (B) Leaf guard cells from 13-day old seedlings treated without and with NaCl (100 mM), respectively. GUS staining is shown as blue.

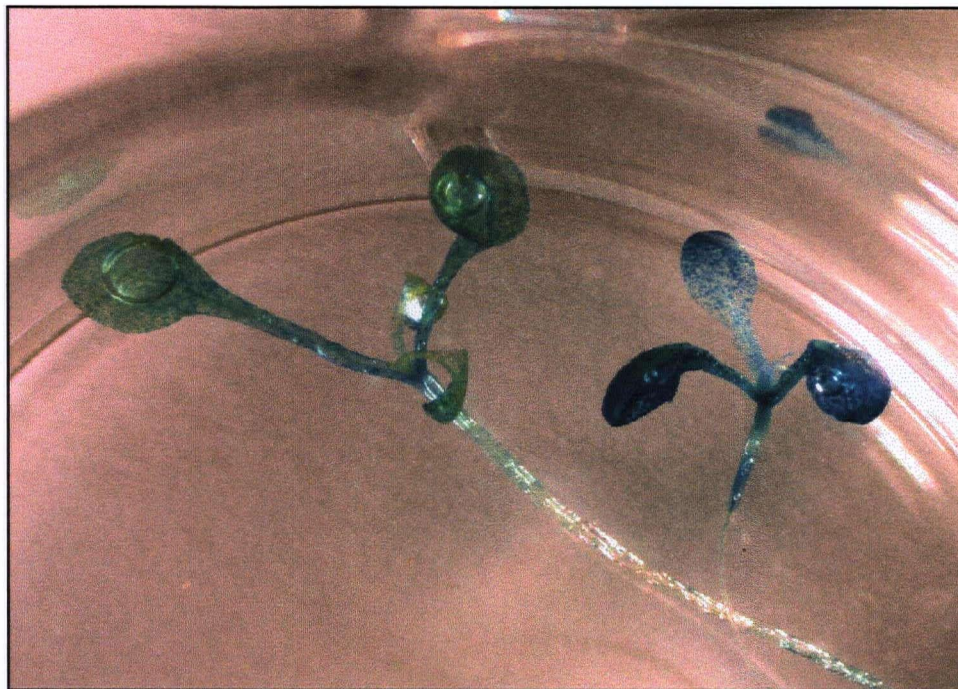


Figure 4.16 Mannitol (5%) causes an increase in GUS activity of the *AtMPK12* promoter::*GUS* reporter seedlings.

(Left) 10-day-old seedlings grown in the absence of mannitol.

(Right) 10-day-old seedlings grown in the presence of 5% mannitol.

4.3.2 Characterization of SALK T-DNA insertion lines

To gain more insight into the function of AtMPK12 in plants, I characterized a mutant line in which the *AtMPK12* gene has been disrupted by a T-DNA insertion in the first exon (Alonso *et al.*, 2003). In collaboration with an undergraduate student, Janet Chung, a homozygous line (line 28) of the *atmpk12* mutant was recovered from screening an accession from the SALK T-DNA insertional mutation collection (SALK_074849), using a PCR genotyping approach (Figure 4.17).

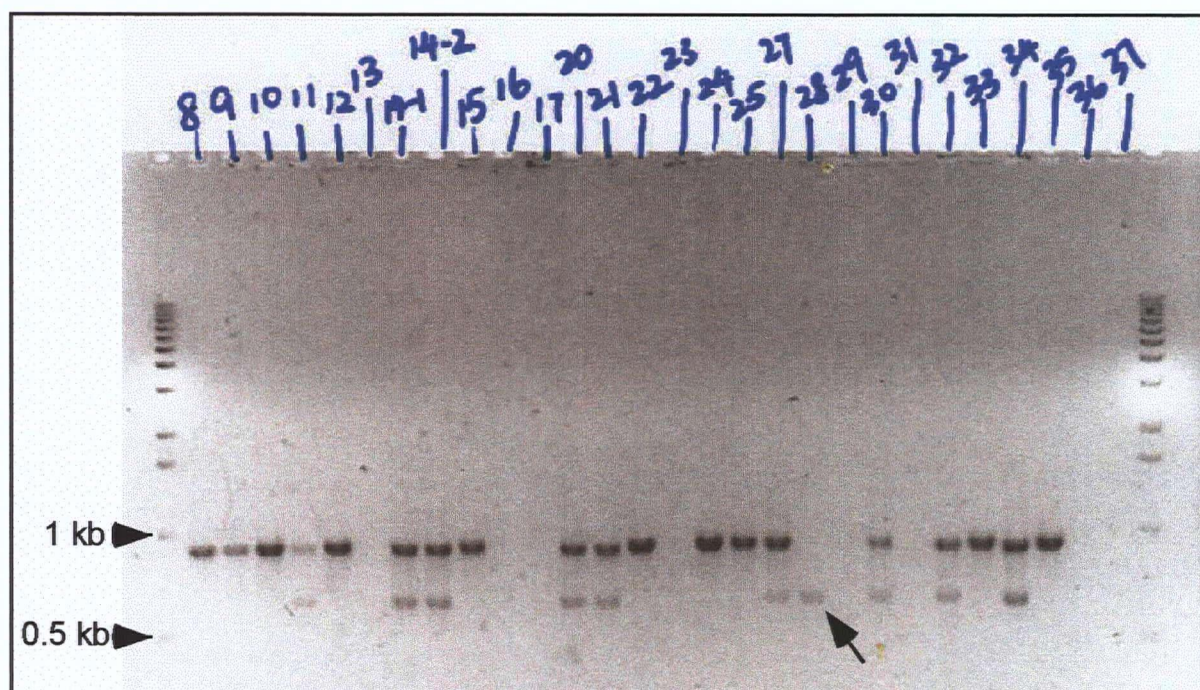


Figure 4.17 PCR screening of *AtMPK12* T-DNA insertional lines (SALK-074849) to identify a plant homozygous for recessive mutant alleles of the *AtMPK12* gene. Line 28 represents a homozygous *atmpk12* mutant that has T-DNA insertions in both chromosomes. An arrow indicates a single band of an amplification product from line 28 (see more details in Section 4.2.7.2).

4.3.3 Phenotypic analysis of the *atmpk12* plants

Under normal growth conditions on MS agar medium, the young *atmpk12* mutant seedlings showed a mixture of both dwarf phenotype (~37 %) and normal-looking phenotype (~ 63 %) in the population (Figure 4.18 A and B). However, the *atmpk12* mutant plants displaying dwarf phenotypes were segregated away in the next generation, leaving only homogenous wild-type looking plants (Figure 4.18 C). This result indicates that the dwarf phenotypes in the previous generation were not an outcome of the *AtMPK12* mutation. It was confirmed by PCR genotyping that the plants with the homogenous phenotypes are *atmpk12* homozygous mutants that contain T-DNA inserts in both chromosomes.

4.4 Discussion

4.4.1 *AtMPK12* promoter activity pattern is guard cell-specific throughout plant development

Epidermal tissues of *Arabidopsis* leaves and stems contain three distinct cell types: stomatal guard cells, trichomes, and epidermal pavement cells (Melaragno *et al.*, 1993). My results show that the *AtMPK12* promoter activity was confined to the stomatal guard cells and was not detected in pavement cells or trichomes (Figure 4.12 B and Figure 4.11 D). In addition, my results reveal that the *AtMPK12* promoter directs *GUS* expression specifically to the guard cells in a range of developmental contexts, since *GUS*-expressing guard cells were detected in cotyledons, hypocotyls, and siliques, as well as in specific floral tissues such as sepals, anthers and the stylar region of pistils (Figure 4.11 H and J). However, the activity was not detected uniformly in all guard cells. The level of *GUS* activity appears to be related to the size of the guard cells, or perhaps their state of development (Figure 4.12 B).

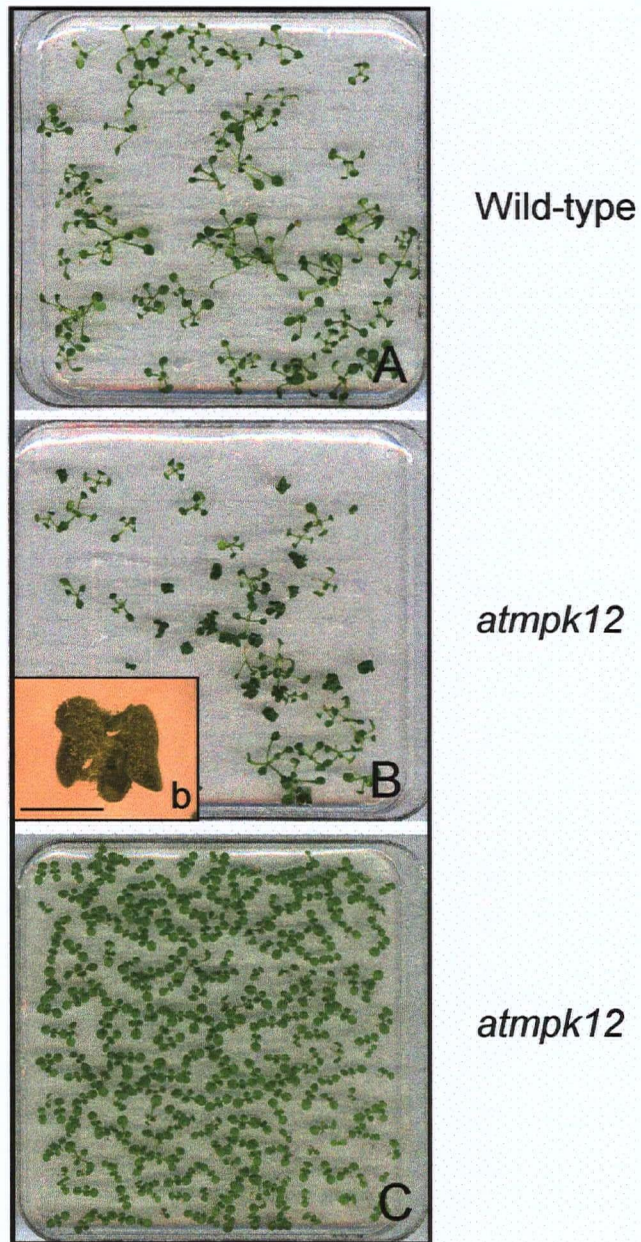


Figure 4.18 Phenotypic analysis of wild-type and *atmpk12* mutant plants on growth medium (1.2 % agar and 3 % sucrose)

(A) 12-day-old wild-type plants

(B) 12-day-old *atmpk12* mutants with both dwarf and wild-type looking plants.

(B inset b) a closer view of a dwarf plant; black bars = 2 mm

(C) 12-day-old *atmpk12* mutants in the next generation with homogeneous wild-type looking plants.

4.4.2 AtMPK12 may be required for guard cell development.

Two aspects of the promoter activity and gene expression patterns of *AtMPK12* are noteworthy. First, the pattern of GUS activity driven by the *AtMPK12* promoter included strong expression in mature stomatal guard cells. This indicates the involvement of *AtMPK12* in later stages of stomatal development and/or in stomata function. Similarly, *GUS*-expressing guard cells were not detectable in the stylar region of young pistils, but were detectable in the same region of mature siliques (Figure 4.11 J), indicating again that *AtMPK12* expression is most pronounced at later stages of stomatal development.

The second observation is that *AtMPK12* was highly expressed in callus, a tissue that contains actively dividing cells (Chapter 2, Figure 2.2). This indicates that *AtMPK12* may also be involved in a specific cell division process in plants. It is known that formation of *Arabidopsis* stomata requires at least one asymmetric and one symmetric division (Figure 4.2 and Nadeau and Sack 2003). Thus, *AtMPK12* may be required for controlling specific cell division counts during stomatal development. These two observations indicate that *AtMPK12* may function differently at different developmental stages.

In contrast to *AtMPK12*, transcription of other stomata-associated genes, e.g. *SDD1* and *TMM*, is particularly active in developing cells in the stomatal pathway. The *TMM* promoter was active in both daughter cells of the asymmetric division, i.e. the meristemoids and their neighbor cells (Nadeau and Sack, 2002a). Similarly, the *SDD1* promoter was active in the smaller stomata precursor cells, the meristemoids and guard mother cells, whereas its activity decreased during guard cell formation and maturation (Von Groll *et al.*, 2002). These genes are proposed to regulate early events in asymmetric cell division (Berger and Altmann, 2000; Geisler *et al.*, 2000). The pattern of *AtMPK12* promoter activity with the late

developmental events in the stomatal pathway indicates that AtMPK12 might be involved in the terminal differentiation of a guard mother cell to form guard cells.

4.4.3 Guard cell-specific AtMPK12 is involved in osmotic stress response.

Some members of the plant MAPK gene family have been previously identified as salt or osmotic stress-responsive genes; for example, AtMKK2, AtMPK4, AtMPK6, SIMKK, SIMK, NtMEK2, SIPK and WIPK (Chapter 4 Introduction and references therein). In my study, an increase in *AtMPK12* promoter activity upon NaCl treatments in stomatal guard cells indicates the involvement of the *AtMPK12* gene product in transducing the salt stress signal in these specialized cells.

Protein phosphorylation plays an important role in the regulation of stomatal aperture and in ion transport in guard cells (Li *et al.*, 1998), and the guard-cell specific activity pattern of the *AtMPK12* promoter is similar to that of the promoter of the *KAT1* gene, which encodes a potassium channel (Figure 4.12 and Nakamura *et al.*, (1995)). Another ion transporter gene, *AtNHX1* (*Arabidopsis thaliana* sodium proton exchanger 1) is also exclusively expressed in stomatal guard cells (Shi and Zhu, 2002). It is tempting to suggest that AtMPK12 might function in regulation of one or more classes of ion channels that control stomata opening and closing. Interestingly, expression of the *AtNHX1* gene was also increased by treatment of leaves with NaCl, KCl or ABA (Shi and Zhu, 2002), and overexpression of the *AtNHX1* gene conferred increased salt tolerance (Apse *et al.*, 1999). AtNHX1 has been proposed to regulate Na⁺ compartmentation in the vacuole under salt stress (Zhu, 2001b).

I also showed that mannitol treatment enhanced the activity of the *AtMPK12* promoter in leaf stomata and in roots. One common feature of both salt and mannitol stresses is osmotic stress (Kreps *et al.*, 2002), presumably because these agents generate a common water deficiency stress. This triggers the expression of genes whose products are involved in cell and/or whole plant protection from the water deficit, locally or distantly. For example, more osmolytes are synthesized, as is the plant hormone abscisic acid (ABA), and more water channels are produced or activated. It has been established that roots exposed to drought synthesize ABA and export it from root xylem to leaves, where it induces stomatal closure (Wilkinson and Davies, 2002). It has been demonstrated that injection of ABA into the xylem (Zhang and Outlaw, 2001a) and slow drying of the entire roots (Zhang and Outlaw, 2001b) increase the concentration of xylem-derived ABA up to 30-fold in guard cells (Outlaw, 2003). Together, the observation of *AtMPK12* promoter activity in both stomatal guard cells and root tissues would be consistent with the involvement of this gene in osmotic stress response. However, it does not appear that expression of *AtMPK12* is directly regulated by ABA, since exogenously applied ABA had no significant effect on the *AtMPK12* promoter-GUS activity in this study (data not shown). This result is consistent with SOS1 work (Shi *et al.*, 2000) in that *SOS1* can be induced transcriptionally by NaCl, but not by ABA. Although, my results indicate that ABA does not control the *AtMPK12* gene at the transcriptional level, this does not exclude the possibility that ABA could have an effect at the post-transcriptional level. For example, the activation of AtMPK4 and AtMPK6 in response to osmotic stresses was not associated with changes in the amount of the cognate mRNA or protein (Ichimura *et al.*, 2000). Similarly, ABA had no detectable effect on the transcript level of the protein kinase, *OST1*, or on the level of *OST1* promoter-GUS activity,

but it did induce the activation of the OST1 kinase. Notably, *OST1* expression and its promoter activity are also associated with the guard cells (Mustilli *et al.*, 2002).

4.4.5 Concluding remarks

Through molecular biology and reverse genetics approaches, I have identified a novel guard cell-specific MAPK, AtMPK12, that may be involved in correct guard cell development/patterning in normal growth conditions. In addition, I have shown that expression of *AtMPK12* is also salt-stress and osmotic-stress regulated. The mechanisms/pathways within which AtMPK12 operates in guard cell development or patterning and in response to salt and osmotic stress signal transduction remain largely unknown. Identification of AtMPK12 upstream regulators (e.g. MAPKKs and MAPKKKs) and downstream targets (e.g. transcription factors or other proteins) would be a priority. *AtMPK12* gene expression has been shown to be upregulated in *yda* mutant and downregulated in ΔN -YDA, a constitutively active version of YDA (Supporting online material in Bergmann *et al.*, 2004). This data raises the question whether YODA is an upstream MAPKKK signaling to AtMPK12. Biochemical investigations will be required to address this question, and further detailed characterization of the phenotypes of the *atmpk12* mutant would be required to address questions on the role(s) of AtMPK12 at specific stages during guard cell development and function.

CHAPTER 5

Overall Thesis Discussion and Future Directions

5.1 Transcriptional profiling approach versus developmental signaling

In my thesis research I screened *Arabidopsis* *MAPK* and *MAPKK* genes for their expression pattern, selected the most interesting candidate genes based on these expression patterns, formed hypotheses concerning their possible function(s), and tested the hypotheses with more specific experiments. However, many of the *MAPK* gene family members appear to function without marked changes over time and development at the transcriptional level. Therefore, expression profiling provides only limited information. Notably, all of the candidate genes chosen for further detailed functional characterization in this study appear to be involved in plant development. They are well differentiated in their expression in *Arabidopsis* cells, tissues and organs, which is not surprising given the basis of their selection. For these family members, at least, the pattern of transcript levels for particular MAPK signaling molecules can provide an initial indication of their molecular function.

It is interesting that some *MAPK/MAPKK* genes display large differences in transcriptional activity during development whereas others apparently do not. There are at least two possible explanations.

(1) The gene products may be required for routine functioning of specific cells or tissues, and these cells are increasing in number or size at a particular point in development. In this scenario, a MAPK/MAPKK gene produces more mRNA in order to generate more of the encoded proteins in order to meet the needs of multiple copies of similar cell types, or to execute more of the same process in existing cells. The amount of transcript may be critical

for production of a certain threshold level of a protein that regulates downstream targets. For example, in the case of the *PID* gene, the amount of its gene product is critical for its function in regulating PIN protein localization (Kaplinsky and Barton, 2004).

(2) In the case of the *AtMKK6* and *AtMPK13* genes, their gene products are presumably required for particular functions associated with initiation of a new tissue, lateral root primordia, within the pericycle.

5.2 Characterization of developmentally regulated genes using an inducible RNAi approach

Timing is critical in developmental processes; therefore, I used an inducible expression system in my study. The inducible RNAi approach is good for the functional analysis of developmentally regulated genes because gene expression can be interfered at a certain point during a biological process of interest. For example, I was able to use *AtMKK6*RNAi and *AtMPK13*RNAi for a lateral root formation assay by inducing the RNAi to interfere with the formation of lateral roots at the age that plants started to form these organs. (see Chapter 3).

5.3. Future directions

My thesis makes a significant contribution to the characterization of the *MAPK* gene family in plants, but there are many issues that need to be pursued further. Some of these issues would require new methodology and specific molecular tools, e.g. protein-specific antibodies. Suggestions for both complementary work and in-depth exploration of issues arising from my thesis results are presented as follows.

5.3.1 Systematic analysis of the *MAPKKK* genes

When I started my Ph.D. thesis in the year 1999, expression data for *Arabidopsis* genes was sparse in the publicly available databases, but extensive gene expression data is now available such as TAIR (<http://www.arabidopsis.org/links/microarrays.jsp>), MPSS (<http://mpss.udel.edu/at/>), Plantsp (<http://plantsp.genomics.purdue.edu/>) and GENEVESTIGATOR: *Arabidopsis* Microarray Database and Analysis Toolbox (<https://www.genevestigator.ethz.ch/>). It would therefore not require expensive and time-consuming experiments to obtain expression profiles for most members of any given gene family. My thesis indicates that a transcriptional profiling survey would be a useful entry point for systematic analysis of the *MAPKKK* genes, the class of *MAPK* gene family that presumably functions at the top of MAPK cascades. Since *MAPKK* and *MAPK* genes, the middle and the bottom components of these cascades, are transcriptionally regulated, it would be expected that some *AtMKKK* genes would also be transcriptionally regulated. Such transcriptional profiling would be a useful approach to identification of candidate genes worthy of further functional characterization. For example, the *Arabidopsis* orthologs of *NPK1* namely, *ANP1*, *ANP2* and *ANP3*, are highly expressed in organs that are rich in dividing cells (Nishihama *et al.*, 1997). These kinases are prime candidates to be tested for being upstream components of AtMKK6 and/or AtMPK13.

5.3.2 Use inducible promoters to drive *AtMPK12* gene constructs in stomata of transgenic plants

The *AtMPK12* gene is expressed in guard cells of most aerial tissues under normal growth conditions. This pattern indicates that ATMPK12 may be involved in stomatal development.

Therefore, I anticipate that loss-of-function or gain-of-function in ATMPK12 would interfere with this developmental process. To clarify the possible function of ATMPK12 in stomatal development, it would be useful to specifically interfere with stomatal *AtMPK12* expression by using an inducible promoter or tissue-specific promoter to drive expression of *AtMPK12* gene constructs (RNAi or over-expression of the gene) and perform analyses of the stomatal development.

5.3.3 Identification of the MAPK protein network

On the one hand, to identify an upstream component of ATMPK12, one could use an *in vivo* phosphorylation assay and identify which ATMKKs can phosphorylate the ATMPK12. On the other hand, one could use microarray analysis with the *AtMPK12* T-DNA mutant or inducible *AtMPK12*RNAi transgenic plants to identify possible downstream targets of ATMPK12.

5.3.4 Further characterization of the mutant and transgenic plants

It would be interesting to investigate the possible roles of the AtMKK6 and AtMPK13 in auxin polar transport and LRP cell-division using immunolocalization techniques (Sugimoto *et al.*, 2000; Friml *et al.*, 2004) with the AtMKK6RNAi and AtMPK13RNAi transgenic plants. In the case of AtMPK12, I am interested in further characterizing *atmpk12* plants to investigate their guard cell function such as guard cell opening and closing.

REFERENCES

- Abel, S., and Theologis, A. (1996). Early genes and auxin action. *Plant Physiol* **111**, 9-17.
- Agrawal, G.K., Rakwal, R., and Iwahashi, H. (2002). Isolation of novel rice (*Oryza sativa* L.) multiple stress responsive MAP kinase gene, OsMSRMK2, whose mRNA accumulates rapidly in response to environmental cues. *Biochem Biophys Res Commun* **294**, 1009-1016.
- Ahlfors, R., Macioszek, V., Rudd, J., Brosche, M., Schlichting, R., Scheel, D., and Kangasjarvi, J. (2004). Stress hormone-independent activation and nuclear translocation of mitogen-activated protein kinases in *Arabidopsis thaliana* during ozone exposure. *Plant J* **40**, 512-522.
- Ahn, N.G., Seger, R., Bratlien, R.L., Diltz, C.D., Tonks, N.K., and Krebs, E.G. (1991). Multiple components in an epidermal growth factor-stimulated protein kinase cascade. In vitro activation of a myelin basic protein/microtubule-associated protein 2 kinase. *J Biol Chem* **266**, 4220-4227.
- Alonso, J.M., Stepanova, A.N., Leisse, T.J., Kim, C.J., Chen, H., Shinn, P., Stevenson, D.K., Zimmerman, J., Barajas, P., Cheuk, R., Gadrinab, C., Heller, C., Jeske, A., Koesema, E., Meyers, C.C., Parker, H., Prednis, L., Ansari, Y., Choy, N., Deen, H., Geralt, M., Hazari, N., Hom, E., Karnes, M., Mulholland, C., Ndubaku, R., Schmidt, I., Guzman, P., Aguilar-Henonin, L., Schmid, M., Weigel, D., Carter, D.E., Marchand, T., Risseuw, E., Brogden, D., Zeko, A., Crosby, W.L., Berry, C.C., and Ecker, J.R. (2003). Genome-wide insertional mutagenesis of *Arabidopsis thaliana*. *Science* **301**, 653-657.
- Apse, M.P., Aharon, G.S., Snedden, W.A., and Blumwald, E. (1999). Salt tolerance conferred by overexpression of a vacuolar Na⁺/H⁺ antiport in *Arabidopsis*. *Science* **285**, 1256-1258.
- Asai, T., Tena, G., Plotnikova, J., Willmann, M.R., Chiu, W.L., Gomez-Gomez, L., Boller, T., Ausubel, F.M., and Sheen, J. (2002). MAP kinase signalling cascade in *Arabidopsis* innate immunity. *Nature* **415**, 977-983.
- Baier, M., Kandlbinder, A., Goldack, D., and Dietz, K.-J. (2005). Oxidative stress and ozone: Perception, signalling and response. *Plant, Cell and Environment*, 1-9.
- Ballas, N., Wong, L.M., and Theologis, A. (1993). Identification of the auxin-responsive element, AuxRE, in the primary indoleacetic acid-inducible gene, PS-IAA4/5, of pea (*Pisum sativum*). *J Mol Biol* **233**, 580-596.
- Banno, H., Hirano, K., Nakamura, T., Irie, K., Nomoto, S., Matsumoto, K., and Machida, Y. (1993). NPK1, a tobacco gene that encodes a protein with a domain homologous to yeast BCK1, STE11, and Byr2 protein kinases. *Mol Cell Biol* **13**, 4745-4752.
- Beeckman, T., Burssens, S., and Inze, D. (2001). The peri-cell-cycle in *Arabidopsis*. *J Exp Bot* **52**, 403-411.
- Berger, D., and Altmann, T. (2000). A subtilisin-like serine protease involved in the regulation of stomatal density and distribution in *Arabidopsis thaliana*. *Genes Dev* **14**, 1119-1131.
- Bergmann, D.C. (2004). Integrating signals in stomatal development. *Curr Opin Plant Biol* **7**, 26-32.

- Bergmann, D.C., Lukowitz, W., and Somerville, C.R.** (2004). Stomatal development and pattern controlled by a MAPKK kinase. *Science* **304**, 1494-1497.
- Bhalerao, R.P., Eklof, J., Ljung, K., Marchant, A., Bennett, M., and Sandberg, G.** (2002). Shoot-derived auxin is essential for early lateral root emergence in *Arabidopsis* seedlings. *Plant J* **29**, 325-332.
- Boerjan, W., Cervera, M.T., Delarue, M., Beeckman, T., Dewitte, W., Bellini, C., Caboche, M., Van Onckelen, H., Van Montagu, M., and Inze, D.** (1995). Superroot, a recessive mutation in *Arabidopsis*, confers auxin overproduction. *Plant Cell* **7**, 1405-1419.
- Bogre, L., Ligterink, W., Meskiene, I., Barker, P.J., Heberle-Bors, E., Huskisson, N.S., and Hirt, H.** (1997). Wounding induces the rapid and transient activation of a specific MAP kinase pathway. *Plant Cell* **9**, 75-83.
- Bogre, L., Calderini, O., Binarova, P., Mattauch, M., Till, S., Kiegerl, S., Jonak, C., Pollaschek, C., Barker, P., Huskisson, N.S., Hirt, H., and Heberle-Bors, E.** (1999). A MAP kinase is activated late in plant mitosis and becomes localized to the plane of cell division. *Plant Cell* **11**, 101-113.
- Bolwell, G.P.** (1996). The origin of the oxidative burst in plants. *Biochem Soc Trans* **24**, 438-442.
- Boulton, T.G., Yancopoulos, G.D., Gregory, J.S., Slaughter, C., Moomaw, C., Hsu, J., and Cobb, M.H.** (1990). An insulin-stimulated protein kinase similar to yeast kinases involved in cell cycle control. *Science* **249**, 64-67.
- Brenner, S., Johnson, M., Bridgham, J., Golda, G., Lloyd, D.H., Johnson, D., Luo, S., McCurdy, S., Foy, M., Ewan, M., Roth, R., George, D., Eletr, S., Albrecht, G., Vermaas, E., Williams, S.R., Moon, K., Burcham, T., Pallas, M., DuBridge, R.B., Kirchner, J., Fearon, K., Mao, J., and Corcoran, K.** (2000). Gene expression analysis by massively parallel signature sequencing (MPSS) on microbead arrays. *Nat Biotechnol* **18**, 630-634.
- Brunet, A., Roux, D., Lenormand, P., Dowd, S., Keyse, S., and Pouyssegur, J.** (1999). Nuclear translocation of p42/p44 mitogen-activated protein kinase is required for growth factor-induced gene expression and cell cycle entry. *EMBO J* **18**, 664-674.
- Burnett, E.C., Desikan, R., Moser, R.C., and Neill, S.J.** (2000). ABA activation of an MBP kinase in *Pisum sativum* epidermal peels correlates with stomatal responses to ABA. *J Exp Bot* **51**, 197-205.
- Calderini, O., Glab, N., Bergounioux, C., Heberle-Bors, E., and Wilson, C.** (2001). A novel tobacco mitogen-activated protein (MAP) kinase kinase, NtMEK1, activates the cell cycle-regulated p43Ntf6 MAP kinase. *J Biol Chem* **276**, 18139-18145.
- Calderini, O., Bogre, L., Vicente, O., Binarova, P., Heberle-Bors, E., and Wilson, C.** (1998). A cell cycle regulated MAP kinase with a possible role in cytokinesis in tobacco cells. *J Cell Sci* **111** (Pt 20), 3091-3100.
- Cardinale, F., Meskiene, I., Ouaked, F., and Hirt, H.** (2002). Convergence and divergence of stress-induced mitogen-activated protein kinase signaling pathways at the level of two distinct mitogen-activated protein kinase kinases. *Plant Cell* **14**, 703-711.
- Casimiro, I., Beeckman, T., Graham, N., Bhalerao, R., Zhang, H., Casero, P., Sandberg, G., and Bennett, M.J.** (2003). Dissecting *Arabidopsis* lateral root development. *Trends Plant Sci* **8**, 165-171.

- Casimiro, I., Marchant, A., Bhalerao, R.P., Beeckman, T., Dhooge, S., Swarup, R., Graham, N., Inze, D., Sandberg, G., Casero, P.J., and Bennett, M. (2001). Auxin transport promotes *Arabidopsis* lateral root initiation. *Plant Cell* **13**, 843-852.
- Celenza, J.L., Grisafi, P.L., and Fink, G.R. (1995). A pathway for lateral root-formation in *Arabidopsis thaliana*. *Gene Dev* **9**, 2131-2142.
- Clough, S.J., and Bent, A.F. (1998). Floral dip: a simplified method for *Agrobacterium*-mediated transformation of *Arabidopsis thaliana*. *Plant J* **16**, 735-743.
- Cooper, J.A., Bowen-Pope, D.F., Raines, E., Ross, R., and Hunter, T. (1982). Similar effects of platelet-derived growth factor and epidermal growth factor on the phosphorylation of tyrosine in cellular proteins. *Cell* **31**, 263-273.
- Coruzzi, G.M., and Zhou, L. (2001). Carbon and nitrogen sensing and signaling in plants: emerging 'matrix effects'. *Curr Opin Plant Biol* **4**, 247-253.
- Courchesne, W.E., Kunisawa, R., and Thorner, J. (1989). A putative protein kinase overcomes pheromone-induced arrest of cell cycling in *S. cerevisiae*. *Cell* **58**, 1107-1119.
- Crews, C.M., and Erikson, R.L. (1992). Purification of a murine protein-tyrosine/threonine kinase that phosphorylates and activates the Erk-1 gene product: relationship to the fission yeast *byr1* gene product. *Proc Natl Acad Sci U S A* **89**, 8205-8209.
- Crews, C.M., Alessandrini, A., and Erikson, R.L. (1992). The primary structure of MEK, a protein kinase that phosphorylates the ERK gene product. *Science* **258**, 478-480.
- Desikan, R., Hancock, J.T., Coffey, M.J., and Neill, S.J. (1996). Generation of active oxygen in elicited cells of *Arabidopsis thaliana* is mediated by a NADPH oxidase-like enzyme. *FEBS Lett* **382**, 213-217.
- Desikan, R., Hancock, J.T., Ichimura, K., Shinozaki, K., and Neill, S.J. (2001). Harpin induces activation of the *Arabidopsis* mitogen-activated protein kinases AtMPK4 and AtMPK6. *Plant Physiol* **126**, 1579-1587.
- Doerner, P., Jorgensen, J.E., You, R., Steppuhn, J., and Lamb, C. (1996). Control of root growth and development by cyclin expression. *Nature* **380**, 520-523.
- Dolan, L., Janmaat, K., Willemsen, V., Linstead, P., Poethig, S., Roberts, K., and Scheres, B. (1993). Cellular-organization of the *Arabidopsis thaliana* root. *Development* **119**, 71-84.
- Droillard, M., Boudsocq, M., Barbier-Brygoo, H., and Lauriere, C. (2002). Different protein kinase families are activated by osmotic stresses in *Arabidopsis thaliana* cell suspensions. Involvement of the MAP kinases AtMPK3 and AtMPK6. *FEBS Lett* **527**, 43-50.
- Dubrovsky, J.G., Doerner, P.W., Colon-Carmona, A., and Rost, T.L. (2000). Pericycle cell proliferation and lateral root initiation in *Arabidopsis*. *Plant Physiol* **124**, 1648-1657.
- Edwards, K., Johnstone, C., and Thompson, C. (1991). A simple and rapid method for the preparation of plant genomic DNA for PCR analysis. *Nucl. Acids Res.* **19**, 1349-.
- Elion, E.A., Grisafi, P.L., and Fink, G.R. (1990). FUS3 encodes a *cdc2*+/CDC28-related kinase required for the transition from mitosis into conjugation. *Cell* **60**, 649-664.
- Epstein, E., Norlyn, J.D., Rush, D.W., Kingsbury, R.W., Kelley, D.B., Cunningham, G.A., and Wrona, A.F. (1980). Saline culture of crops: a genetic approach. *Science* **210**, 399-404.

- Friml, J., Yang, X., Michniewicz, M., Weijers, D., Quint, A., Tietz, O., Benjamins, R., Ouwerkerk, P.B., Ljung, K., Sandberg, G., Hooykaas, P.J., Palme, K., and Offringa, R.** (2004). A PINOID-dependent binary switch in apical-basal PIN polar targeting directs auxin efflux. *Science* **306**, 862-865.
- Frye, C.A., Tang, D., and Innes, R.W.** (2001). Negative regulation of defense responses in plants by a conserved MAPKK kinase. *Proc Natl Acad Sci U S A* **98**, 373-378.
- Fu, S.F., Chou, W.C., Huang, D.D., and Huang, H.J.** (2002). Transcriptional regulation of a rice mitogen-activated protein kinase gene, OsMAPK4, in response to environmental stresses. *Plant Cell Physiol* **43**, 958-963.
- Galweiler, L., Guan, C., Muller, A., Wisman, E., Mendgen, K., Yephremov, A., and Palme, K.** (1998). Regulation of polar auxin transport by AtPIN1 in *Arabidopsis* vascular tissue. *Science* **282**, 2226-2230.
- Geisler, M., Yang, M., and Sack, F.D.** (1998). Divergent regulation of stomatal initiation and patterning in organ and suborgan regions of the *Arabidopsis* mutants too many mouths and four lips. *Planta* **205**, 522-530.
- Geisler, M., Nadeau, J., and Sack, F.D.** (2000). Oriented asymmetric divisions that generate the stomatal spacing pattern in *Arabidopsis* are disrupted by the too many mouths mutation. *Plant Cell* **12**, 2075-2086.
- Grabov, A., Leung, J., Giraudat, J., and Blatt, M.R.** (1997). Alteration of anion channel kinetics in wild-type and abil-1 transgenic *Nicotiana benthamiana* guard cells by abscisic acid. *Plant J* **12**, 203-213.
- Green, R., and Fluhr, R.** (1995). UV-B-Induced PR-1 Accumulation is mediated by active oxygen species. *Plant Cell* **7**, 203-212.
- Gupta, R., Huang, Y., Kieber, J., and Luan, S.** (1998). Identification of a dual-specificity protein phosphatase that inactivates a MAP kinase from *Arabidopsis*. *Plant J* **16**, 581-589.
- Gustin, M.C., Albertyn, J., Alexander, M., and Davenport, K.** (1998a). MAP kinase pathways in the yeast *Saccharomyces cerevisiae*. *Microbiol Mol Biol Rev* **62**, 1264-1300.
- Gustin, M.C., Albertyn, J., Alexander, M., and Davenport, K.** (1998b). MAP kinase pathways in the yeast *Saccharomyces cerevisiae*. *Microbiol Mol Biol Rev* **62**, 1264-+.
- Halfter, U., Ishitani, M., and Zhu, J.K.** (2000). The *Arabidopsis* SOS2 protein kinase physically interacts with and is activated by the calcium-binding protein SOS3. *Proc Natl Acad Sci U S A* **97**, 3735-3740.
- Hamal, A., Jouannic, S., Leprince, A.-S., Kreis, M., and Henry, Y.** (1999). Molecular characterization and expression of an *Arabidopsis thaliana* L. MAP kinase kinase cDNA, AtMAP2K[alpha]. *Plant Science* **140**, 49-64.
- Hardin, S.C., and Wolniak, S.M.** (1998). Molecular cloning and characterization of maize ZmMEK1, a protein kinase with a catalytic domain homologous to mitogen- and stress-activated protein kinase kinases. *Planta* **206**, 577-584.
- Hasegawa, P.M., Bressan, R.A., Zhu, J.K., and Bohnert, H.J.** (2000). Plant cellular and molecular responses to high salinity. *Annu Rev Plant Physiol Plant Mol Biol* **51**, 463-499.
- Herskowitz, I.** (1995). MAP kinase pathways in yeast: for mating and more. *Cell* **80**, 187-197.

- Hey, S.J., Bacon, A., Burnett, E.C., and Neill, S.J. (1997). Absciscic acid signal transduction in epidermis cells of *Pisum sativum* L. *Argenteum*: both dehydrin mRNA accumulation and stomatal responses require protein phosphorylation and dephosphorylation. *Planta* **202**, 85-92.
- Higo, K., Ugawa, Y., Iwamoto, M., and Korenaga, T. (1999). Plant cis-acting regulatory DNA elements (PLACE) database: 1999. *Nucleic Acids Res* **27**, 297-300.
- Himanen, K., Boucheron, E., Vanneste, S., de Almeida Engler, J., Inze, D., and Beeckman, T. (2002). Auxin-mediated cell cycle activation during early lateral root initiation. *Plant Cell* **14**, 2339-2351.
- Hirt, H. (2000). MAP kinases in plant signal transduction. *Results Probl Cell Differ* **27**, 1-9.
- Hobbie, L., and Estelle, M. (1994). Genetic approaches to auxin action. *Plant Cell Environ* **17**, 525-540.
- Huang, X., Stettmaier, K., Michel, C., Hutzler, P., Mueller, M.J., and Durner, J. (2004). Nitric oxide is induced by wounding and influences jasmonic acid signaling in *Arabidopsis thaliana*. *Planta* **218**, 938-946.
- Huang, Y., Li, H., Gupta, R., Morris, P.C., Luan, S., and Kieber, J.J. (2000). ATMPK4, an *Arabidopsis* homolog of mitogen-activated protein kinase, is activated in vitro by AtMEK1 through threonine phosphorylation. *Plant Physiol* **122**, 1301-1310.
- Ichimura, K., Mizoguchi, T., Hayashida, N., Seki, M., and Shinozaki, K. (1998a). Molecular cloning and characterization of three cDNAs encoding putative mitogen-activated protein kinase kinases (MAPKKs) in *Arabidopsis thaliana*. *DNA Res* **5**, 341-348.
- Ichimura, K., Mizoguchi, T., Yoshida, R., Yuasa, T., and Shinozaki, K. (2000). Various abiotic stresses rapidly activate *Arabidopsis* MAP kinases ATMPK4 and ATMPK6. *Plant J* **24**, 655-665.
- Ichimura, K., Mizoguchi, T., Irie, K., Morris, P., Giraudat, J., Matsumoto, K., and Shinozaki, K. (1998b). Isolation of ATMEKK1 (a MAP kinase kinase kinase)-interacting proteins and analysis of a MAP kinase cascade in *Arabidopsis*. *Biochem Biophys Res Commun* **253**, 532-543.
- Ishikawa, M., Soyano, T., Nishihama, R., and Machida, Y. (2002). The NPK1 mitogen-activated protein kinase kinase kinase contains a functional nuclear localization signal at the binding site for the NACK1 kinesin-like protein. *Plant J* **32**, 789-798.
- Ishitani, M., Liu, J., Halfter, U., Kim, C.S., Shi, W., and Zhu, J.K. (2000). SOS3 function in plant salt tolerance requires N-myristoylation and calcium binding. *Plant Cell* **12**, 1667-1678.
- Jefferson, R.A. (1987). Assaying chimeric genes in plants: The GUS gene fusion system. *plant molecular biology reporter* **5**, 387-405.
- Johnson, P.R., and Ecker, J.R. (1998). The ethylene gas signal transduction pathway: a molecular perspective. *Annu Rev Genet* **32**, 227-254.
- Jonak, C., and Hirt, H. (2002). Glycogen synthase kinase 3/SHAGGY-like kinases in plants: an emerging family with novel functions. *Trends in Plant Science* **7**, 457-461.
- Jonak, C., Okresz, L., Bogre, L., and Hirt, H. (2002). Complexity, cross talk and integration of plant MAP kinase signalling. *Curr Opin Plant Biol* **5**, 415-424.
- Jonak, C., Kiegerl, S., Ligterink, W., Barker, P.J., Huskisson, N.S., and Hirt, H. (1996). Stress signaling in plants: a mitogen-activated protein kinase pathway is activated by cold and drought. *Proc Natl Acad Sci U S A* **93**, 11274-11279.

- Jouannic, S., Hamal, A., Leprince, A.S., Tregear, J.W., Kreis, M., and Henry, Y. (1999).** Characterisation of novel plant genes encoding MEKK/STE11 and RAF-related protein kinases. *Gene* **229**, 171-181.
- Kaplinsky, N.J., and Barton, M.K. (2004).** Plant biology. Plant acupuncture: sticking PINs in the right places. *Science* **306**, 822-823.
- Kieber, J.J., Rothenberg, M., Roman, G., Feldmann, K.A., and Ecker, J.R. (1993).** CTR1, a negative regulator of the ethylene response pathway in *Arabidopsis*, encodes a member of the raf family of protein kinases. *Cell* **72**, 427-441.
- Kiegerl, S., Cardinale, F., Siligan, C., Gross, A., Baudouin, E., Liwosz, A., Eklof, S., Till, S., Bogre, L., Hirt, H., and Meskiene, I. (2000).** SIMKK, a mitogen-activated protein kinase (MAPK) kinase, is a specific activator of the salt stress-induced MAPK, SIMK. *Plant Cell* **12**, 2247-2258.
- Knetsch, M., Wang, M., Snaar-Jagalska, B.E., and Heimovaara-Dijkstra, S. (1996).** Absciscic acid induces mitogen-activated protein kinase activation in barley aleurone protoplasts. *Plant Cell* **8**, 1061-1067.
- Kovtun, Y., Chiu, W.L., Zeng, W., and Sheen, J. (1998).** Suppression of auxin signal transduction by a MAPK cascade in higher plants. *Nature* **395**, 716-720.
- Kovtun, Y., Chiu, W.L., Tena, G., and Sheen, J. (2000).** Functional analysis of oxidative stress-activated mitogen-activated protein kinase cascade in plants. *Proc Natl Acad Sci U S A* **97**, 2940-2945.
- Kreps, J.A., Wu, Y., Chang, H.S., Zhu, T., Wang, X., and Harper, J.F. (2002).** Transcriptome changes for *Arabidopsis* in response to salt, osmotic, and cold stress. *Plant Physiol* **130**, 2129-2141.
- Krysan, P.J., Jester, P.J., Gottwald, J.R., and Sussman, M.R. (2002).** An *Arabidopsis* mitogen-activated protein kinase kinase kinase gene family encodes essential positive regulators of cytokinesis. *Plant Cell* **14**, 1109-1120.
- Kyriakis, J.M., App, H., Zhang, X.F., Banerjee, P., Brautigan, D.L., Rapp, U.R., and Avruch, J. (1992).** Raf-1 activates MAP kinase-kinase. *Nature* **358**, 417-421.
- Lange-Carter, C.A., Pleiman, C.M., Gardner, A.M., Blumer, K.J., and Johnson, G.L. (1993).** A divergence in the MAP kinase regulatory network defined by MEK kinase and Raf. *Science* **260**, 315-319.
- Larkin, J.C., Brown, M.L., and Schiefelbein, J. (2003).** How do cells know what they want to be when they grow up? Lessons from epidermal patterning in *Arabidopsis*. *Annu Rev Plant Biol* **54**, 403-430.
- Larkin, J.C., Marks, M.D., Nadeau, J., and Sack, F. (1997).** Epidermal cell fate and patterning in leaves. *Plant Cell* **9**, 1109-1120.
- Laskowski, M.J., Williams, M.E., Nusbaum, H.C., and Sussex, I.M. (1995).** Formation of lateral root meristems is a two-stage process. *Development* **121**, 3303-3310.
- Le Deunff, E., Davoine, C., Le Dantec, C., Billard, J.P., and Huault, C. (2004).** Oxidative burst and expression of germin/oxo genes during wounding of ryegrass leaf blades: comparison with senescence of leaf sheaths. *Plant J* **38**, 421-431.
- Lescot, M., Dehais, P., Thijs, G., Marchal, K., Moreau, Y., Van de Peer, Y., Rouze, P., and Rombauts, S. (2002).** PlantCARE, a database of plant cis-acting regulatory elements and a portal to tools for in silico analysis of promoter sequences. *Nucleic Acids Res* **30**, 325-327.

- Leung, J., and Giraudat, J.** (1998). Absciscic acid signal transduction. *Annu Rev Plant Physiol Plant Mol Biol* **49**, 199-222.
- Leung, J., Merlot, S., and Giraudat, J.** (1997). The *Arabidopsis* *ABSCISIC ACID INSENSITIVE 2* (*ABI2*) and *ABI1* genes encode redundant protein phosphatases 2C involved in absciscic acid signal transduction. *Plant Cell* **9**, 759-771.
- Leung, J., Bouvier-Durand, M., Morris, P.-C., Guerrier, D., Cheddor, F., and Giraudat, J.** (1994). *Arabidopsis* ABA-response gene *ABI1*: features of a calcium-modulated protein phosphatase. *Science* **264**, 1448-1452.
- Li, J., and Assmann, S.M.** (1996). An absciscic acid-activated and calcium-independent protein kinase from guard cells of fava bean. *Plant Cell* **8**, 2359-2368.
- Li, J., Lee, Y.R., and Assmann, S.M.** (1998). Guard cells possess a calcium-dependent protein kinase that phosphorylates the KAT1 potassium channel. *Plant Physiol* **116**, 785-795.
- Li, J., Wang, X.Q., Watson, M.B., and Assmann, S.M.** (2000). Regulation of absciscic acid-induced stomatal closure and anion channels by guard cell AAPK kinase. *Science* **287**, 300-303.
- Ligterink, W., and Hirt, H.** (2001). Mitogen-activated protein (MAP) kinase pathways in plants: versatile signaling tools. *Int Rev Cytol* **201**, 209-275.
- Liu, J., Ishitani, M., Halfter, U., Kim, C.S., and Zhu, J.K.** (2000). The *Arabidopsis thaliana* *SOS2* gene encodes a protein kinase that is required for salt tolerance. *Proc Natl Acad Sci U S A* **97**, 3730-3734.
- Liu, S., and Zhu, J.K.** (1997). An *Arabidopsis* mutant that requires increased calcium for potassium nutrition and salt tolerance. *PNAS* **94**, 14960-14964.
- Liu, S., and Zhu, J.K.** (1998). A calcium sensor homolog required for plant salt tolerance. *Science* **280**, 1943-1945.
- Liu, Y., and Zhang, S.** (2004). Phosphorylation of 1-aminocyclopropane-1-carboxylic acid synthase by MPK6, a stress-responsive mitogen-activated protein kinase, induces ethylene biosynthesis in *Arabidopsis*. *Plant Cell* **16**, 3386-3399.
- Liu, Y., Jin, H., Yang, K.Y., Kim, C.Y., Baker, B., and Zhang, S.** (2003). Interaction between two mitogen-activated protein kinases during tobacco defense signaling. *Plant J* **34**, 149-160.
- Luan, S.** (2002). Signalling drought in guard cells. *Plant Cell Environ* **25**, 229-237.
- Lukowitz, W., Roeder, A., Parmenter, D., and Somerville, C.** (2004). A MAPKK kinase gene regulates extra-embryonic cell fate in *Arabidopsis*. *Cell* **116**, 109-119.
- MacRobbie, E.A.C.** (1997). Signalling in guard cells and regulation of ion channel activity. *J Exp Bot* **48**, 515-528.
- Malamy, J.E., and Benfey, P.N.** (1997). Organization and cell differentiation in lateral roots of *Arabidopsis thaliana*. *Development* **124**, 33-44.
- Malamy, J.E., and Ryan, K.S.** (2001). Environmental regulation of lateral root initiation in *Arabidopsis*. *Plant Physiol* **127**, 899-909.
- MAPK Group.** (2002). Mitogen-activated protein kinase cascades in plants: a new nomenclature. *Trends Plant Sci* **7**, 301-308.
- Matsuoka, D., Nanmori, T., Sato, K., Fukami, Y., Kikkawa, U., and Yasuda, T.** (2002). Activation of AtMEK1, an *Arabidopsis* mitogen-activated protein kinase kinase, in vitro and in vivo: analysis of active mutants expressed in *E. coli* and generation of the active form in stress response in seedlings. *Plant J* **29**, 637-647.

- Mayrose, M., Bonshtien, A., and Sessa, G.** (2004). LeMPK3 is a mitogen-activated protein kinase with dual specificity induced during tomato defense and wounding responses. *J Biol Chem* **279**, 14819-14827.
- McNellis, T.W., Mudgett, M.B., Li, K., Aoyama, T., Horvath, D., Chua, N.H., and Staskawicz, B.J.** (1998). Glucocorticoid-inducible expression of a bacterial avirulence gene in transgenic *Arabidopsis* induces hypersensitive cell death. *Plant J* **14**, 247-257.
- Mehdy, M.C.** (1994). Active oxygen species in plant defense against pathogens. *Plant Physiol* **105**, 467-472.
- Melaragno, J.E., Mehrotra, B., and Coleman, A.W.** (1993). Relationship between endopolyploidy and cell size in epidermal tissue of *Arabidopsis*. *Plant Cell* **5**, 1661-1668.
- Melikant, B., Giuliani, C., Halbmayer-Watzina, S., Limmongkon, A., Heberle-Bors, E., and Wilson, C.** (2004). The *Arabidopsis thaliana* MEK AtMKK6 activates the MAP kinase AtMPK13. *FEBS Lett* **576**, 5-8.
- Meskiene, I., Baudouin, E., Schweighofer, A., Liwosz, A., Jonak, C., Rodriguez, P.L., Jelinek, H., and Hirt, H.** (2003). Stress-induced protein phosphatase 2C is a negative regulator of a mitogen-activated protein kinase. *J Biol Chem* **278**, 18945-18952.
- Meyer, K., Leube, M.P., and Grill, E.** (1994). A protein phosphatase 2C involved in ABA signal transduction in *Arabidopsis thaliana*. *Science* **264**, 1452-1455.
- Meyers, B.C., Lee, D.K., Vu, T.H., Tej, S.S., Edberg, S.B., Matvienko, M., and Tindell, L.D.** (2004a). *Arabidopsis* MPSS. an online resource for quantitative expression analysis. *Plant Physiol* **135**, 801-813.
- Meyers, B.C., Tej, S.S., Vu, T.H., Haudenschild, C.D., Agrawal, V., Edberg, S.B., Ghazal, H., and Decola, S.** (2004b). The use of MPSS for whole-genome transcriptional analysis in *Arabidopsis*. *Genome Res* **14**, 1641-1653.
- Mikolajczyk, M., Awotunde, O.S., Muszynska, G., Klessig, D.F., and Dobrowolska, G.** (2000). Osmotic stress induces rapid activation of a salicylic acid-induced protein kinase and a homolog of protein kinase ASK1 in tobacco cells. *Plant Cell* **12**, 165-178.
- Mizoguchi, T., Ichimura, K., and Shinozaki, K.** (1997). Environmental stress response in plants: the role of mitogen-activated protein kinases. *Trends Biotechnol* **15**, 15-19.
- Mizoguchi, T., Irie, K., Hirayama, T., Hayashida, N., Yamaguchi-Shinozaki, K., Matsumoto, K., and Shinozaki, K.** (1996). A gene encoding a mitogen-activated protein kinase kinase kinase is induced simultaneously with genes for a mitogen-activated protein kinase and an S6 ribosomal protein kinase by touch, cold, and water stress in *Arabidopsis thaliana*. *Proc Natl Acad Sci U S A* **93**, 765-769.
- Mizoguchi, T., Ichimura, K., Irie, K., Morris, P., Giraudat, J., Matsumoto, K., and Shinozaki, K.** (1998). Identification of a possible MAP kinase cascade in *Arabidopsis thaliana* based on pairwise yeast two-hybrid analysis and functional complementation tests of yeast mutants. *FEBS Lett* **437**, 56-60.
- Mizoguchi, T., Gotoh, Y., Nishida, E., Yamaguchi-Shinozaki, K., Hayashida, N., Iwasaki, T., Kamada, H., and Shinozaki, K.** (1994). Characterization of two cDNAs that encode MAP kinase homologues in *Arabidopsis thaliana* and analysis of the possible role of auxin in activating such kinase activities in cultured cells. *Plant J* **5**, 111-122.

- Morris, P.C.** (2001). MAP kinase signal transduction pathways in plants. *New Phytol* **151**, 67-89.
- Morris, P.C., Guerrier, D., Leung, J., and Giraudat, J.** (1997). Cloning and characterisation of MEK1, an *Arabidopsis* gene encoding a homologue of MAP kinase kinase. *Plant Mol Biol* **35**, 1057-1064.
- Mustilli, A.C., Merlot, S., Vavasseur, A., Fenzi, F., and Giraudat, J.** (2002). *Arabidopsis* OST1 protein kinase mediates the regulation of stomatal aperture by abscisic acid and acts upstream of reactive oxygen species production. *Plant Cell* **14**, 3089-3099.
- Nadeau, J.A., and Sack, F.D.** (2002a). Control of stomatal distribution on the *Arabidopsis* leaf surface. *Science* **296**, 1697-1700.
- Nadeau, J.A., and Sack, F.D.** (2002b). *The Arabidopsis Book*. (Rockville, MD: American Society of Plant Biologists).
- Nadeau, J.A., and Sack, F.D.** (2003). Stomatal development: cross talk puts mouths in place. *Trends Plant Sci* **8**, 294-299.
- Nakagami, H., Kiegerl, S., and Hirt, H.** (2004). OMTK1, a novel MAPKKK, channels oxidative stress signaling through direct MAPK interaction. *J Biol Chem* **279**, 26959-26966.
- Nakamura, R.L., McKendree, W.L., Jr., Hirsch, R.E., Sedbrook, J.C., Gaber, R.F., and Sussman, M.R.** (1995). Expression of an *Arabidopsis* potassium channel gene in guard cells. *Plant Physiol* **109**, 371-374.
- Nakashima, M., Hirano, K., Nakashima, S., Banno, H., Nishihama, R., and Machida, Y.** (1998). The expression pattern of the gene for NPK1 protein kinase related to mitogen-activated protein kinase kinase kinase (MAPKKK) in a tobacco plant: correlation with cell proliferation. *Plant Cell Physiol* **39**, 690-700.
- Nishihama, R., and Machida, Y.** (2000). The MAP kinase cascade that includes MAPKKK-related protein kinase NPK1 controls a mitotic process in plant cells. *Results Probl Cell Differ* **27**, 119-130.
- Nishihama, R., Banno, H., Kawahara, E., Irie, K., and Machida, Y.** (1997). Possible involvement of differential splicing in regulation of the activity of *Arabidopsis* ANP1 that is related to mitogen-activated protein kinase kinase kinases (MAPKKKs). *Plant J* **12**, 39-48.
- Nishihama, R., Ishikawa, M., Araki, S., Soyano, T., Asada, T., and Machida, Y.** (2001). The NPK1 mitogen-activated protein kinase kinase kinase is a regulator of cell-plate formation in plant cytokinesis. *Genes Dev* **15**, 352-363.
- Nuhse, T.S., Peck, S.C., Hirt, H., and Boller, T.** (2000). Microbial elicitors induce activation and dual phosphorylation of the *Arabidopsis thaliana* MAPK 6. *J Biol Chem* **275**, 7521-7526.
- Ouaked, F., Rozhon, W., Lecourieux, D., and Hirt, H.** (2003). A MAPK pathway mediates ethylene signaling in plants. *Embo J* **22**, 1282-1288.
- Outlaw.** (2003). Integration of cellular and physiological functions of guard cells. *Crit Rev Plant Sci* **22**, 503-529.
- Outlaw, W.H., Jr.** (1983). Current concepts on the role of potassium in stomatal movements. *Physiol Plant* **59**, 302-311.
- Pages, G., Lenormand, P., L'Allemain, G., Chambard, J.C., Meloche, S., and Pouyssegur, J.** (1993). Mitogen-activated protein kinases p42mapk and p44mapk are required for fibroblast proliferation. *Proc Natl Acad Sci U S A* **90**, 8319-8323.

- Pandey, S., and Assmann, S.M.** (2004). The *Arabidopsis* putative G protein-coupled receptor GCR1 interacts with the G protein alpha subunit GPA1 and regulates abscisic acid signaling. *Plant Cell* **16**, 1616-1632.
- Pearson, G., Robinson, F., Beers Gibson, T., Xu, B.E., Karandikar, M., Berman, K., and Cobb, M.H.** (2001). Mitogen-activated protein (MAP) kinase pathways: regulation and physiological functions. *Endocr Rev* **22**, 153-183.
- Pei, Z.M., Kuchitsu, K., Ward, J.M., Schwarz, M., and Schroeder, J.I.** (1997). Differential abscisic acid regulation of guard cell slow anion channels in *Arabidopsis* wild-type and *abi1* and *abi2* mutants. *Plant Cell* **9**, 409-423.
- Petersen, M., Brodersen, P., Naested, H., Andreasson, E., Lindhart, U., Johansen, B., Nielsen, H.B., Lacy, M., Austin, M.J., Parker, J.E., Sharma, S.B., Klessig, D.F., Martienssen, R., Mattsson, O., Jensen, A.B., and Mundy, J.** (2000). *Arabidopsis* map kinase 4 negatively regulates systemic acquired resistance. *Cell* **103**, 1111-1120.
- Piao, H.L., Lim, J.H., Kim, S.J., Cheong, G.W., and Hwang, I.** (2001). Constitutive over-expression of AtGSK1 induces NaCl stress responses in the absence of NaCl stress and results in enhanced NaCl tolerance in *Arabidopsis*. *Plant J* **27**, 305-314.
- Pollok, B.A., and Heim, R.** (1999). Using GFP in FRET-based applications. *Trends Cell Biol* **9**, 57-60.
- Poovaiah, B.W., Friedmann, M., Reddy, A.S., and Rhee, J.K.** (1988). Auxin induced delay of abscission: The involvement of calcium ions and protein phosphorylation in bean plants. *Physiol Plant* **73**, 354-359.
- Prestamo, G., Testillano, P.S., Vicente, O., Gonzalez-Melendi, P., Coronado, M.J., Wilson, C., Heberle-Bors, E., and Risueno, M.C.** (1999). Ultrastructural distribution of a MAP kinase and transcripts in quiescent and cycling plant cells and pollen grains. *J Cell Sci* **112** (Pt 7), 1065-1076.
- Rashotte, A.M., Brady, S.R., Reed, R.C., Ante, S.J., and Muday, G.K.** (2000). Basipetal auxin transport is required for gravitropism in roots of *Arabidopsis*. *Plant Physiol* **122**, 481-490.
- Ray, L.B., and Sturgill, T.W.** (1987). Rapid stimulation by insulin of a serine/threonine kinase in 3T3-L1 adipocytes that phosphorylates microtubule-associated protein 2 in vitro. *Proc Natl Acad Sci U S A* **84**, 1502-1506.
- Raz, V., and Fluhr, R.** (1993). Ethylene signal is transduced via protein phosphorylation events in plants. *Plant Cell* **5**, 523-530.
- Reddy, A.S., Chengappa, S., and Poovaiah, B.W.** (1987). Auxin-regulated changes in protein phosphorylation in pea epicotyls. *Biochem Biophys Res Commun* **144**, 944-950.
- Reed, R.C., Brady, S.R., and Muday, G.K.** (1998). Inhibition of auxin movement from the shoot into the root inhibits lateral root development in *Arabidopsis*. *Plant Physiol* **118**, 1369-1378.
- Roelfsema, M.R., Levchenko, V., and Hedrich, R.** (2004). ABA depolarizes guard cells in intact plants, through a transient activation of R- and S-type anion channels. *Plant J* **37**, 578-588.
- Rossomando, A.J., Payne, D.M., Weber, M.J., and Sturgill, T.W.** (1989). Evidence that pp42, a major tyrosine kinase target protein, is a mitogen-activated serine/threonine protein kinase. *Proc Natl Acad Sci U S A* **86**, 6940-6943.

- Sakai, T., Takahashi, Y., and Nagata, T. (1996). Analysis of the promoter of the auxin-inducible gene, *parC*, of tobacco. *Plant Cell Physiol* **37**, 906-913.
- Sambrook, J., Fritsch, E., and Maniatis, T. (1989). *Molecular cloning: a laboratory manual*, 2nd edition. (New York: Cold Spring Harbor Laboratory Press).
- Samuel, M.A., and Ellis, B.E. (2002). Double jeopardy: both overexpression and suppression of a redox-activated plant mitogen-activated protein kinase render tobacco plants ozone sensitive. *Plant Cell* **14**, 2059-2069.
- Samuel, M.A., Miles, G.P., and Ellis, B.E. (2000). Ozone treatment rapidly activates MAP kinase signalling in plants. *Plant J* **22**, 367-376.
- Schraudner, M., Langebartels, C., and Sandermann, H., Jr. (1996). Plant defence systems and ozone. *Biochem Soc Trans* **24**, 456-461.
- Schroeder, J.I., Kwak, J.M., and Allen, G.J. (2001a). Guard cell abscisic acid signalling and engineering drought hardness in plants. *Nature* **410**, 327-330.
- Schroeder, J.I., Allen, G.J., Hugouvieux, V., Kwak, J.M., and Waner, D. (2001b). Guard cell signal transduction. *Annu Rev Plant Physiol Plant Mol Biol* **52**, 627-658.
- Seger, R., Ahn, N.G., Posada, J., Munar, E.S., Jensen, A.M., Cooper, J.A., Cobb, M.H., and Krebs, E.G. (1992). Purification and characterization of mitogen-activated protein kinase activator(s) from epidermal growth factor-stimulated A431 cells. *J Biol Chem* **267**, 14373-14381.
- Seo, S., Sano, H., and Ohashi, Y. (1999). Jasmonate-based wound signal transduction requires activation of WIPK, a tobacco mitogen-activated protein kinase. *Plant Cell* **11**, 289-298.
- Seo, S., Okamoto, M., Seto, H., Ishizuka, K., Sano, H., and Ohashi, Y. (1995). Tobacco MAP kinase: a possible mediator in wound signal transduction pathways. *Science* **270**, 1988-1992.
- Shi, H., and Zhu, J.K. (2002). Regulation of expression of the vacuolar Na^+/H^+ antiporter gene *AtNHX1* by salt stress and abscisic acid. *Plant Mol Biol* **50**, 543-550.
- Shi, H., Ishitani, M., Kim, C., and Zhu, J.K. (2000). The *Arabidopsis thaliana* salt tolerance gene *SOS1* encodes a putative Na^+/H^+ antiporter. *Proc Natl Acad Sci U S A* **97**, 6896-6901.
- Shpak, E.D., McAbee, J.M., Pillitteri, L.J., and Torii, K.U. (2005). Stomatal patterning and differentiation by synergistic interactions of receptor kinases. *Science* **309**, 290-293.
- Skene, K. (2000). Pattern formation in cluster roots: Some developmental and evolutionary considerations. *Ann Bot-London* **85**, 901-908.
- Soyano, T., Nishihama, R., Morikiyo, K., Ishikawa, M., and Machida, Y. (2003). NQK1/NtMEK1 is a MAPKK that acts in the NPK1 MAPKKK-mediated MAPK cascade and is required for plant cytokinesis. *Genes Dev* **17**, 1055-1067.
- Stals, H., and Inze, D. (2001). When plant cells decide to divide. *Trends Plant Sci* **6**, 359-364.
- Strompen, G., El Kasmi, F., Richter, S., Lukowitz, W., Assaad, F.F., Jurgens, G., and Mayer, U. (2002). The *Arabidopsis* HINKEL gene encodes a kinesin-related protein involved in cytokinesis and is expressed in a cell cycle-dependent manner. *Curr Biol* **12**, 153-158.

- Sugimoto, K., Williamson, R.E., and Wasteneys, G.O.** (2000). New techniques enable comparative analysis of microtubule orientation, wall texture, and growth rate in intact roots of *Arabidopsis*. *Plant Physiol* **124**, 1493-1506.
- Takahashi, Y., Soyano, T., Sasabe, M., and Machida, Y.** (2004). A MAP kinase cascade that controls plant cytokinesis. *J Biochem (Tokyo)* **136**, 127-132.
- Takenaka, K., Gotoh, Y., and Nishida, E.** (1997). MAP kinase is required for the spindle assembly checkpoint but is dispensable for the normal M phase entry and exit in *Xenopus* egg cell cycle extracts. *J Cell Biol* **136**, 1091-1097.
- Talbott, L.D., and Zeiger, E.** (1998). The role of sucrose in guard cell osmoregulation. *J Exp Bot* **49**, 329-337.
- Tanaka, H., Ishikawa, M., Kitamura, S., Takahashi, Y., Soyano, T., Machida, C., and Machida, Y.** (2004). The AtNACK1/HINKEL and STUD/TETRASPORE/AtNACK2 genes, which encode functionally redundant kinesins, are essential for cytokinesis in *Arabidopsis*. *Genes Cells* **9**, 1199-1211.
- Teige, M., Scheikl, E., Eulgem, T., Doczi, R., Ichimura, K., Shinozaki, K., Dangl, J.L., and Hirt, H.** (2004). The MKK2 pathway mediates cold and salt stress signaling in *Arabidopsis*. *Mol Cell* **15**, 141-152.
- Tena, G., Asai, T., Chiu, W.L., and Sheen, J.** (2001). Plant mitogen-activated protein kinase signaling cascades. *Curr Opin Plant Biol* **4**, 392-400.
- Thiel, G., MacRobbie, E.A., and Blatt, M.R.** (1992). Membrane transport in stomatal guard cells: the importance of voltage control. *J Membr Biol* **126**, 1-18.
- Urao, T., Yamaguchi-Shinozaki, K., and Shinozaki, K.** (2000). Two-component systems in plant signal transduction. *Trends Plant Sci* **5**, 67-74.
- Usami, S., Banno, H., Ito, Y., Nishihama, R., and Machida, Y.** (1995). Cutting activates a 46-kilodalton protein kinase in plants. *Proc Natl Acad Sci U S A* **92**, 8660-8664.
- Van Haute, E., Joos, H., Maes, M., Warren, G., Van Montagu, M., and Schell, J.** (1983). Intergeneric transfer and exchange recombination of restriction fragments cloned in pBR322: a novel strategy for the reversed genetics of the Ti plasmids of *Agrobacterium tumefaciens*. *Embo J* **2**, 411-417.
- von Groll, U., and Altmann, T.** (2001). Stomatal cell biology. *Curr Opin Plant Biol* **4**, 555-560.
- Von Groll, U., Berger, D., and Altmann, T.** (2002). The subtilisin-like serine protease SDD1 mediates cell-to-cell signaling during *Arabidopsis* stomatal development. *Plant Cell* **14**, 1527-1539.
- Voronin, V., Touraev, A., Kieft, H., van Lammeren, A.A., Heberle-Bors, E., and Wilson, C.** (2001). Temporal and tissue-specific expression of the tobacco ntf4 MAP kinase. *Plant Mol Biol* **45**, 679-689.
- Voronin, V., Aionesei, T., Limmongkon, A., Barinova, I., Touraev, A., Lauriere, C., Coronado, M.J., Testillano, P.S., Risueno, M.C., Heberle-Bors, E., and Wilson, C.** (2004). The MAP kinase kinase NtMEK2 is involved in tobacco pollen germination. *FEBS Lett* **560**, 86-90.

- Wang, X.Q., Ullah, H., Jones, A.M., and Assmann, S.M.** (2001). G protein regulation of ion channels and abscisic acid signaling in *Arabidopsis* guard cells. *Science* **292**, 2070-2072.
- Widmann, C., Gibson, S., Jarpe, M.B., and Johnson, G.L.** (1999). Mitogen-activated protein kinase: conservation of a three-kinase module from yeast to human. *Physiol Rev* **79**, 143-180.
- Wilkinson, S., and Davies, W.J.** (2002). ABA-based chemical signalling: the co-ordination of responses to stress in plants. *Plant Cell Environ* **25**, 195-210.
- Wilson, C., Eller, N., Gartner, A., Vicente, O., and Heberle-Bors, E.** (1993). Isolation and characterization of a tobacco cDNA clone encoding a putative MAP kinase. *Plant Mol Biol* **23**, 543-551.
- Wilson, C., Voronin, V., Touraev, A., Vicente, O., and Heberle-Bors, E.** (1997). A developmentally regulated MAP kinase activated by hydration in tobacco pollen. *Plant Cell* **9**, 2093-2100.
- Wu, S.J., Ding, L., and Zhu, J.K.** (1996). *SOS1*, a genetic locus essential for salt tolerance and potassium acquisition. *Plant Cell* **8**, 617-627.
- Yahraus, T., Chandra, S., Legendre, L., and Low, P.S.** (1995). Evidence for a mechanically induced oxidative burst. *Plant Physiol* **109**, 1259-1266.
- Yang, C.Y., Spielman, M., Coles, J.P., Li, Y., Ghelani, S., Bourdon, V., Brown, R.C., Lemmon, B.E., Scott, R.J., and Dickinson, H.G.** (2003). TETRASPORE encodes a kinesin required for male meiotic cytokinesis in *Arabidopsis*. *Plant J* **34**, 229-240.
- Yang, K.Y., Liu, Y., and Zhang, S.** (2001). Activation of a mitogen-activated protein kinase pathway is involved in disease resistance in tobacco. *Proc Natl Acad Sci U S A* **98**, 741-746.
- Yang, M., and Sack, F.D.** (1995). The too many mouths and four lips mutations affect stomatal production in *Arabidopsis*. *Plant Cell* **7**, 2227-2239.
- Yuasa, T., Ichimura, K., Mizoguchi, T., and Shinozaki, K.** (2001). Oxidative stress activates ATMPK6, an *Arabidopsis* homologue of MAP kinase. *Plant Cell Physiol* **42**, 1012-1016.
- Zhang, B., Ramonell, K., Somerville, S., and Stacey, G.** (2002). Characterization of early, chitin-induced gene expression in *Arabidopsis*. *Mol Plant Microbe Interact* **15**, 963-970.
- Zhang, S., and Klessig, D.F.** (1998). The tobacco wounding-activated mitogen-activated protein kinase is encoded by SIPK. *Proc Natl Acad Sci U S A* **95**, 7225-7230.
- Zhang, S., and Klessig, D.F.** (2001). MAPK cascades in plant defense signaling. *Trends Plant Sci* **6**, 520-527.
- Zhang, S.Q., and Outlaw, W.H., Jr.** (2001a). Abscisic acid introduced into the transpiration stream accumulates in the guard-cell apoplast and causes stomatal closure. *Plant Cell Environ* **24**, 1045-1054.

- Zhang, S.Q., and Outlaw, W.H., Jr.** (2001b). Gradual long-term water stress results in abscisic acid accumulation in the guard-cell symplast and guard-cell apoplast of intact *Vicia faba* L. plants. *J Plant Growth Regul* **20**, 300-307.
- Zhou, F., Menke, F.L., Yoshioka, K., Moder, W., Shirano, Y., and Klessig, D.F.** (2004). High humidity suppresses *ssi4*-mediated cell death and disease resistance upstream of MAP kinase activation, H₂O₂ production and defense gene expression. *Plant J* **39**, 920-932.
- Zhu, J.-K.** (2000). Genetic analysis of plant salt tolerance using *Arabidopsis*. *Plant Physiol* **124**, 941-948.
- Zhu, J.-K.** (2001a). Cell signaling under salt, water and cold stresses. *Curr Opin Plant Biol* **4**, 401-406.
- Zhu, J.-K.** (2001b). Plant salt tolerance. *Trends in Plant Science* **6**, 66-71.
- Zwerg, K., and Hirt, H.** (2001). Recent advances in plant MAP kinase signalling. *Biol Chem* **382**, 1123-1131.